

https://dspace.org/

Mineralogical, petrographic and geochemical characteristics of shales of the Karoo supergroup, South Africa

Tshibalo, Rudzani

2021

https://hdl.handle.net/10539/33205

Downloaded from a DSpace repository. https://dspace.org/

MINERALOGICAL, PETROGRAPHIC AND GEOCHEMICAL CHARACTERISTICS OF SHALES OF THE KAROO SUPERGROUP, SOUTH AFRICA

By

Rudzani Tshibalo

Supervisor:

Dr Zubair Jinnah

A thesis submitted to the

Faculty of Science, University of the Witwatersrand

in fulfilment of the requirements for the degree of Master of Science



School of Geosciences

University of the Witwatersrand, Johannesburg

DECLARATION

I, Rudzani Tshibalo, hereby declare that this research study is my own unaided work. It is being submitted for the Degree of Master of Science in Economic Geology to the University of the Witwatersrand, Johannesburg. It has not been submitted before for any degree or examination to any other university.

RTshibalo

(Signature of Candidate)

22nd day of September year 2021

ABSTRACT

The main objective of this research study is to gain a mineralogical and geochemical understanding of the potential of the source rocks of the Ecca Group to predict the success of hydraulic fracturing in the study area. A total of 12 samples were collected from the Prince Albert, Whitehill and Collingham Formations along the R67 provincial route between Grahamstown and Fort Beaufort in the Eastern Cape Province of South Africa. These samples were subjected to petrographic, mineralogical and geochemical analyses using petrographic microscopy, x-ray diffraction, x-ray fluorescence and inductively coupled plasma mass spectrometry.

The main mineral constituents of the Lower Ecca Group in the study area are quartz (65.6 wt.%), illite (12.19 wt.%), smectite (0.99 wt.%), chlorite (1.19 wt.%), calcite (12.19 wt.%) and dolomite (1.19 wt.%). The Prince Albert and Whitehill Formations contain a high amount of quartz, some carbonates and the least amount of clay, while the Collingham Formation contains a high amount of quartz, some clay and the least amount of carbonate. The mineralogical composition of the Lower Ecca Group compares favourably with gas-producing shales such as the Barnett Shale of the Fort Worth Basin in the United States. The Lower Ecca Group has high quartz (68.6 wt.%) content relative to the Barnett Shale (43 wt.%). The concentration of clay minerals in the Lower Ecca Group (4.8 wt.%) is generally lower than in the Barnett Shale (31 wt.%). Dolomite is the dominant carbonate mineral in the Barnett Shale, while calcite predominates in the Lower Ecca Group. In essence, the Lower Ecca Group of the Main Karoo Basin contains a high brittle mineral and low ductile mineral content relative to the Barnett Shale.

The petrographic analysis reveals that the mudstones and shales from the study area have been altered mainly due to carbonate and quartz cementations. Post-depositional diagenesis, such as the precipitation of calcite cements, occurs mainly in the Prince Albert Formation. The petrographic analysis shows that quartz and calcite cements are the most abundant, occurring mainly as fracture filling, pore-space filling and grain and matrix replacement. The deformation in the study area is largely linked to the Cape Fold Belt and assisted by dissolution. Large-ion lithophile elements (Rb, Ba, Sr, Th and U), high field strength elements (Zr, Hf, Y and Nb) and transition trace elements (Sc, V, Cr, Co, Pb, Ni and Zn) in the mudstones and shales of the

study area are generally depleted compared to the upper continental crust. The concentrations of Cu, Ni, Zn and V are depleted in the Lower Ecca Group relative to the Barnett and Marcellus Shales in the United States. The concentration of major elements in the current study is generally higher than in the Barnett Shale, while the SiO_2 content averages 63 wt.% in the study area-higher than in the Barnett Shale (15.16 wt.%).

The Whitehill Formation of the Main Karoo Basin and the Barnett Shale of the Fort Worth Basin share the following similarities: they are composed of black carbonaceous shales, high brittle mineral constituents and high total organic content accommodated by an anoxic depositional environment. Based on this research study, the Prince Albert, Whitehill and Collingham Formations possess more brittle mineral content (quartz and carbonate) than ductile mineral content (clay). An increase in brittle minerals generally suggests that the formations are conducive to hydraulic fracturing. The overall mineralogy promotes natural fractures and the generation of induced network fractures. The Collingham Formation may enable a good seal and trap shale gas from migrating out of the shale below due to the high clay content (9.1 wt.%) compared to the Prince Albert (3.69 wt.%) and Whitehill Formations (8.75 wt.%). The performance of hydraulic fracturing would be successful if these formations were to be developed. Diagenetic transformations (cementation) may cause loss of porosity, permeability reductions and reservoir quality degradation, increasing the requirement for hydraulic fracturing and additional stimulation methods to enhance shale gas recovery and flow capacity.

ACKNOWLEDGEMENTS

First, I would like to thank God the Almighty for giving me the strength and courage to execute this research. I express my sincere gratitude to my supervisor, Dr Zubair Jinnah, Senior Lecturer at the University of the Witwatersrand, for providing valuable guidance and constructive criticism.

I also take this opportunity to express a deep sense of gratitude to my employer, the Department of Energy of South Africa, for opening this door of opportunity and for their profound contribution in providing financial assistance.

Special mention is made of the efforts of Mr Marlin Patchappa and his team for performing the XRF and ICP-MS analyses and Mr Caiphus Majola and his team for preparing the samples and thin sections. The efforts of Dr Sabine Verryn of XRD Analytical and Consulting in performing XRD analysis are gratefully acknowledged. I am thankful to Mr Bongani Hlungwani for providing his assistance during fieldwork and data collection.

I am grateful to my dearest grandmother (Mrs Tshililo Makwarela Tshibalo), my father (Mr Ndivhudzannyi Carlson Tshibalo) and my siblings for their continued support, guidance and encouragement.

I am thankful to the members of the University of the Witwatersrand for their endorsement and reassurance during the course of my research.

TABLE OF CONTENTS

DECLARATION ..... **ii**
ABSTRACT ..... **iii**
ACKNOWLEDGEMENTS ..... **v**
LIST OF FIGURES ..... **ix**
LIST OF TABLES ..... **xii**
ABBREVIATIONS ..... **xiii**
CHAPTER 1: INTRODUCTION **1**
1.1 Background 1
1.2 Economic potential of the shale formations in the Ecca Group 3
1.3 Shale gas and hydraulic fracturing 4
1.4 Problem statement 7
1.5 Aims and objectives of the research 7
1.5.1 General aim 7
1.5.2 Specific objectives 8
1.6 Location of the study area 8
CHAPTER 2: GEOLOGICAL SETTING **10**
2.1 Main Karoo Basin 10
2.2 Stratigraphy 13
2.2.1 Dwyka Group (glacial) 14
2.2.2 Ecca Group (marine) 14
2.2.3 Beaufort Group 22
2.2.4 Stormberg Group 23
2.3 Depositional environments 23
2.3.1 Prince Albert Formation 25
2.3.2 Whitehill Formation 26
2.3.3 Collingham Formation 26
2.4 Shale mineralogy 27
2.4.1 Prince Albert Formation 28
2.4.2 Whitehill Formation 29
2.4.3 Collingham Formation 29
2.5 Geochemistry of shales 29

2.5.1 Organic geochemistry 30
2.5.2 Inorganic geochemistry 31
2.6 Previous studies on Ecca Group mineralogy and geochemistry 31
CHAPTER 3: METHODOLOGY AND INSTRUMENTATION 33
3.1 Desktop study 33
3.2 Fieldwork 33
3.3 Laboratory analysis 34
3.3.1 Sample preparation 34
3.3.2 Petrographic microscope 35
3.3.3 X-ray diffraction 37
3.3.4 X-ray fluorescence 38
3.3.5 Inductively coupled plasma mass spectrometry 39
CHAPTER 4: DATA PRESENTATION 41
4.1 Fieldwork data 41
4.1.1 Prince Albert Formation lithologic description 45
4.1.2 Whitehill Formation lithologic description 46
4.1.3 Collingham Formation lithologic description 47
4.2 Petrographic data 48
4.2.1 Petrography of the Prince Albert Formation 48
4.2.2 Petrography of the Whitehill Formation 50
4.2.3 Petrography of the Collingham Formation 52
4.3 Mineralogical data 54
4.3.1 Prince Albert Formation 58
4.3.2 Whitehill Formation 59
4.3.3 Collingham Formation 59
4.4 Major element data 61
4.4.1 Prince Albert Formation 61
4.4.2 Whitehill Formation 62
4.4.3 Collingham Formation 63
4.5 Trace element data 66
4.5.1 Prince Albert Formation 67
4.5.2 Whitehill Formation 67
4.5.3 Collingham Formation 67
CHAPTER 5: DATA ANALYSIS AND INTERPRETATION 69

5.1 Fieldwork data analysis 69
5.2 Petrographic data analysis 70
5.3 Mineralogical data analysis 73
5.3.1 Silica mineralogy 74
5.3.2 Carbonate mineralogy 75
5.3.3 Clay mineralogy 76
5.4 Major element data analysis 81
5.5 Trace element data analysis 86
CHAPTER 6: CONCLUSIONS 95
REFERENCES 98

LIST OF FIGURES

Figure 1.1: (a) Shows hydraulic induced fractures; (b) indicates the existence characteristics of absorbed gas and free gas in a shale gas reservoir.....6
Figure 1.2: Map showing the study area situated along the R67 provincial route from Grahamstown to Fort Beaufort in the Eastern Cape Province.....9
Figure 2.1: Shows the location of the Main Karoo and Kalahari Basins and other smaller basins in southern Africa.....10
Figure 2.2: Lithostratigraphy of the Karoo Supergroup 12
Figure 2.3: Dwyka diamictite with clasts of different sizes, shapes and sources 14
Figure 2.4: Five lithofacies of the Prince Albert Formation along the southern basin margin 17
Figure 2.5: Thin-bedded wave-ripple wackes in the Waterford Formation.....22
Figure 3.1: Schematic illustration of a jaw crusher 35
Figure 3.2: Thin sections preparation procedure 36
Figure 3.3: Petrographic microscope attached with camera for photomicrography.....36
Figure 3.4: Schematic diagram of X-ray diffraction pattern.....37
Figure 3.5: X-ray fluorescence spectroscopy instrumentation 38
Figure 3.6: Major instrumentation components of the ICP-MS system 39
Figure 3.7: ICP-MS sample introduction area 40
Figure 4.1: Shows mudstone foliation and red stain (due to high iron content) at the Prince Albert Formation (elevation: 466 m; 26° 62′ 73″ E; 33° 21′ 62″ S).....45
Figure 4.2: Shows tuffaceous zone within the Whitehill Formation (elevation: 483 m; 26° 62′ 73″ E; 33° 21′ 62″ S) 46
Figure 4.3: Shows shale and tuff interbeds of Collingham Formation (elevation: 487 m; 26° 62′ 63″ E; 33° 21′ 55″ S).....47
Figure 4.4: Thin section photomicrographs of the Prince Albert Formation viewed under plane polarised light.....49
Figure 4.5: Thin section photomicrographs of the Whitehill Formation viewed under plane and cross polarised light.....51
Figure 4.6: Thin section photomicrographs of the Collingham Formation in the Karoo Basin viewed under plane and cross polarised light 54

Figure 4.7: (a) A ternary plot showing the mineral composition as a percentage of three major components (i.e., quartz, clay and carbonate); (b) pie chart depicting the percentage distribution of quartz, clay and carbonate minerals in mudstones across the Prince Albert Formation.....58
Figure 4.8: (a) A ternary plot showing mineral composition as a percentage of three major components (i.e., quartz, clay and carbonate); (b) pie chart depicting the percentage distribution of quartz, clay and carbonate minerals in shales across the Whitehill Formation.....59
Figure 4.9: (a) A ternary plot showing the mineral composition as a percentage of three major components (i.e., quartz, clay and carbonate); (b) pie chart depicting the percentage distribution of quartz, clay and carbonate minerals in shales across the Collingham Formation.....60
Figure 4.10: (a) A ternary plot of the major oxides (XRF) showing the Prince Albert mudstones rich in SiO_2 relative to Al_2O_3 and CaO; (b) a ternary plot showing mineral composition (XRD) as a percentage of three major components (i.e., quartz, clay = illite + chlorite + smectite and carbonate = calcite + dolomite) in mudstones across the Prince Albert Formation.....62
Figure 4.11: (a) A ternary plot of the major oxides (XRF) showing Whitehill shales rich in SiO_2 relative to Al_2O_3 and CaO (i.e., quartz = SiO_2, clay = Al_2O_3 and carbonate = CaO); (b) a ternary plot showing the mineral composition (XRD) as a percentage of three major components (i.e., quartz, clay = illite + chlorite + smectite and carbonate = calcite + dolomite) across shales in the Whitehill Formation.....63
Figure 4.12: (a) A ternary plot of the major oxides (XRF) showing Collingham shales rich in SiO_2 relative to Al_2O_3 and CaO; (b) a ternary plot showing mineral composition (XRD) as a percentage of three major components (i.e., quartz, clay = illite + chlorite + smectite and carbonate = calcite + dolomite) across shales in the Collingham Formation.....64
Figure 4.13: UCC normalised trace element concentrations of mudstones and shales of the Prince Albert, Whitehill and Collingham Formations (arranged in LILE, HFSE and TTE).....66
Figure 5.1: Silica mineral composition in the three formations.....75
Figure 5.2: Carbonate mineral composition in the three formations.....76
Figure 5.3: Clay mineral composition in the three formations.....77

Figure 5.4: Major elements (reported in weight%) of shale samples from the three formations 82
Figure 5.5: (a-d) Hacker diagrams of major oxides (Na_2O, CaO, Fe_2O_3 and Al_2O_3) versus SiO_2 (negative correlations) 84
Figure 5.6: (a-c) Hacker diagrams of major oxides (Fe_2O_3, TiO_2 and K_2O versus Al_2O_3), positively correlated; (d) negatively correlated Na_2O/K_2O 85
Figure 5.7: Average trace elements (ppm) in the studied samples 87
Figure 5.8: (a-d) Bivariate plot diagrams of K_2O and Rb, Cr and Ni, Zr and Hf and Al_2O_3 and Rb showing good strong correlations 89
Figure 5.9: Ni versus TiO_2 plot diagram to characterise source rock composition in the study area 90
Figure 5.10: Zr versus TiO_2 plots diagram to discriminate provenance of the rocks in the study area 91

LIST OF TABLES

Table 2.1: Lithostratigraphy of the Karoo Supergroup in the Eastern Cape Province compiled by the Council of Geoscience, South Africa 13
Table 2.2: Lithostratigraphy of the Ecca Group in the Eastern Province of South Africa 15
Table 2.3: Stratigraphic subdivision of the Prince Albert Formation 16
Table 2.4: Stratigraphic subdivision of the Whitehill Formation 18
Table 2.5: Stratigraphic subdivision of the Collingham Formation 20
Table 2.6: Geologic age and depositional environments of the Karoo Supergroup 24
Table 4.1: Summary of the lithological description in the study area 43
Table 4.2: Comparison of the lithologic description data to the petrographic data in the Prince Albert Formation 50
Table 4.3: Comparison of the lithologic description data to the petrographic data in the Whitehill Formation 52
Table 4.4: Comparison of the lithologic description data to the petrographic data in the Collingham Formation 54
Table 4.5: Qualitative and quantitative XRD laboratory test results of the three formations reported in weight% (wt.%) 57
Table 4.6: Major element concentrations of the studied samples reported in weight% 65
Table 4.7: Trace element composition in ppm (arranged in LILE, HFSE and TTE groups) 68
Table 5.1: XRF data (major elements) of the Barnett Shale compared with the current study (Ecca Group) 86
Table 5.2: Trace element data of the Barnett Shale compared with the current study (Colwell, 2014) 92
Table 5.3: Comparison of the Marcellus Shale trace element data to this study 93

ABBREVIATIONS

BI	Brittleness index
CFB	Cape fold belt
GPS	Global positioning system
HFSE	High field strength elements
ICP-MS	Inductively coupled plasma mass spectrometry
LILE	Large-ion lithophile elements
PAAS	Post-Archean Australian Shale
PPM	Parts per million
Tcf	Trillion cubic feet
TOC	Total organic content
UCC	Upper continental crust
TTE	Transition trace elements
Wt.%	Weight percentage
XRD	X-ray diffraction
XRF	X-ray fluorescence

CHAPTER 1: INTRODUCTION

1.1 Background

South Africa is faced with the challenge of meeting the future energy demands of an expanding economy (Burton et al., 2018; Von Ketelhodt and Wöcke, 2008). Another challenge is the fact that the country is highly carbon-intensive (Burton et al., 2018). Concerns have been expressed over the country's unsustainable dependency on coal. These concerns have also been prompted by the risks associated with the greenhouse gas emissions that drive global climate change (Niemack, 2009).

South Africa must acquire alternative sources of energy, such as shale gas, that are less carbon-intensive than coal (Niemack, 2009). Although coal and petroleum have traditionally been the important resources required to generate energy, natural gas is now attracting more interest in the energy sector. The main reason is that natural gas offers an efficient and greener source of energy (Wanniarachchi et al., 2015).

However, the extremely low permeability of the host rock (shale) is a major difficulty in shale gas development. In general, shales contain a large clay content that assists to absorb and store gas (Rogen and Fabricius, 2002; Ross and Bustin, 2009). A large amount of clay minerals in shales makes the shale unfavourable for hydraulic fracturing purposes due to the enhancement of the ductility of the formation. Thus, the reduction in the brittleness of the shale leads to a poor response to the fracking process (Zhang et al., 2017a).

Ye et al. (2020) also documented that an excessive quartz or carbonate content hinders fracture development in shales. Shale is defined as a hard mudrock and is composed of variable proportions of quartz silt with a grain size of less than 0.032 mm and clay crystals generally less than 0.004 mm (Merriman et al., 2003). Gas-shale is a formation of organic-rich shale, formed from deposits of mud, silt, clay and organic matter (Broderick et al., 2011). The basic requirements for shale gas development include an understanding of mineralogy, organic richness, brittleness, maturation, thickness, gas in place, permeability and pore pressure (Chopra et al., 2014).

The mineralogy of shale is one major determining parameter of how efficiently the induced fractures will stimulate shale to release gas (Chopra et al., 2014). Furthermore, the characterisation of shale gas reservoirs depends on the depositional environment, i.e., marine or non-marine (continental) shale. Marine shale has a lower clay content and is composed of brittle minerals (such as quartz, feldspar and carbonates) which respond better to fracking during hydraulic stimulation.

On the other hand, non-marine shales tend to be high in clay content and are ductile and less responsive to hydraulic stimulation. In this manner, the brittleness in marine shale is generally higher than in non-marine shale and produces cracks more easily (Chopra et al., 2014). These findings were also supported by Deng et al. (2018); they indicated that the mineralogical composition of continental shale can considerably affect the brittleness of shale gas formation. Generally, the brittle index (BI) of continental shales is lower than that of marine shales.

A study undertaken by Ye et al. (2020) highlighted that a quartz content of greater than 70% decreases rock brittleness, while quartz content between 20% and 70% shows good brittleness. The key parameters that control the hydraulic fracturing process include shales containing high quartz content as well as carbonates. Therefore, shale must contain over 30% quartz, some carbonates and preferably a brittle rock material. The mineralogy and petrography of the shale can be determined by using techniques such as thin section microscopy, supplemented by scanning electron microscopy (SEM) (Xue et al., 2015).

For the past few decades, the discovery of shale gas has resulted in a sharp increase in the number of researchers in this field (Wang & Li, 2017). However, in terms of the Karoo Basin, recent studies have focused on the geothermal history and petrophysical characteristics of shale units at specific points within the basin (De Kock et al., 2017). The Karoo Basin has been singled out as an area with great potential for shale gas and current resource estimates of 390 trillion cubic feet (Tcf) are speculatively based on properties such as carbonaceous shale thickness, area, depth, thermal maturity and, most of all, the total organic carbon content (De Kock et al., 2017). Attempts have been made to correlate the trace element geochemistry of shales with their mineralogy to distinguish the depositional environment of shales (Hofmeyr, 1971). In addition to the properties listed above, it is of considerable importance to investigate and understand the mineralogy and geochemistry of the host rock, hence this study.

In recent years, several studies focusing particularly on the lower formations of the Ecca Group have been undertaken. This includes the study by Geel et al. (2013) that emphasised the petrography and geochemistry of the Lower Ecca Group. The study results indicated that marine shales are enriched in V and Cr, while the fresh-water shales are enriched in Cu. These researchers further suggested that the deposition of these rocks took place in stratified water bodies in oxygen-deficient conditions. According to Hofmeyr (1971), elements such as V, Cr and Cu are reliable indicators of the shale depositional environment.

Another study by Danchin (1970) focusing on the geochemistry of the black shales of the Ecca Group indicates that the rock units have high calcite, illite and apatite content. The high concentrations of calcite and apatite provided evidence that the sediments were deposited in an alkaline-water (pH > 7.8) environment (Danchin, 1970). A study by Maake (2018) about the mineralogy and geochemistry of the shales of the Lower Ecca Group (the Prince Albert, Whitehill and Collingham Formations) indicates that shales are characterised by discontinuous parallel laminae while dolomite and calcite are the dominant carbonate minerals. Calcite occurs mainly as pore-filling cement and grain replacement. The lithology of the Whitehill Formation consists of calcite veins, pyrite, quartz and micaceous minerals thought to be associated with organic-rich sediments.

In this study, the mineralogical and geochemical data obtained by various techniques, such as fieldwork, petrographic microscopy, x-ray diffraction (XRD), x-ray fluorescence (XRF) and inductively coupled plasma mass spectrometry (ICP-MS), were used to assess whether hydraulic fracturing in the study area is feasible or not.

1.2 Economic potential of the shale formations in the Ecca Group

The Karoo Basin of South Africa formed as a successor basin to the early Palaeozoic Cape Basin along the southwestern margin of Gondwana (Geel et al., 2015). This sequence of predominantly sedimentary rocks preserves a world-class assemblage of fossils, spanning a time range from the Late Carboniferous to the Early Jurassic periods (Rubidge & Hancox, 2002). The Karoo Supergroup is stratigraphically divided into several groups defined by their age and sedimentological characteristics: Dwyka, Ecca, Beaufort, Stormberg and Drakensberg (Johnson et al., 2006). The study area is located within the Ecca Group which is divided into

the Prince Albert, Whitehill, Collingham, Ripon, Fort Brown and Waterford Formations (Catuneanu et al., 2005).

Although the Permian black shales of the Karoo Basin have been classified as potential unconventional gas resources, the Whitehill Formation of the southern basin is the main target for future shale gas exploration and production (Costin et al., 2019; Geel et al., 2021). The Whitehill Formation is the most favourable formation for gas exploitation due to high organic richness, porosity resulting from the decomposition of organic matter and mineral induced brittleness (Geel et al., 2015). The formation has a high total organic content (TOC) of ~5 wt.% (Geel et al., 2021). The high TOC content in the Whitehill Formation indicates organic matter preservation, suggesting anoxic conditions (Geel & Bordy, 2021). The characteristics of the Whitehill Formation as a suitable shale gas host compare favourably with gas-producing fields in the United States (Geel et al., 2015). The Prince Albert and Collingham Formations have an average TOC content of 0.181 wt.% and 1.44 wt.%, respectively (Geel & Bordy, 2021; Geel et al., 2021).

1.3 Shale gas and hydraulic fracturing

Hydraulic fracturing is the process of enhancing the extraction and flow from unconventional reservoirs through the generation of a fracture network (Gehne & Benson, 2019). The development of a fracture network is crucial in the development of the shale formation. Hydraulic fracture propagation depends on geologic and engineering factors controlling the fracture and extending into the network in the shale reservoir (Ren et al., 2014).

Several geologic factors control hydraulic fracturing in shales: rock mineral composition (higher brittle mineral content), rock mechanics properties (stronger elastic characteristic), horizontal stress field (smaller horizontal differential stress) and distribution of natural fractures (better developed natural fractures). These factors cause better extension and propagation of hydraulic fractures in the network. The engineering conditions of the fracturing process require higher treating net pressure, lower fluid viscosity and a larger fracturing scale (Ren et al., 2014). The present study focuses on the distribution of mineral composition as one of the geologic factors that affect hydraulic fracture propagation in shales.

In terms of mineralogical composition, the brittleness of shale is estimated based on the mineralogical composition of the rock. Quartz and some other minerals are considered brittle minerals, while clay is considered a plastic/ductile mineral (Xia et al., 2019). The presence of clay in a reservoir may destroy its porosity and permeability. Illitic cement may cause a negative effect on permeability, while smectitic clays swell in the presence of water. The smectitic reservoirs are very susceptible to deformation if drilled with conventional water-based mud; oil-based mud is used instead (Deshpande, 2008).

Different mineral compositions also control the brittleness of shale and further influence reservoir reconstruction. The general requirement for brittle mineral content in shale is that it must be higher than 30% to obtain a good fracturing effect (Zhang, Shi & Li, 2018). The existence of brittle mineral content plays an important role in rock brittleness prediction. Usually, quartz > dolomite > calcite > clay improves the brittleness for hydraulic fracturing in an unconventional reservoir (Mohamed et al., 2019). Brittleness is the key factor that affects the fracture network of shale reservoirs during hydraulic fracturing.

Ductile shale, on the other hand, will seal natural gas and fracture cracks. Ductile shale enables a good seal, traps the hydrocarbons from migrating out of the shale below and creates a good fracture barrier for a reservoir. Brittle shale is more prone to natural fracture and easily forms a complex network through hydraulic fracturing (Rickman et al., 2008; Wang et al., 2017; Xia et al., 2019). To achieve commercial development value, the accumulated thickness of a shale reservoir must reach at least 15 m and the buried depth must be < 4000 m (Zhang et al., 2018). Figure 1.1 shows hydraulic induced and natural fractures in shale.

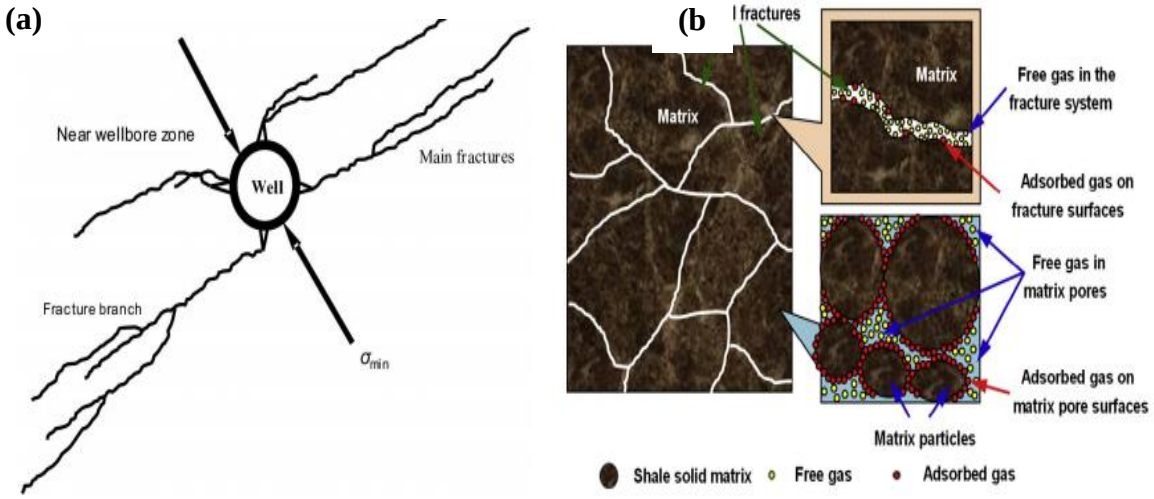


Figure 1.1: (a) Shows hydraulic induced fractures; (b) indicates the existence characteristics of absorbed gas and free gas in a shale gas reservoir (Zhang, Chen & Zhao, 2019)

The higher content of brittle minerals such as quartz and calcite can result in the formation of natural fractures. During fracturing and stimulation, complex induced fractures (Figure 1.1) can be formed more easily and achieve the extension and connection of fracture networks (Jiang et al., 2016). Brittle rocks may facilitate hydraulic fracturing due to low fracture closure rates. However, recent investigations in the Lower Ecca Group suggest that brittle rocks may demonstrate the poor ability of the rock to develop a complex fracture network during hydraulic fracturing due to a high Young's modulus and fracture toughness (Geel & Bordy, 2021).

The Lower Ecca Group has high maturity and that influences diagenetic mineral precipitation, impacting an overall brittleness. According to geochemical results by Geel et al. (2021), the Prince Albert and Collingham Formations are the strongest and most brittle due to their high proportion and intermediate mineral fractions. The brittleness of the Lower Ecca Group suggests easy fracking. However, the irregular spatial distribution of fracture zones, veining and carbonate horizons may enhance or diminish the quality of hydraulic fracturing (Geel et al., 2021).

According to Gale et al. (2007), when natural fractures are encountered during hydraulic fracturing, they are opened up to fluids and provide a network connected to the wellbore. The length and width of the fractures generated by hydraulic fracturing are the most important

factors for gas production from the reservoir. The extension of the hydraulic fractures is significantly influenced by the brittleness of the reservoir (Xia et al., 2019).

Brittle shale can be easily treated because there are more natural fractures and the fractures can be connected after the hydraulic fracturing (Rickman et al., 2008; Xia et al., 2019). In high brittleness shales, the proppant may provide a high-conductivity flow path for hydrocarbons to migrate to the wellbore; in more ductile shales, the fracture becomes more like conventional bi-wing fracture geometry (Rickman et al., 2008).

1.4 Problem statement

More than a decade ago, Dondo and Nhleko (2008) indicated that the Karoo Basin hosts a potential shale gas resource that has not been adequately explored with advanced technology such as hydraulic fracturing. Fast-forward to the present and it turns out that the current resource estimates are not sufficient to define and identify a region within the Karoo Basin with high gas content and high brittleness – a 'sweet spot' (De Kock et al., 2017).

As shale gas plays become more important, a better understanding and more knowledge become vital to supporting future exploration and exploitation (Abouelresh et al., 2017). Thus, a systematic approach should be considered to minimise and eliminate these uncertainties. This research will provide geological data with improved accuracy to support future exploration and exploitation of shale gas using hydraulic fracturing processes.

1.5 Aims and objectives of the research

1.5.1 General aim

The economic feasibility of hydraulic fracturing to enhance the recovery of shale gas in the Karoo Basin has not been widely studied and reported. This research aims to gain a mineralogical and geochemical understanding of the source rock to predict the success of hydraulic fracturing and to guide the development of shale gas in the study area.

1.5.2 Specific objectives

The study has three specific objectives:

- To determine the mineralogical signatures of the source rock using the XRD technique and petrographic microscope;
- To determine the geochemical signatures of the source rock for major and trace elements using XRF and inductively coupled plasma mass spectrometry (ICP-MS), respectively; and
- To systematically assess and predict if the mineral composition of the source is conducive for hydraulic fracturing.

1.6 Location of the study area

This research project focuses mainly on the lower geological formations of the Ecca Group of the Karoo Basin. The Ecca Group was selected for this project because it comprises the Prince Albert and Whitehill Formations which have been identified for shale gas development. Cole and Mosavel (2016) categorised these two formations as shale gas 'sweet spots'. It has been reported that the Whitehill Formation provides the best target for shale gas development since it has similar TOC content to several gas-producing shales in the United States. Furthermore, the maturity levels of shales within the Whitehill Formation are conducive to the production of dry gas (Cole & Mosavel, 2016).

The study area is located between Grahamstown and Fort Beaufort along the R67 provincial route in the Eastern Cape Province of South Africa (Figure 1.2). The study area was selected mainly because the rocks of the Lower Ecca Group are well exposed along the R67 route due to road cuttings and are easily accessible. Secondly, the orientation of the rock beds and the Ecca stratigraphic succession can be easily identified and mapped.

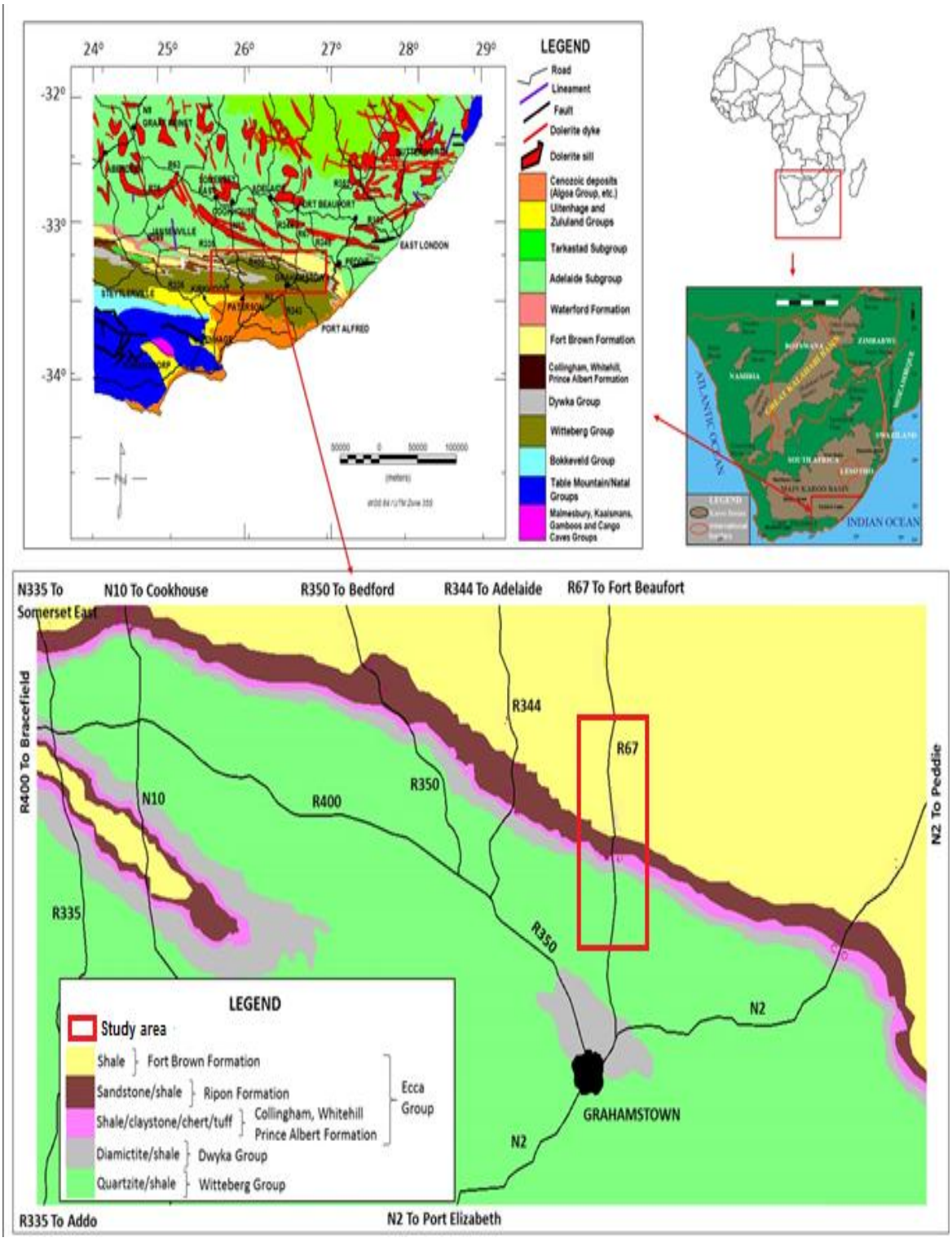


Figure 1.2: Map showing the study area situated along the R67 provincial route from Grahamstown to Fort Beaufort in the Eastern Cape Province (Baiyegunhi, Liu & Gwavava, 2017a)

CHAPTER 2: GEOLOGICAL SETTING

2.1 Main Karoo Basin

According to Johnson et al. (1996), the Karoo Supergroup (Karoo Basin) in southern Africa occurs in the extensive Main Karoo and Kalahari Basins, as well as several other smaller basins (Figure 2.1). The basin has an areal extent of approximately 550 000 km^2 (Cadle et al., 1993) and comprises about 5 500 m of deep marine and fluvial deposits (Flint et al., 2011). The beginning of the Karoo depositional sequence is generally placed in the Late Carboniferous period (300 Ma). This was after a major inversion tectonic event along the southern margin of the supercontinent that led to the assemblage of Pangea (Catuneanu et al., 2005).

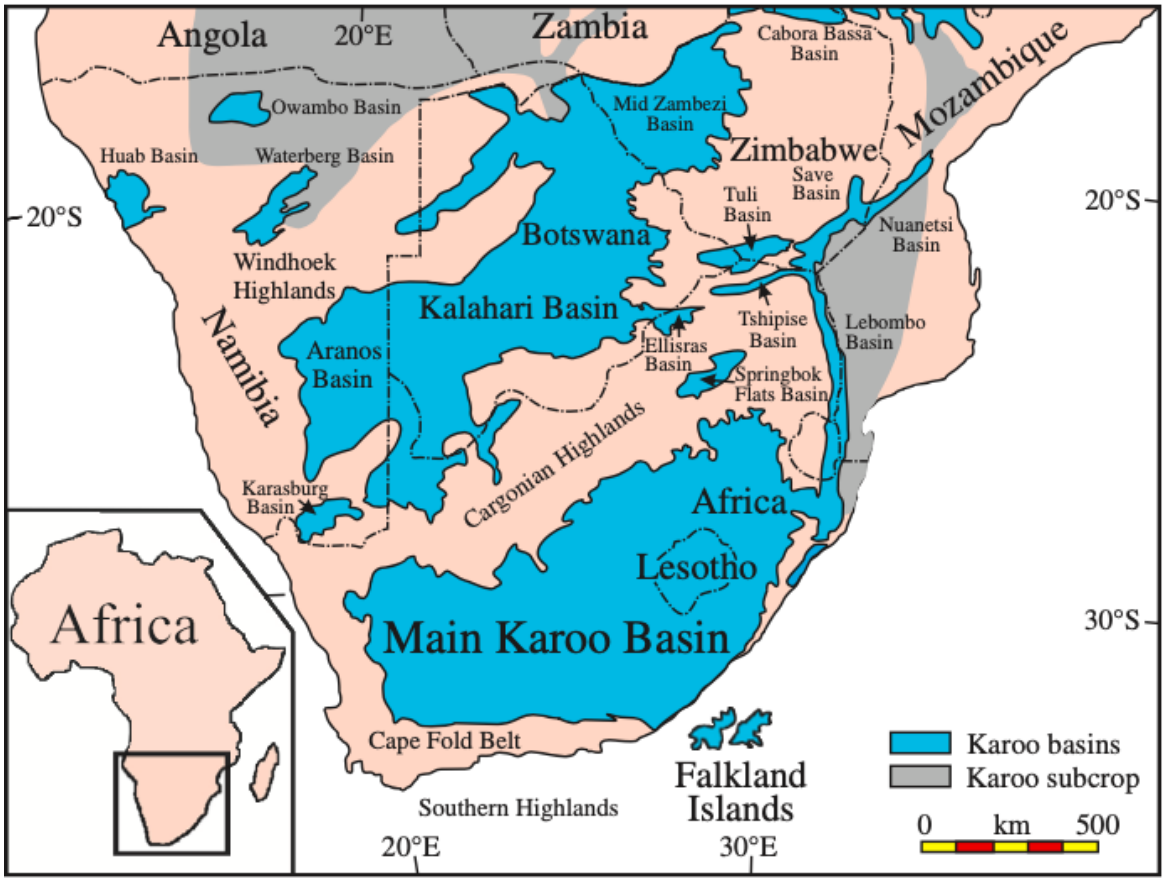


Figure 2.1: Shows the location of the Main Karoo and Kalahari Basins and other smaller basins in southern Africa (Catuneanu et al., 2005; Isbell et al., 2008)

The age of the Karoo Supergroup ranges from the Late Carboniferous to the Early Jurassic (Flint et al., 2011; Rubidge & Hancox, 2002). This period (300–280 Ma) was marked by large-

scale episodes of subsidence, producing a series of interconnected marine basins (Flint et al., 2011). The sedimentary rocks of the Karoo Supergroup contain a world-class assemblage of fossil vertebrates (Rubidge & Hancox, 2002). These fossil vertebrates of the Karoo Supergroup include fish, amphibians and a great diversity of reptiles (Damiani & Rubidge, 2003).

The following main geodynamic events are recognised in the deposition of the Karoo Supergroup: the deposition of the sediments and uplift of the Cape Fold Belt (CFB), the breakup of the ancient supercontinent (Gondwana) and the intrusion of Karoo dolerite and basalt (Woodford, Chevallier & Botha, 2003). The shifts in tectonic and climatic conditions from the southern margins of Africa during Karoo time also caused the litho-stratigraphic character of the Karoo sequence to change significantly across the African continent (Catuneanu et al., 2005).

Lithologically, the Supergroup is split into five main groups: Dwyka, Ecca, Beaufort, Stormberg and Drakensberg (Cadle et al., 1993; Catuneanu et al., 2005; Johnson et al., 1996; Figure 2.2). These groups are defined according to their sedimentological characteristics (Catuneanu et al., 2005) and they represent sediments deposited in glacial, marine, fluviodeltaic, fluviolacustrine and dry-wet desert environments, respectively (Cadle et al., 1993).

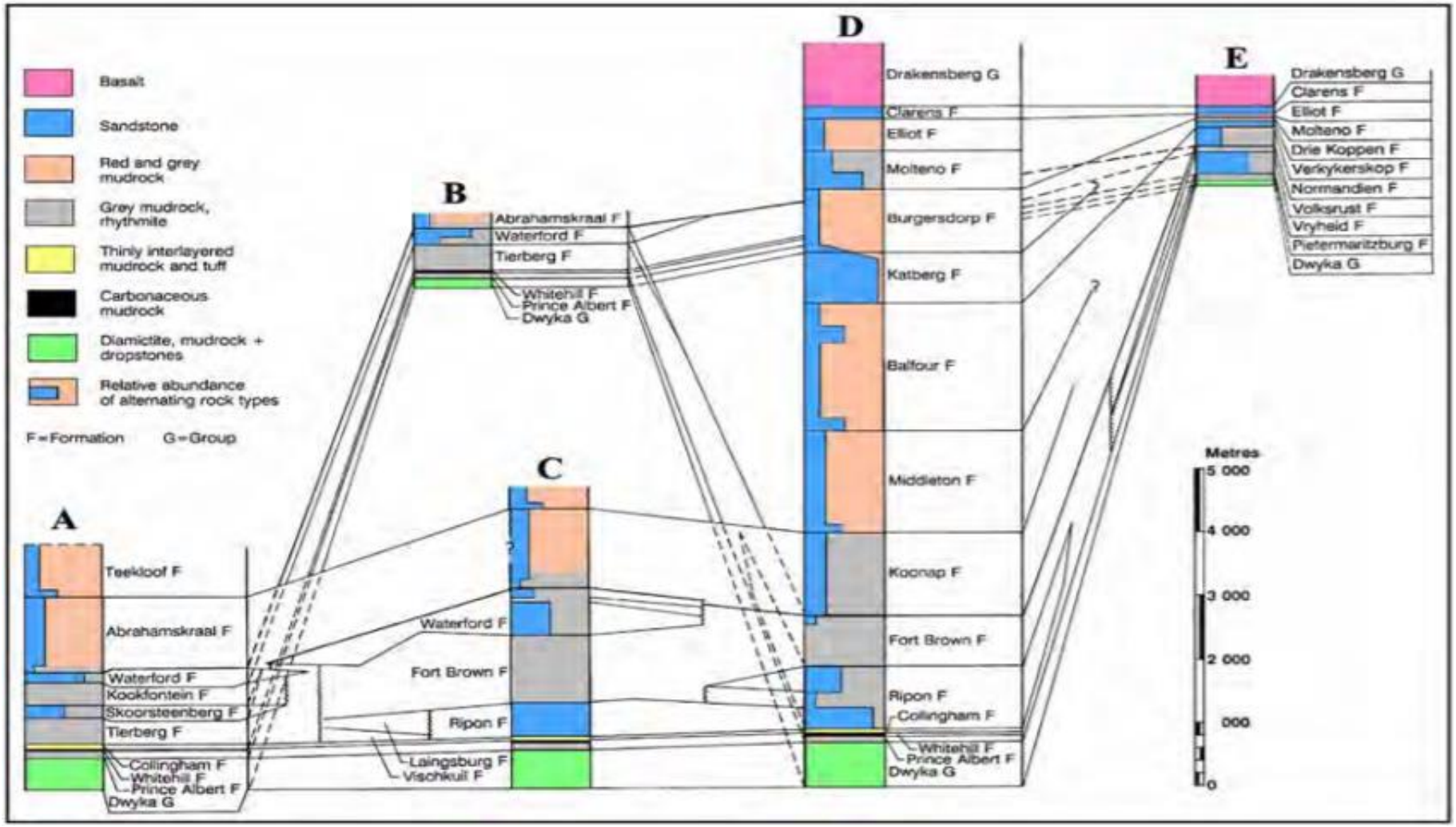


Figure 2.2: Lithostratigraphy of the Karoo Supergroup (Johnson et al., 1997; Woodford et al., 2003)

2.2 Stratigraphy

The stratigraphy of the Karoo Supergroup (Table 2.1) is divided into five groups based on differences in lithostratigraphy as indicated: Dwyka (Westphalian to Early Permian), Ecca (Permian), Beaufort (Permian-Triassic), Stormberg and Drakensberg (Adeniyi et al., 2018; Fildani et al., 2009).

Table 2.1: Lithostratigraphy of the Karoo Supergroup in the Eastern Cape Province compiled by the Council of Geoscience, South Africa (modified from Mepaiyeda et al., 2020)

SUPERGROUP	GROUP	SUBGROUP	FORMATION	MEMBER	LITHOLOGY
KAROO	DRAKENSBERG		Drakensberg Basalts		Basalt, Pyroclastic Deposits
	STORMBERG		Clarens		Sandstone
			Elliot		Mudstone, Sandstone
			Molteno		Sandstone, Khaki Shale
	BEAUFORT	TARKASTAD	Burgersdorp		Mudstone, Sandstone, Shale
			Katberg		Sandstone, Mudstone, Shale
			Balfour	Palingkloof	Mudstone, Sandstone, Shale
				Elandsberg	Sandstone, Siltstone
				Barberskrans	Sandstone, Khaki Shale
				Daggaboersnek	Shale, Sandstone, Siltstone
				Oudeberg	Sandstone, Khaki Shale
			Middleton		Shale, Sandstone, Mudstone
			Koonap		Sandstone, Mudstone
	ECCA		Waterford		Sandstone, Shale
			Fort Brown		Shale, Sandstone
			Ripon		Sandstone, Shale
			Collingham		Shale, Yellow Claystone
			Whitehill		Black Shale, Chert
			Prince Albert		Khaki Shale
	DWYKA		Dwyka Glacial Beds		Diamictite, Tillite, Shale

2.2.1 Dwyka Group (glacial)

The glaciogenic Dwyka Group (glacial deposits) is a succession of diamictites (Figure 2.3) and glacio-fluvial deposits with a thickness of up to 800 m (Flint et al., 2011). This group represents the first depositional sequence in the Main Karoo Basin and was formed during the Carboniferous-Permian glaciation of southern Gondwana (Belica et al., 2017; Lanci et al., 2013; Wheeler, 2015). It marked the beginning of Karoo Basin sedimentation at approximately 300-310 Ma (Flint et al., 2011). The diamictite of the Dwyka Group is superseded by the horizontally stratified Permian Ecca Group (Lanci et al., 2013; Von Brunn, 1996).



Figure 2.3: Dwyka diamictite with clasts of different sizes, shapes and sources (photo by Mervine)

2.2.2 Ecca Group (marine)

The Ecca Group sequence was deposited between the Late Carboniferous Dwyka Group and the Late Permian-Middle Triassic Beaufort Group (Catuneanu et al., 2005). The group was mainly deposited in a large body of water and consisted of approximately 2 000 m of sediments. The Ecca Group sediments comprise rhythmites, mudstones, sandstones and shales (Johnson, 1976). The rocks of the Lower Ecca Group are composed of interbedded mudstones and sandstones that represent turbidite deposits accumulated within a shallow inland sea (Johnson et al., 2006). In the southwestern Karoo Basin, the Ecca Group is an approximately 1 300 m

thick succession of predominantly siliciclastic sediments capped by the fluvial Beaufort Group (Flint et al., 2011).

The Ecca Group is subdivided into six formations (Table 2.2), in ascending order, the Prince Albert, Whitehill, Collingham, Ripon, Fort Brown and Waterford Formations (Johnson et al., 2006). These formations reflect the lateral variation in the lithologic characteristics of the Ecca succession (Johnson et al., 1997). This study focuses on the Lower Ecca Group formations – the Prince Albert, Whitehill and Collingham Formations.

Table 2.2: Lithostratigraphy of the Ecca Group in the Eastern Province of South Africa (modified after Johnson et al., 2006)

Group	Formation	Lithology	Ages
Ecca	Waterford	Sandstone, mudstone	258–251 Ma
	Fort Brown	Sandstone, shale	262–258 Ma
	Ripon	Sandstone, shale	267–262 Ma
	Collingham	Shale, claystone, tuff, siltstones, sandstones	274–279 Ma
	Whitehill	Black carbonaceous shale, chert	275 Ma
	Prince Albert	Khaki shale, siltstones	280–275 Ma

The Lower Ecca Group comprises shale and chert shale beds with scattered ashes (Prince Albert Formation), black carbonaceous shales with pelagic organisms (Whitehill Formation) and interbedded mudstone and fine-grained sandstone succession with abundant intercalated ashes (Collingham Formation; Fildani et al., 2009; Hodgson et al., 2006). The consolidated thickness of the Prince Albert, Whitehill and Collingham Formations is approximately 1 300 m of the total thickness of the Ecca Group (Flint et al., 2011).

2.2.2.1 Prince Albert Formation

The Lower Permian Prince Albert Formation forms the lowermost unit within the Permian Ecca Group in the central and southwestern parts of the Main Karoo Basin (Mosavel & Cole, 2019). In the Main Karoo Basin, the Prince Albert Formation, which overlies the Dwyka Group, consists mainly of mudrocks (Johnson et al., 1996; Johnson et al., 1997) and has a

maximum thickness of 180 m (Danchin, 1970; Flint et al., 2011). The Prince Albert Formation is overlain by approximately 30 m of black carbonaceous claystone of the Whitehill Formation. This formation is mainly composed of claystone and cherty claystone beds with intertidal and supratidal carbonates (Flint et al., 2011) and dark grey to greyish-black and dark greenish-grey mudstone with subordinate sandstone in places (Mosavel & Cole, 2019). Nyathi (2014) subdivided the stratigraphy of the Prince Albert Formation in the study area into two members – lower and upper – comprising clay lithology (Table 2.3).

Table 2.3: Stratigraphic subdivision of the Prince Albert Formation (modified after Nyathi, 2014)

GROUP	FORMATION	MEMBER	UNIT NO	CLAY	THICKNESS (m)	SEDIMENTARY STRUCTURES	LITHOLOGY
ECCA GROUP	Prince Albert Formation	Upper Member	2		15.1	Lamination Folding	• Folded and well-laminated dark grey shale. • The colour of the shale is reddish-brown due to weathering of iron-bearing minerals. • Lenticular siltstone beds are found intercalated within the shales. • The siltstone is also folded due to tectonic movement.
		Lower Member	1		104.9	Lamination Crumbling Thin Bedding	• The Member is made up of thin-bedded and well-laminated dark grey shale. • The shale has been obscured by a khaki colour due to weathering. • The khaki colour typifies the rocks at the bottom of the Prince Albert Formation. • The shale is strongly crumbled due to fine grain size and purer clay mineral content. • The Formation disconformably overlays the Dwyka Group diamictite and is also disconformably overlain by the Whitehill Formation. • It is rich in soft clay minerals and crumbled due to lamination.

Visser (1992) on the other hand, subdivided the Prince Albert lithostratigraphy into five units based on the lithological description in ascending order (Figure 2.4);

- Mudstone-shale facies with minor claystone breccia, wacke and chert; chert pinches out southward, while dolomitic limestone content increases northward.
- Chert shale facies are composed of reddish markers and abundant pyrite.
- Greenish-grey shale-chert facies are made up of phosphorite in the south; dolomitic limestone content increases northwards and chert pinches out towards the north.
- Olive-grey micaceous shale facies consist of phosphorite in the south.
- Dark grey shale-phosphorite facies consist of carbonaceous and dolomitic limestone, pyrite and tuffaceous beds.

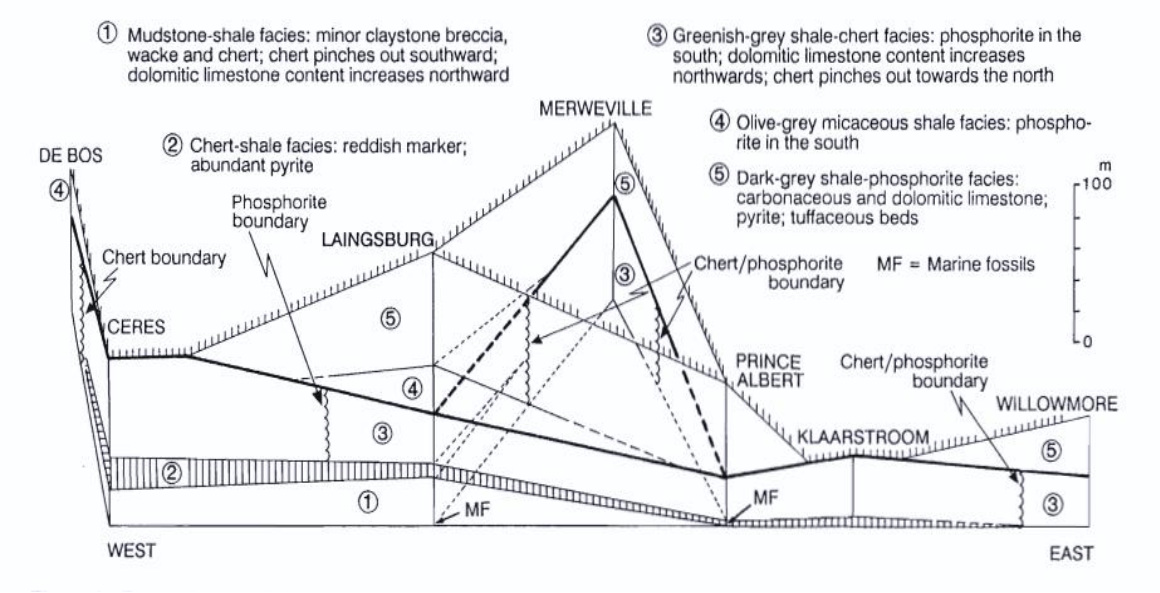


Figure 2.4: Five lithofacies of the Prince Albert Formation along the southern basin margin (Visser, 1992)

2.2.2.2 Whitehill Formation

The Whitehill Formation is contained in the lower part of the Permian Ecca Group which forms part of the Late Carboniferous-Early Jurassic Karoo Supergroup. The formation is made up of diagenetic carbonate, chert and phosphate concretions which vary from spherical and ellipsoidal to tube-like bodies within the shales (Smithard et al., 2015). The Whitehill Formation is 21 m thick and is regarded as a marker horizon consisting of carbonaceous shale.

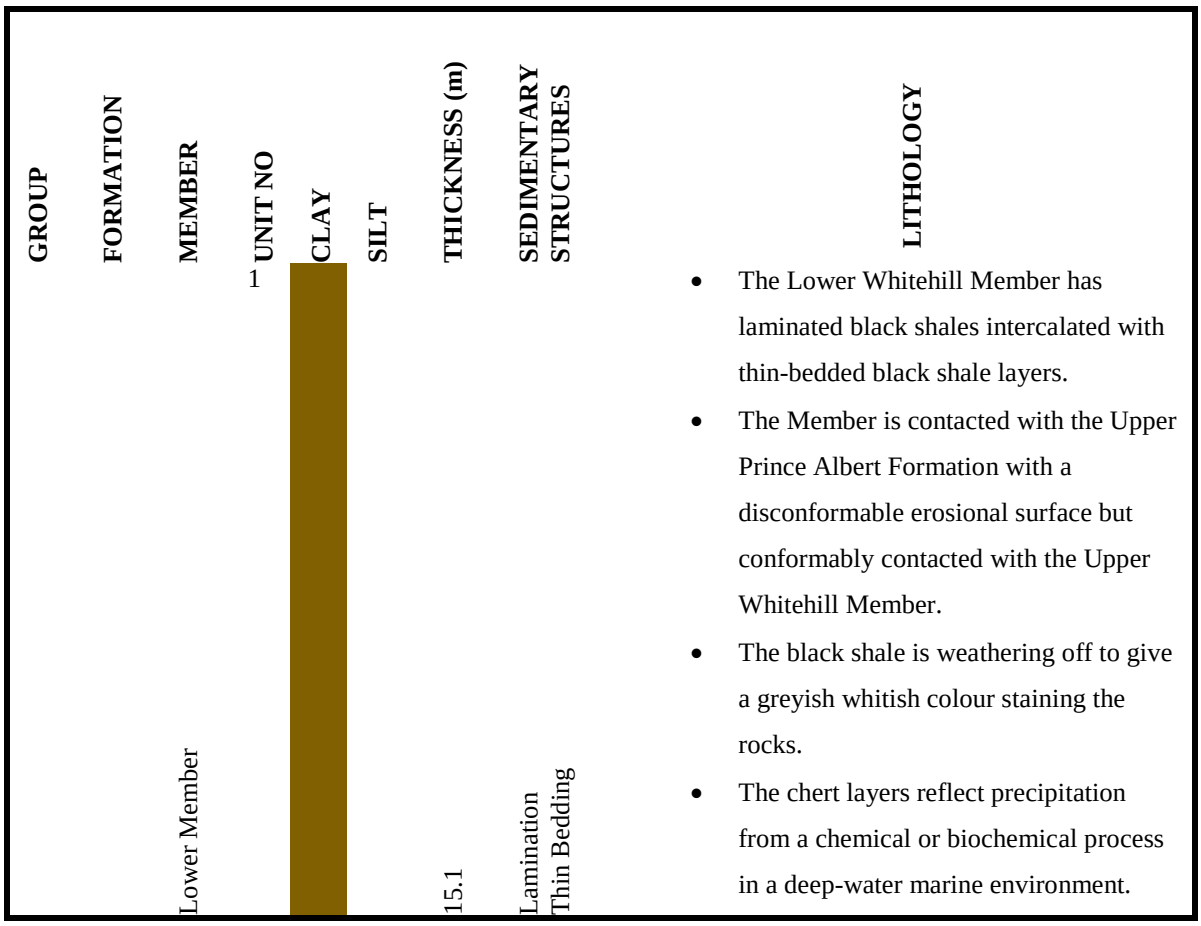
Folding and faulting are major sedimentary structures of the Whitehill Formation (Kingsley, 1981).

The transitioning between the Prince Albert and Whitehill Formations involves a thin upward-coarsening sequence grading from carbonaceous mudrock into silty shale (Johnson et al., 1997). The mudrocks/black carbonaceous shales of the Whitehill Formation weather white due to the diagenetic alteration of the sulphur (pyrite) content of the sulphates (Smithard et al., 2015), making it a useful marker during field mapping as it is easily distinguishable from the underlying and overlying shale units (Johnson et al., 1996; Johnson et al., 1997; Visser, 1992).

Lithologically, the formation can be subdivided into deep-water facies characterised by chert and carbonate concretions and shallow water facies characterised by numerous silty horizons and subordinate carbonate beds; chert is noticeably absent (Visser, 1992). Based on the lithologic characteristics, the Whitehill Formation can be divided into lower and upper members composed of clay and silt (Table 2.4; Nyathi, 2014).

Table 2.4: Stratigraphic subdivision of the Whitehill Formation (modified after Nyathi, 2014)

GROUP	FORMATION	MEMBER	UNIT NO	CLAY	SILT	THICKNESS (m)	SEDIMENTARY STRUCTURES	LITHOLOGY
Ecca Group	Whitehill Formation	Upper Member	2			10.1	Lamination Thin Bedding	• The Upper Whitehill Member is separated from the lower part by a normal fault line. • Grey well-laminated shale and thin-bedded fine to silt grained mudstone are the constituent rocks. • Minor chert layers are also found and are very short and thin compared to those at the bottom of the formation. • Minor chert and the weak grey colour of the rocks are evidence of very little organic matter at the time of the deposition of terrigenous sediments.



2.2.2.3 Collingham Formation

According to Flint et al. (2011), the Collingham Formation is composed of dark carbonaceous claystone interbedded with thin-bedded siliciclastic turbidites with a high concentration of ash beds. The formation comprises a rhythmic alternation of thin ultra-tabular beds (average 5 cm) of hard, dark grey, siliceous mudrock and very thin beds (average 2 cm) of softer yellowish tuff (Johnson et al., 1997; Kingsley, 1981). The thickness of the Collingham Formation is between 30 m and 70 m (Johnson et al., 1997; Flint et al., 2011). The sedimentary structures observed include laminations, cross-laminations, thin-medium bedding and ripple laminations (Table 2.5; Nyathi, 2014).

Table 2.5: Stratigraphic subdivision of the Collingham Formation (modified after Nyathi, 2014)

GROUP	FORMATION	MEMBER	UNIT NO	CLAY	SILT	THICKNESS (m)	SEDIMENTARY STRUCTURES	LITHOLOGY
Ecca Group	Collingham Formation	Upper Member	2			35.1	Cross Lamination Convolute Bedding Ripple Lamination Lamination Thin Bedding Medium Bedding	• Dark-black rhythmite. • Well-laminated claystone alternating with thin to medium bedded mudstone. • All the rocks are originally dark-greyish in colour; however, the claystone layers have adopted a weathered pale yellowish colour due to the weathering and purer clay content. • The claystone and mudstone constitute multiple cyclotherms of repeated couplets called rhythmite, similar to classic flysch or turbidite deposits. • The characteristics of the grain size, dark colour, lamination structure and rhythmite cycles reflect lower energy in a deeper marine depositional environment. • The rhythmite probably was formed on or near the continental slope area. • The rhythmite is well jointed and has both vertical and horizontal joints. • Convolute bedding and recumbent bedding are also typical of the continental slope setting. • Thin-bedded fine mudstone and siltstone with well-laminated shale conformably overlaying the Whitehill Formation.
		Lower Member	1			20.1	Lamination Thin bedding	

2.2.2.4 Ripon Formation

The Ripon Formation is generally 600–700 m thick. It consists of poorly sorted, fine to very fine-grained lithofeldspathic sandstone alternating with dark grey clastic rhythmite and mudrock (Woodford et al., 2003). The Ripon Formation is subdivided into three members: Pluto's Vale (alternation of sandstone and shale), Wonderfontein (mainly shale) and Trumpeters (alternation of sandstone and shale, mainly shale). The Pluto's Vale Member is the lowest stratigraphic member of the Ripon Formation and overlies the Collingham Formation (Kingsley, 1981; Walters & Tucker, 2020). This formation contains dark grey, fine to very fine-grained feldspathic sandstones interbedded with rhythmites along with mudrocks (Johnson, 1976). The sedimentary structures include graded bedding, convolute lamination, bouma sequence, groove cast and slumping (Kingsley, 1981).

The presence of clay clasts in the sand, load cast structures and convolute lamination indicate that the deposition rate of the turbidites was fast (Kingsley, 1981). The formation consists of poorly sorted medium to fine-grained sandstone, alternating with siltstones and shales and occurring at a depth between 1 000 and > 3 500 m in the southern part of the Karoo Basin. The Ripon Formation contains siltstone and three distinct sandstone lithologies: very fine-grained sandstones, fine-grained sandstones and medium-grained sandstones (Campbell et al., 2016).

2.2.2.5 Fort Brown Formation

The initial stage of sedimentation of the Fort Brown Formation was characterised by slow mud deposition but, subsequently, a fast regression occurred and a typical coarsening-upward sequence was formed (Kingsley, 1981). Individual laminae and beds in the Fort Brown Formation are either poorly laminated or massive in the lower part of this formation and well-laminated and graded in the upper part. This formation is 670 m thick. The Fort Brown Formation consists of rhythmite and mudrock with minor sandstone intercalations and displays an overall coarsening-upward tendency (Woodford et al., 2003).

2.2.2.6 Waterford Formation

The Waterford Formation (Upper Ecca) conformably overlies the Fort Brown Formation. This formation varies from 150 m to 580 m in thickness and is more arenaceous than the underlying

formation. The lithofacies of the Waterford Formation are mostly arenaceous (Rubidge et al., 2000). Dominant lithologies include fine greyish to khaki, massive lithofeldspathic sandstones or wackes and dark grey mudrock (Figure 2.5). The lithologies show well-developed wave-rippled bedding planes and extensive evidence of soft-sediment deformation including spectacular ball-and-pillow load structures and chaotic slump facies. The delta-top sediments of the Waterford Formation can be distinguished from the conformably overlying Lower Beaufort Group fluvial succession based on sedimentological characteristics. The sedimentological characteristics include, among others, the predominance of upward-coarsening, sandstone-dominated packages, thin-bedded rhythmites, common large-scale wave ripples, ball-and-pillow and chaotically slumped horizons (Almond, 2016).



Figure 2.5: Thin-bedded wave-ripple wackes in the Waterford Formation (Almond, 2016)

2.2.3 Beaufort Group

The Beaufort Group is subdivided into the Adelaide and Tarkastad subgroups (Van der Walt et al., 2010). The subgroups are distinguished by a greater sandstone-to-mudstone ratio (Rutherford et al., 2015). The fluvio-lacustrine sedimentary rocks of the Beaufort Group were deposited within the Main Karoo Basin of South Africa between the Middle Permian and the Early Triassic (Day & Rubidge, 2014). The upper sedimentary units of the Beaufort Group

(Tarkastad Subgroup) include predominantly thick sandstones of approximately > 10 m beds of the Katberg Formation (Lanci et al., 2013). The coarser-grained rocks are found near the CFB, while mudstone, shale and fine-grained sandstones dominate the central and northern part of the basin (Woodford et al., 2003). The rocks of the Beaufort Group of the Karoo Supergroup cover approximately 60% of the surface of South Africa and comprise an approximately 3 000 m thick succession of sedimentary rocks that are richly fossiliferous (Van der Walt et al., 2010).

2.2.4 Stormberg Group

The Stormberg Group is subdivided into three main formations, in ascending order: the Molteno, Elliot and Clarens Formations. The thickness of the Molteno Formation varies from less than 10 m to over 100 m. This formation is characterised by light coloured sandstones which consist of moderately to poorly sorted and sub-rounded to subangular grain shapes. The contact between the Molteno Formation and the underlying Beaufort Group is sharp, while the upper contact with the Elliot is gradational (Eriksson, 1984).

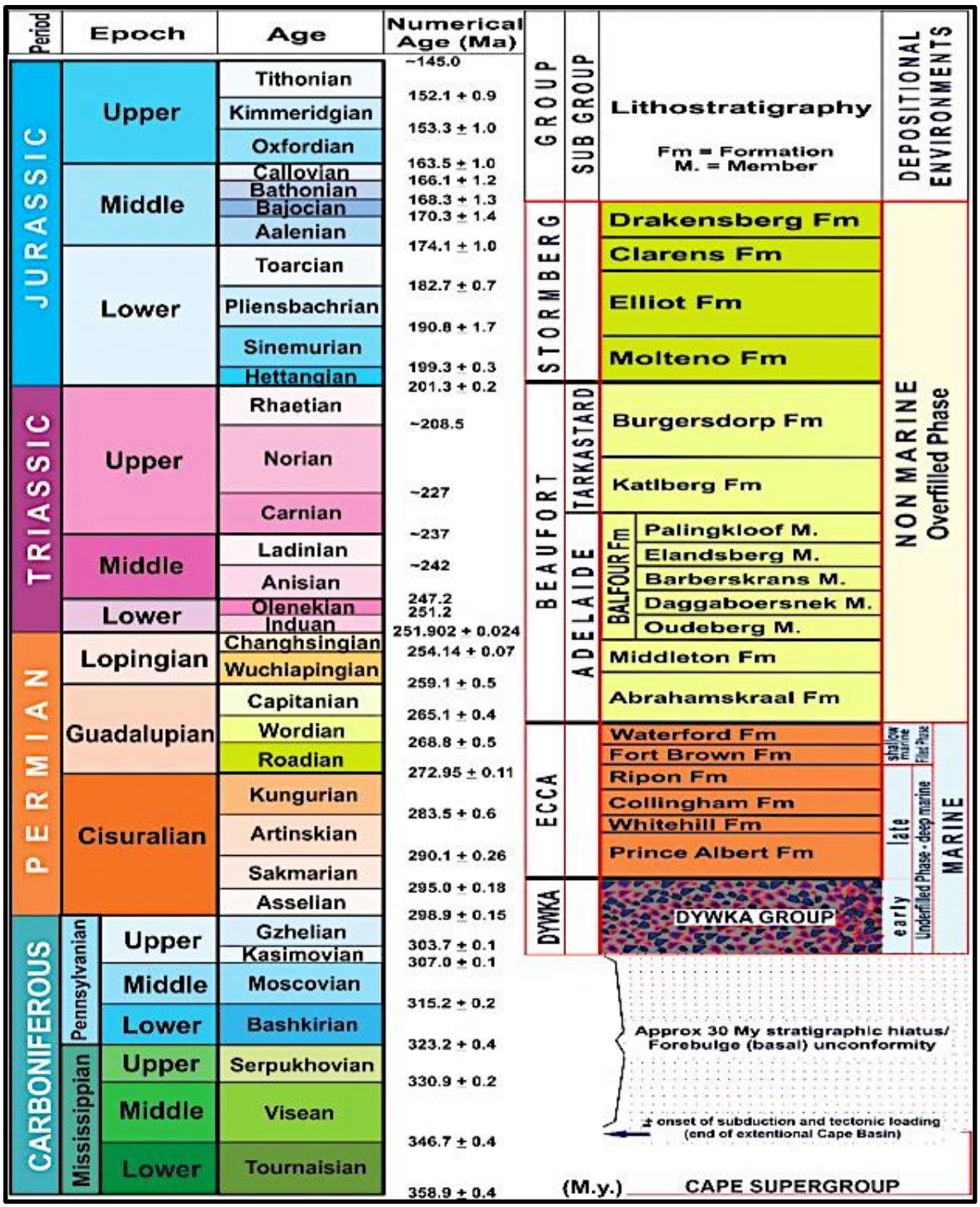
The youngest unit of the Stormberg Group, the Lower Jurassic Clarens Formation is characterised by the presence of white, cream or pink fine-grained sandstone and silty sandstone beds. The Clarens Formation is the uppermost sedimentary rock unit in the Karoo Supergroup and has thickly bedded sandstones with a variable thickness ranging from 10 m to 300 m (Bordy & Head, 2018). The age of the Elliot Formation in the Main Karoo Basin ranges from Late Triassic to Early Jurassic. The sandstones are mainly fine to medium-grained. The Elliot Formation shows no lateral transitions into either the underlying Molteno or overlying Clarens Formations (Bordy & Eriksson, 2015).

2.3 Depositional environments

Depositional environments vary geographically in the Karoo Basin (Table 2.6) and range from marine to lacustrine for the Dwyka to Lower Ecca Groups of southern Africa (Herbert & Compton, 2007). The Karoo Basin of South Africa represents about 100 million years of sedimentation, from ca. 280 Ma to ca. 180 Ma. The deposition of Karoo sedimentary rocks occurred during the Late Carboniferous period across Gondwana and continued until the

beginning of the breakup of this supercontinent during the Middle Jurassic period (ca. 183 Ma; Geel et al., 2013).

Table 2.6: Geologic age and depositional environments of the Karoo Supergroup (Adeniyi, 2016)



The order of deposition of the sedimentary mega-succession Karoo Supergroup is as follows: the Dwyka Group (Westphalian to Early Permian), containing glaciogenic deposits; the Ecca Group (Permian), a siliciclastic sedimentary succession; and the Beaufort Group (Permo-Triassic), containing fluvial deposits (Fildani et al., 2009; Flint et al., 2011; Hodgson, 2006; Johnson et al., 2006). The lower part of the Karoo Sequence (Dwyka, Ecca and Beaufort Formations) was deposited during the Permian and Early Triassic. The upper part of the sequence, the Stormberg (Molteno, Elliot and Clarens Formations) and the Drakensberg groups, was separated from the lower Karoo by a lacuna that occupied the entire Middle Triassic (Veevers, et al., 1994).

The stratigraphic column of the Karoo Supergroup (Table 2.6) shows that the glacial diamictite and shale of the Dwyka Group were deposited during the Late Carboniferous and Early Permian. The overlying Ecca Group, which is characterised by marine and deltaic shale, mudstone and sandstone, was deposited during the Permian (Loock et al., 1994). The bottom upward Ecca Group succession indicates that the depositional environments gradually changed from the deep marine water environment (Prince Albert, Whitehill and Collingham Formations) to the deltaic environment (Ripon Formation) and then to the lacustrine environment (Fort Brown Formation). This means that the sedimentary basin was gradually filling up with sediments and the water depth of the basin was gradually shallowing (Nyathi, 2014).

According to Geel and Bordy (2021), the deposition of the lower Prince Albert Formation fluctuated between marine and fresh-water conditions due to repeated episodes of meltwater influx in the western part of the Main Karoo Basin. The Rb/K ratios indicate that the depositional environments of the Whitehill and Collingham Formations were predominantly marine. The V/Cr ratios indicate anoxic to dysoxic conditions for the Prince Albert Formation and dysoxic to oxic conditions for the Whitehill and Collingham Formations. The depositional environment in the eastern Main Karoo Basin suggests that salinity conditions fluctuated and were not fully marine.

2.3.1 Prince Albert Formation

The Prince Albert Formation forms the lowermost unit within the Permian Ecca Group in the central and southwestern part of the Main Karoo Basin. The sedimentation of the Prince Albert

Formation is associated with a major transgressive event following the final melting of the Dwyka Group ice sheets (Mosavel & Cole, 2019). The presence of pyrite indicates that the depositional environments changed from brackish in the Prince Albert to marine in the Whitehill Formation and marine to brackish in the Collingham Formation (Nolte et al., 2019).

The presence of thinly bedded shale, mudstone, claystone breccia, silty rhythmite and fine-grained wacke in the Prince Albert Formation suggests deposition by sediment gravity flow and subordinate suspension setting (Visser, 1992). The Prince Albert Formation mudrocks reflect the suspension setting of mud deposited in a marine environment (Johnson et al., 1997). The rocks of the Prince Albert Formation contain almost no clastic input, yet they were deposited in relatively shallow water. This indicates the absence of a clastic source area and supports the absence of the CFB during this time (Flint et al., 2011).

2.3.2 Whitehill Formation

The thinly laminated Whitehill shales are formed by the slow suspension settling of mud, whereas the interbedded siltstone and sandstone were deposited by tractional bottom currents in a shallow environment as shown by cross-bedding and ripple lamination (Visser, 1992). The marine Whitehill Formation is characterised by black, laminated, carbonaceous shales deposited largely from suspension setting under anoxic bottom conditions (Flint et al., 2011; Johnson et al., 1997) and was deposited as black organic muds (Visser, 1992).

Black et al. (2016) proposed that, after the deposition in an intertidal marine/terrestrial environment, the formation – as part of the lower Karoo Supergroup – underwent shallow to intermediate burial, resulting in the formation of illite/smectite, accompanied by the dissolution of grains. This was followed by the deeper burial of sediments, where compaction resulted in rock types of average density (2.06–2.67 g/cm^3). Based on the Rb/K ratios, the depositional environment for the Whitehill Formation in the western Main Karoo Basin suggests fully marine conditions (Geel & Bordy, 2021).

2.3.3 Collingham Formation

Facies of the Collingham Formation indicate relatively quiet conditions during the deposition of the greater part of the formation (Viljoen, 1994). The great lateral extent and fine-grained

character of individual beds reflect deposition from suspension in relatively deep water (Johnson et al., 1997). During the Collingham Formation deposition, sediments likely originated from nearby regions dominated by the Cape Supergroup and Cape Granite Suite (Geel & Bordy, 2021).

2.4 Shale mineralogy

Mineralogically, shales and mudstones contain minerals and other detrital minerals such as quartz, feldspar and other organic matter (Bennett et al., 1991). Some mudstones contain a high proportion of carbonate minerals, such as calcite or siderite, while some black shales contain a high proportion of organic matter (Merriman et al., 2003). The mineral composition of the Ecca Group includes quartz (monocrystalline quartz and polycrystalline quartz), feldspar (albite, microcline and orthoclase), micas (muscovite and biotite) and lithics (Baiyegunhi et al., 2019).

Shale is a combination of clay minerals – illite, kaolinite and chlorite, non-clay minerals – silica (quartz), and carbonate minerals – calcite or dolomite (Butt, 2012; Rodriguez et al., 2014). Illite is the most abundant clay mineral in shale (Butt, 2012). Shale often contains smaller amounts of other carbonates, pyrite and feldspars (Rodriguez et al., 2014). Shales may contain trace minerals and elements such as barite, celestine, siderite, arsenic, barium, molybdenum, uranium, vanadium and zinc (Rodriguez et al., 2014). These are the average percentages of different minerals in shale: clay (58%), quartz (28%), feldspar (6%), carbonates (5%) and iron oxide (2%; Pettijohn, 1975). The mineralogy of shale plays a significant role in how the formation can be fractured (Ratcliffe & Scmimdt, 2012).

Shale is a sedimentary rock, composed mainly of clay-sized mineral grains. Shale is also called mudrock and is formed from the compaction of at least 50% silt and clay-size particles. The characteristics of shale, mudstone, siltstone and slate may vary depending on their geological age and the extent to which they have been buried and altered by tectonic events (Butt, 2012). Shales tend to occur in geologically older rocks. They lack plasticity and have a well-developed slaty cleavage (Merriman et al., 2003). The mudstone and shale have been compacted and hardened by burial in thick sedimentary deposits (Merriman et al., 2003).

The mineral composition of shales dictates their chemical properties and is regarded as the main factor that determines their physical properties, especially relating to their stability and

cementing quality during the hydraulic fracturing process (Gąsiński, 2017; Haddad et al., 2017). In most cases, inadequate cementing is due to the presence of swelling clay layers (Karpiński & Szkodo, 2015). The type and amount of clay minerals determine the physical (i.e., permeability, fracability, wettability) and chemical properties of shale rocks (Dargahi, et al., 2013). In case the stimulation is accomplished by using fresh water, the clay content within the formation may swell and expand, which reduces the flow path areas against the fluid production (Haddad et al., 2017).

The understanding of the mineralogy of gas-bearing shale is crucial when planning a well drilling, stimulation and completion programme and also assists in locating a potential gas reservoir (Nicolas & Bamburak, 2009). The knowledge of the mineral composition of shales plays a significant role in identifying optimal proppants, fracture fluids and pumping schedules (Gąsiński, 2017). The presence and abundance of quartz and swelling clay minerals do not only indicate a unit's potential as an economic gas reservoir but also provide important information for planning a drilling programme (Nicolas & Bamburak, 2009).

It is also significant to understand the relationship between clay mineralogy and the physical parameters (permeability, fracability, wettability) required to develop a shale gas reservoir. The higher the number of clay minerals present, the lower the rock brittleness; a lower clay abundance is usually associated with improved reservoir permeability (Dargahi et al., 2013). The higher the quartz content, the better the rock will respond to hydraulic fracturing due to the brittle material. Similarly, the less swelling clay there is in the target zone, the less chance there is of formation damage during drilling (Zhang et al., 2013).

2.4.1 Prince Albert Formation

Mineralogically, the Prince Albert Formation consists predominantly of illite, kaolinite and halloysite (Ferreira, 2014). XRD analyses indicate that the Prince Albert Formation consists of quartz (52%), illite (21%), muscovite (23%), chlorite (4%) and pyrite (0.2%). The gradational contact between the Dwyka Group and the Prince Albert Formation has a mineralogical composition of quartz (53%), illite (21%), anorthite (8%), muscovite (15%), chlorite (3%) and pyrite (0.2%; Geel et al., 2015).

2.4.2 Whitehill Formation

The Whitehill Formation shales comprise mostly clays such as illite (Geel et al., 2013), smectite (in the form of montmorillonite), muscovite and quartz (Ferreira, 2014; Geel et al., 2015) and contain both framboidal and euhedral pyrite grains (Geel et al., 2013). The formation consists mostly of black shales that are occasionally interlayered with grey, fine-grained siltstone layers (Geel et al., 2015). The Whitehill Formation is a white weathering black shale with dolomite concretions at the base of the formation (Geel et al., 2013). The shales weather white due to an oxidation reaction among their pyrite, dolomite and calcite content to form gypsum growth in veins. Pyrite within shales also creates oxidation staining and the weathered shales vary in surface colouration from white to grey and pink (Geel et al., 2015). The XRD analyses undertaken on the Whitehill Formation showed the following minerals: quartz (32%), calcite (6%), albite (7%) and dolomite (9%; Geel et al., 2015).

2.4.3 Collingham Formation

The clay minerals of the Collingham Formation consist mainly of illite and kaolinite (Ferreira, 2014). Under the light microscope, the boundaries between clay minerals and tuffs can be observed. The SEM analysis revealed that framboidal pyrite occurs close to contact with the Whitehill Formation (Geel et al., 2015). The Collingham Formation mineral composition is as follows: quartz (62%), calcite (2%), albite (10%), muscovite (10%), chlorite (8%), biotite (3%), illite (13%) and pyrite (0.3%; Geel et al., 2015).

2.5 Geochemistry of shales

One of the objectives of this study is to determine the geochemical signatures of the source rock for major and trace elements to assess the characteristics of the shales from the study area. The geochemical technique is an important tool in the exploration of natural gas. One of the important features of shale gas production is the ‘fracability’ of the formations being drilled. The fracability of these formations is controlled by the organic and inorganic composition of the sediments (Ractliffe & Schmidt, 2012). The mineralogical and chemical characteristics of shale are controlled by the properties of the parent rock and the depositional environment (Okeke & Okogbue, 2011).

Geochemistry is divided into organic (carbon-bearing) and inorganic subdisciplines (Olatunde, 2011). According to Ratcliffe and Schmidt (2011), organic geochemistry techniques can be powerful tools to locate ore bodies and identify unique organic signatures such as the source, age, thermal maturity, depositional environment and degree of biodegradation of organic matter contained in sedimentary rocks (Olatunde, 2016). Inorganic geochemical techniques provide the mineralogical composition of shale, relative and absolute ages of mineral growth and dissolution, the presence and migration of fluids and temperatures at which minerals grew or dissolved (Finlay & Martin, 2013).

Elements such as Y, Zr, Nb, Hf, Ta, Th and U are associated with heavy minerals, such as zircon, which are resistant to weathering (Nyakairu & Koeberl, 2001). Selected trace elements such as La, Ce, Nd, Y, Th, Zr, Hf, Nb, Sc, Co and Ti are immobile sedimentary processes (Bhatia & Crook, 1986). Ni and V are highly concentrated in the organic material of marine shales, while Pb, Zn, Cu and Sn are most abundant in fresh-water shales. The concentrations of B, Li and Rb are high in marine shales (Degens et al., 1957), while the non-marine shales are high in Ga (Degens et al., 1957; Tourtelot, 1964).

The average elemental composition of Ba, Th, Zr, La, Ce, Nd, Sm, Tb, Tm, Yb, V and Cr is higher in immature shales compared to mature and post-mature shales. Post-mature shales have elevated concentrations of U, Sr and Co and higher inorganic carbonate content which may increase Sr content in the shales (Abanda & Hannigan, 2006). Black shales are often rich in organic matter and trace elements such as Co, Cr, Cu, Mo, Ni, V, Mn and Zn (El-Anwar, 2017).

2.5.1 Organic geochemistry

Organic geochemical data indicate that the average TOC content of shale in the Prince Albert Formation is 0.37 wt.%, in the Whitehill Formation ~5 wt.% and the Collingham Formation 0.62 wt.% (Geel et al., 2015; Geel et al., 2021). Gas reservoirs are considered to have resource potential when TOC values in shales are generally above 2%. The Prince Albert and Collingham Formations do not qualify as a source rock for natural gas because TOC values are < 1% (Black et al., 2016).

TOC average values are 4.5% in the Whitehill Formation, making it the prime focus for potential shale gas prospects (Geel et al., 2013). The TOC of shale varies between 0.11 and

2.32 wt.% with an average of 0.52 wt.%. The TOC analysis shows high values in the carbonaceous shales of the Whitehill Formation. The values obtained in the Prince Albert Formation are significantly lower than that of those in the Whitehill Formation, while the Collingham Formation shows the lowest values, which could be an indication of the oxidation of organic matter in the outcrop. In addition to oxidation, a decrease in TOC values may also be a result of thermal maturation (Ferreira, 2014).

2.5.2 Inorganic geochemistry

Inorganic geochemical characteristics within the Lower Ecca Group indicate that SiO_2/Al_2O_3 ratios are highest in the Prince Albert Formation and lowest in the Whitehill Formation. CaO and MgO peaks, which correspond with the occurrence of carbonate rock, occur in the Whitehill Formation (Geel et al., 2015). The chemical analyses show that the Collingham Formation is silica-rich and very low in organic carbon. These two properties suggest that the Collingham Formation is more brittle and easily fractured than the underlying carbon-rich Whitehill Formation (Black et al., 2016).

Geochemical signatures in the southern Karoo indicate that the black shales are variably enriched with SiO_2 relative to Al_2O_3 and CaO, indicating detrital sources. Elements such as CaO and P_2O_5 have a negative correlation with Al_2O_3 suggesting that they are from a biogenic source. Increasing Zr and Hf abundance up the stratigraphic succession suggests an increase in felsic content with time (Andersson et al., 2004). The geochemical study of sandstones and shales from the Ecca Group indicates that their trace element data are generally comparable with the trace element data of upper continental crust (UCC) and Post-Archean Australian Shale (PAAS). The concentration of high field strength elements (HFSE) such as Hf, Zr and SiO_2 are higher in sandstones than in shales (Baiyegunhi, 2015; Baiyegunhi et al., 2017b). The source provenance ratios suggest that the sediments are from felsic source rock (Maake, 2018).

2.6 Previous studies on Ecca Group mineralogy and geochemistry

The geochemical analysis of the sandstones and shales from the Ecca Group in the Eastern Cape Province indicates a high concentration of SiO_2. The concentrations of Al_2O_3, CaO and Fe_2O_3 are moderately high, while the concentrations of TiO_2, MnO, MgO, Na_2O, K_2O and P_2O_5 are generally low. The sandstones in the area are higher in SiO_2 content when compared

to the shales. Generally, shales have higher Ce, Cu, Ga, La, Nb, Nd, Rb, Sc, Sr, Th and Y content than sandstones. The sandstones are higher in Hf and Zr than the shales. It is suggested that the high Sr content in shales indicates that Sr may be associated with calcite minerals. Mineralogically, the shales are dominated by kaolinite (Baiyegunhi et al., 2017a).

The lithology of the Lower Ecca formations of the Jansenville area indicates calcite veins, pyrite, quartz and micaceous minerals. This, however, indicates different diagenetic processes from the Prince Albert to the Collingham Formations in relation to pyrite and carbonates. The big grains of pyrite and carbonate concretions and calcite veins observed within the Whitehill Formation are thought to be associated with organic-rich sediments. The carbonates consist of dolomite and calcite. Calcite occurs mainly as a cement in pores and grain replacement and calcite veins are common in the Whitehill Formation. The shales consist of discontinuous, wavy and straight parallel laminae. These shales exhibit different degrees of trace element enrichment relative to global average shale, the approximate order being Pb > V > Zn > Cr > Cu > Co > Ni (Maake, 2018).

Mineralogically, the clay minerals of the Prince Albert, Whitehill and Collingham Formations consist mainly of illite, kaolinite and smectite derived from a combination of the weathering of feldspars and pyroclastics as well as the alteration of other clay minerals. The clays of the Whitehill Formation consist mainly of smectite and muscovite. The clay minerals of the Collingham Formation consist mainly of illite and kaolinite (Ferreira, 2014).

The carbonaceous shales of the Whitehill Formation show high TOC values, while these values are significantly lower in the Prince Albert Formation. The Collingham Formation has the lowest TOC values and could be an indication of the oxidation of organic matter. Sedimentological investigation reveals that the upper Prince Albert Formation is dominated by shale with thin beds of carbonate and the Whitehill Formation consists mainly of carbonaceous shale with relatively more resistant shale beds (Ferreira, 2014).

The study indicates that the petrology of the Ecca Group is mainly alterrigenous rocks with an absence of conglomerates. The study also indicates that there are no carbonate rocks in the Ecca Group. Mineralogically, feldspar, quartz and micas occur as major minerals in the rocks. Clay minerals include kaolinite, smectite, illite and sericite. Accessory minerals include hematite, rutile and zircon (Nyathi, 2014).

CHAPTER 3: METHODOLOGY AND INSTRUMENTATION

This chapter presents the research methodology and data collection techniques – desktop study, fieldwork and laboratory work. The first stage of the methodology involved analysing the existing data by reviewing the literature; field and laboratory work complemented the literature analysis. This chapter introduces the four analytical methods used for this study. These include petrographic microscopy, XRD, XRF and ICP-MS.

3.1 Desktop study

A desktop study involves a preliminary investigation and involves collating available relevant data such as that from previous studies on the Karoo Supergroup and additional work that has been carried out in the study area for correlation purposes.

3.2 Fieldwork

Fieldwork was carried out during the dry season, July to August 2019. This involved a visual inspection of the rocks before sample collection. Rock texture, fabric, colour, variations in grain size and lithology were carefully observed and the data were recorded. Samples were collected from the three formations in the Lower Ecca Group. Different sedimentary features were described, measured and photographed. The equipment included a camera, geological hammer, field book, hand lens, clinorule, tape measure, sample bags, maps and global positioning system (GPS).

Sampling was somewhat random and some sequences received more attention than others. The main criteria used to select the sampling point is the colour of the rock (dark), which often indicates an increased amount of organic carbon. Lavelle (2014) indicates that the colourations of shales differ based on the minerals present and the carbon content of the rock.

Twelve samples were selected to represent the Lower Ecca Group from the three formations along the R67 route between Grahamstown and Fort Beaufort in the Eastern Cape Province. Samples 1 to 4 were taken from the Prince Albert Formation. Samples 5 to 8 represent the Whitehill Formation, while samples 9 to 12 were taken from the Collingham Formation. A

geological map covering Grahamstown (Sheet No: 3326), at a scale of 1:250 000, was predominantly used to locate the three lower formations of the Ecca Group. Additionally, a base map was used to provide fundamental/geographic information of the study area. The white band (Whitehill Formation) was used as a marker horizon because it is distinguishable from other formations. The sampling coordinates range between 26° 37′ 38.5″ E and 33° 12′ 8.2″ S.

3.3 Laboratory analysis

The mineralogical and geochemical analyses for this study were obtained using XRD, petrographic microscopy, XRF and ICP-MS. The preparation and analyses of the samples were carried out in the laboratories of the University of the Witwatersrand in Johannesburg and at XRD Analytical Consulting located in Pretoria. The laboratory work was organised into four main parts: sample preparation, analysing mineral composition, interpretation of petrographic properties and geochemical analysis of major and trace elements.

3.3.1 Sample preparation

Sample preparation involves crushing and milling the samples according to geochemical sample preparation procedures. Before crushing and milling the samples, the surfaces of the jaw crusher (Figure 3.1) were cleaned with a wire brush, toilet towel and acetone. A vacuum was used to remove the excess paper towel. A dry sample weighing no more than 250 g was crushed. Jaw crushed samples were milled (powdered) by placing the sample in a milling machine. The milling machine was decontaminated by placing a scoop of cleaning quartz in it and milling for 30 seconds. The milled samples were split and used for XRD, XRF and ICP-MS analyses. The sample preparation process was carried out in the laboratories of the School of Geosciences at the University of the Witwatersrand in Johannesburg.

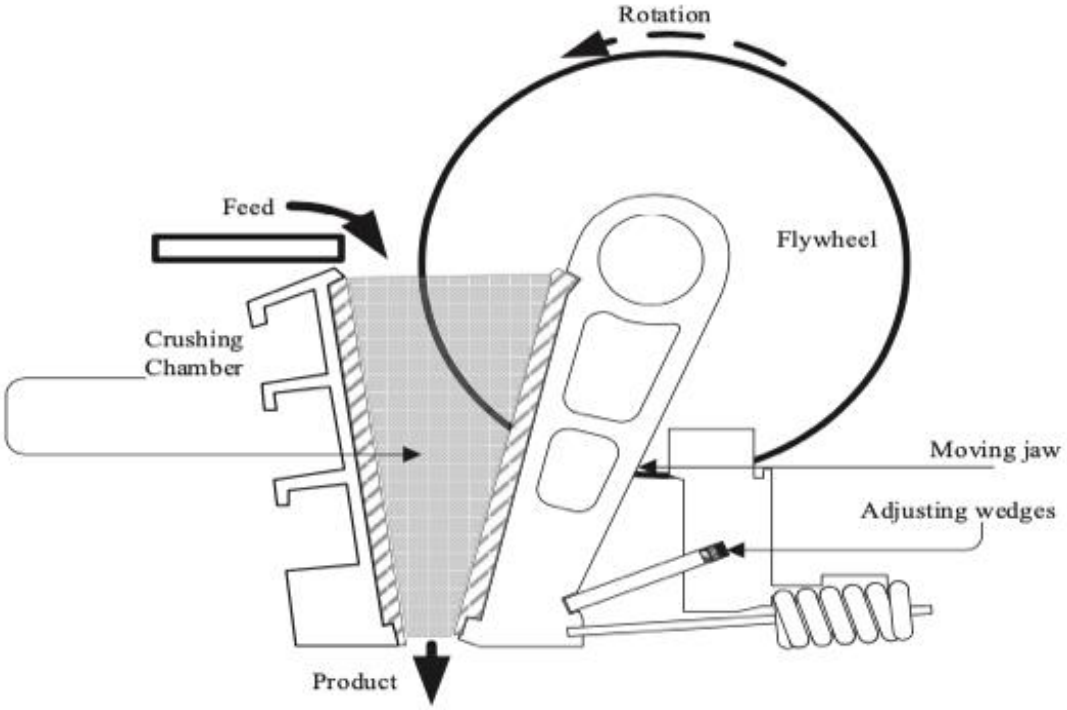


Figure 3.1: Schematic illustration of a jaw crusher (Johansson, 2019)

3.3.2 Petrographic microscope

The preparation of thin sections was carried out in the Thin Section Preparation Laboratory of the School of Geosciences at the University of the Witwatersrand in Johannesburg. The optical microscope was provided by the University of the Witwatersrand and examination of the thin sections was performed in the Microscopy Teaching Laboratory of the School of Geosciences. Twelve petrographic thin sections were prepared and examined under plane polarised light and cross polarised light to provide detailed descriptions of the samples.

To produce a thin section from the rock sample, an area to be cut was marked. The samples were cut perpendicular to the bedding. The rock sample was cut into a smaller rectangular shape and glued onto a glass microscope slide (Figure 3.2). The photomicrographs were captured using a camera integrated with a stereo microscope (Figure 3.3).



Figure 3.2: Thin sections preparation procedure (Paulsen et al., 2013)

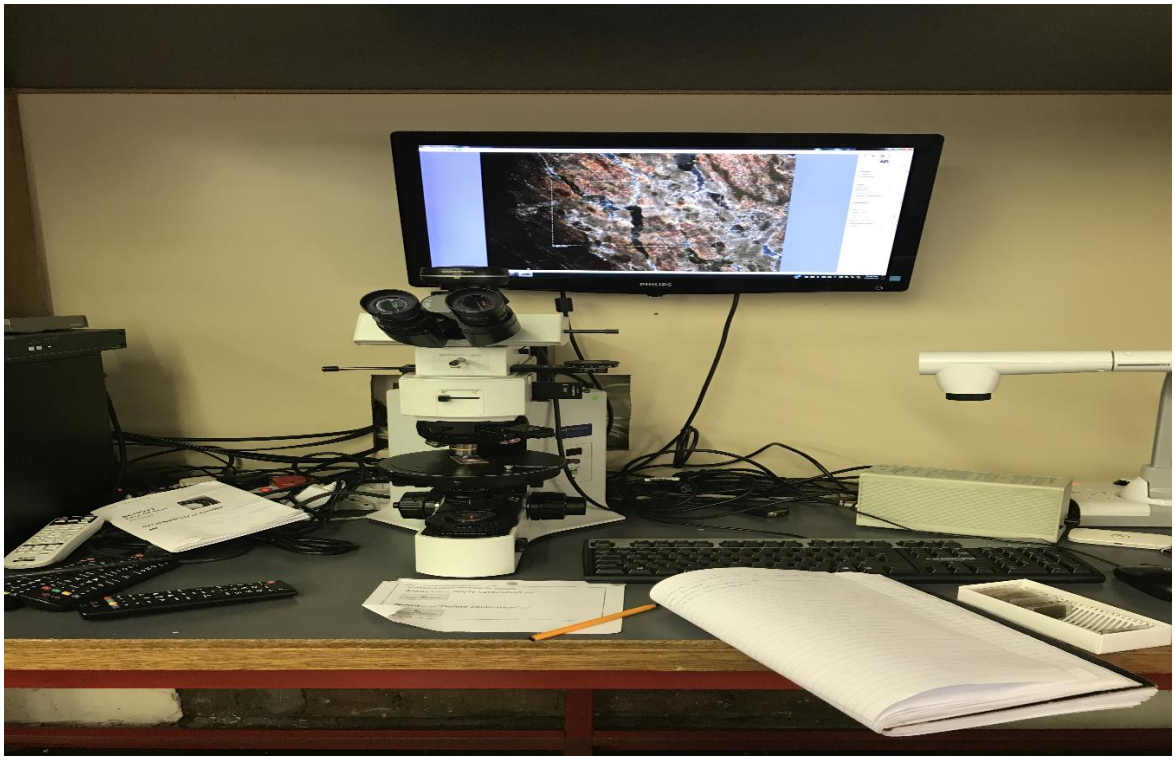


Figure 3.3: Petrographic microscope attached with camera for photomicrography (Photo by the Author)

Scholle and Ulmer-Scholle (2003) emphasised that many minerals commonly found in shale can be identified in thin sections either by reflected light or by transmitted light (polarised or cross polarised) using a petrographic microscope. Clays are found in the matrix of shale samples and appear as very fine-grained crystals with low interference colours. Quartz usually appears as a flat, light to medium grey mineral with rounded edges that display undulatory extinction (Rodriguez et al., 2014).

3.3.3 X-ray diffraction

XRD is the principal tool used to identify and characterise clay and non-clay minerals in shales. Each crystalline phase has a unique powder diffraction pattern which makes it possible to distinguish between compounds. The samples were run on a Malvern Panalytical Aeris diffractometer. This diffractometer is equipped with a pixel x-ray detector and fixed receiving slits with Fe filtered Co-Ka radiation (Figure 3.4). The phases were identified using X'Pert High Score Plus software. The mineral abundance in the samples or relative phase amounts (weight %) were quantified using the Rietveld method. The XRD tests were performed in the laboratories of XRD Analytical and Consulting in Pretoria.

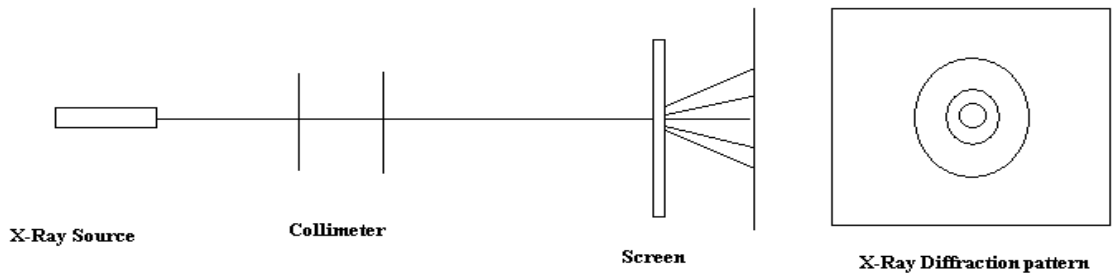


Figure 3.4: Schematic diagram of X-ray diffraction pattern (Butt, 2012)

Using whole-rock geochemical data, relative rock brittleness value can be defined. However, the calculations of mineralogy and brittleness are not as accurate as when direct measurements techniques such as XRD are used (Ratcliffe & Schmidt, 2012). X-ray powder diffraction is the best available technique for the identification and quantification of all minerals present in clay-rich rocks (Środoń et al., 2001). Rock samples of around 50 g are required for most of the analyses (Mowzer, 2012). The application of XRD covered the identification of minerals, characterisation of crystalline materials and identification of fine-grained minerals such as clays and mixed layer clays that are difficult to determine optically (Brady et al., 1995).

3.3.4 X-ray fluorescence

The analysis of the major elements in the studied samples was carried out using an XRF spectrometer (panalytical; Figure 3.5). The analysis was performed in the Earth Laboratory located within the Bernard Price Building of the University of the Witwatersrand in Johannesburg. XRF analysis provides high precision and accuracy, relative ease of use and fast sample preparation. The rock samples were ground into a fine powder before analysis to achieve greater homogeneity in the sample. The powder sample was ignited to about 1000 °C for at least an hour to eliminate the volatile components (Tamponi, Bertoli, Innocenti & Leoni, 2003) and loss on ignition was measured for the studied samples.

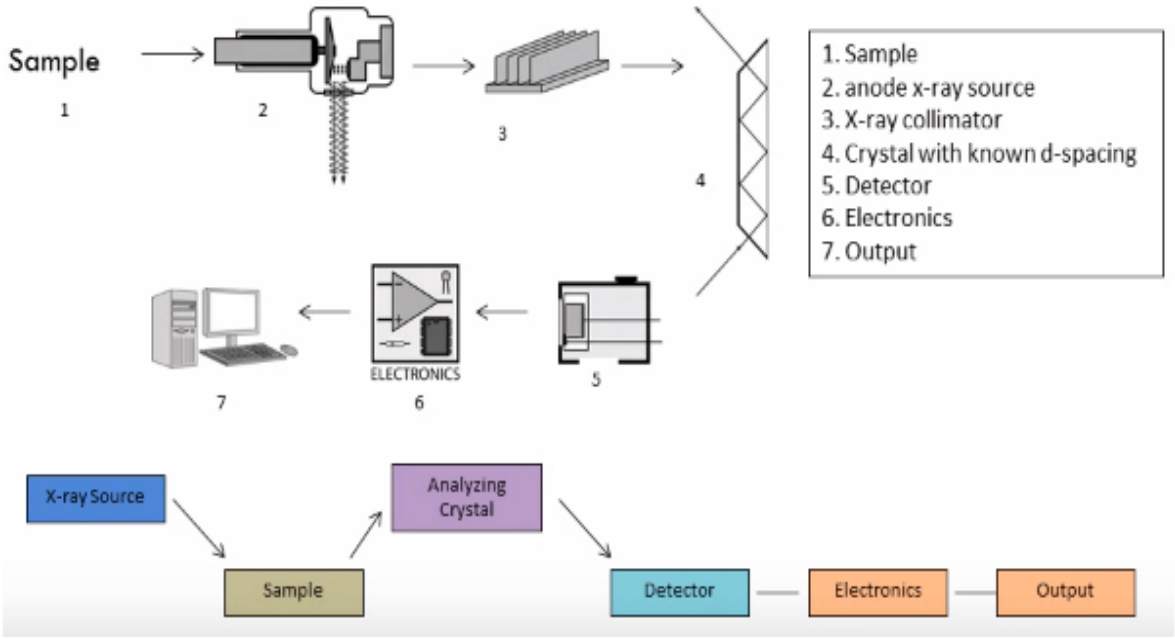


Figure 3.5: X-ray fluorescence spectroscopy instrumentation (Michaud, 2015)

XRF is well recognised as an accurate (Tamponi et al., 2003) and rapid technique and is much less costly for major element determinations on rocks samples (Spencer & Weedmark, 2015; Tamponi et al., 2003). An XRF analytical procedure yields high precision and accuracy which can be considered acceptable for petrological and geochemical purposes (Tamponi et al., 2003). The major rock-forming elements acquired through XRF methods are excellent for identifying rock formations and sub-units in the subsurface which can be correlated from well to well (Spencer & Weedmark, 2015).

3.3.5 Inductively coupled plasma mass spectrometry

The concentrations of the trace elements in the studied samples were analysed by Perkin-Elmer Elan DRC-e ICP-MS instrumentation (quadrupole; Figures 3.6 and 3.7). The procedure was performed in the Earth Laboratory located within the Bernard Price Building of the University of the Witwatersrand in Johannesburg. The procedure involves four stages: sample introduction, ICP torch, interface and mass spectrometry. The samples are fully decomposed into constituent elements and those elements are transformed into ions. Care was taken to ensure that sample preparation did not add contaminants to the specimen. These procedures were also highlighted by Kogel and Lewis (2001).

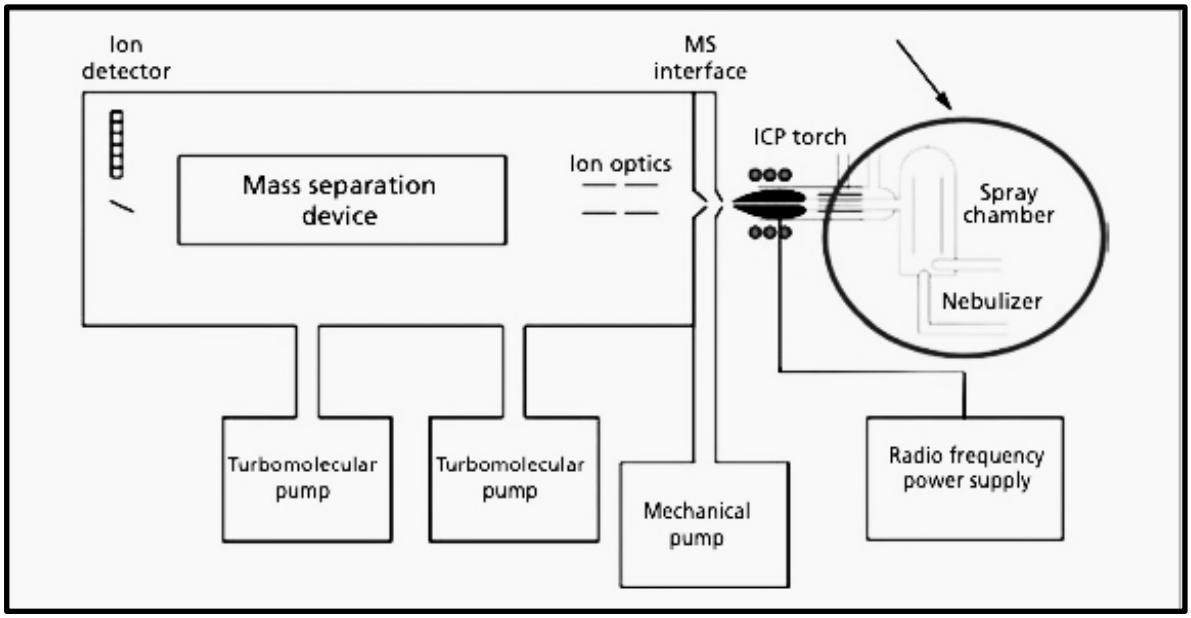


Figure 3.6: Major instrumentation components of the ICP-MS system (Brennan, Dulude & Thomas, 2015)

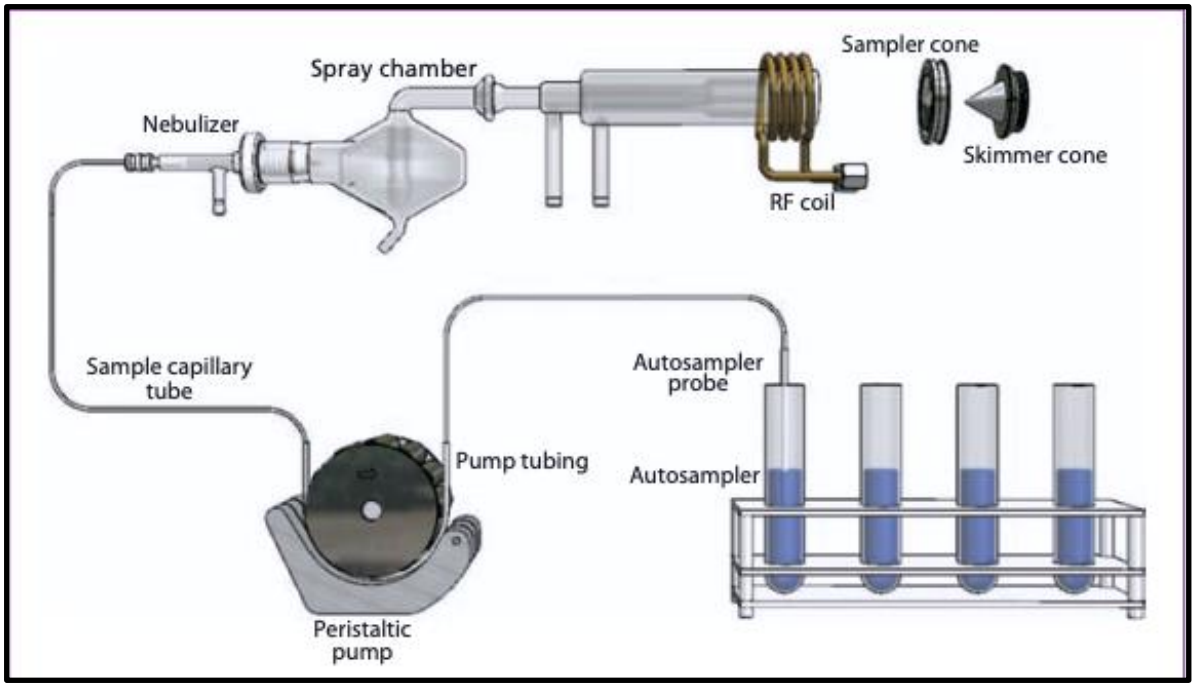


Figure 3.7: ICP-MS sample introduction area (Brennan et al., 2015)

CHAPTER 4: DATA PRESENTATION

This chapter presents the data collected from the field and through laboratory experiments. The research data are divided into five parts – fieldwork, petrographic, mineralogical (XRD), major element (XRF) and trace element (ICP-MS) data.

4.1 Fieldwork data

Table 4.1 summarises the data collected from the study area. In summary, the outcrop at the study area comprises mudstones and shales of the Ecca Group which is part of the Karoo Supergroup. The mudstones and shales of the study area are fine-grained, consisting of a mixture of clay and silt-sized particles. The colour of the lithostratigraphic units varies from grey to black in organic-rich beds and reddish-brown as a result of iron staining. The sedimentary structures seen in the outcrop and hand specimens (samples) include folds, particularly in the Prince Albert Formation, bedding and tuff beds. A detailed description of the lithology of the Prince Albert, Whitehill and Collingham Formations is included under 4.1.1, 4.1.2 and 4.1.3.

Table 4.1: Summary of the lithological description in the study area

Formation	Coordinates	Grain size/Texture	Composition	Deformation/ Sedimentary Structures	Diagnostic Description	Rock name	Basin Evolution; depositional Environment and Age (Baiyegunhi, 2015; Branch et al., 2007; Geel et al., 2013; Johnson et al., 1997; Nyathi, 2014; Viljoen, 1994; Visser, 1992)
Prince Albert	26° 62′ 73″ E 33° 21′ 62″ S	Fine-grained deposit	Clay and silt	Laminated Thinly bedded/ Interlayered Folded	Fine-grained mudstones Clay and silt-sized particles Grey in colour, but the colours of the beds vary from brown to red Non-carbonaceous	Mudstone	Post-Glacial marine Transgression-Suspension setting ~289–275 Ma
Whitehill	26° 62′ 73″ E 33° 21′ 62″ S	Fine-grained deposit	Clay and Silt	Well-laminated Thinly bedded	Fine-grained shales Clay and silt-sized particles Dark grey to black in colour Breaks along the parallel bedding laminae Carbonaceous-rich Tuffaceous horizon	Shales	Lacustrine deposition Slow suspension setting ~279–275 Ma

Formation	Coordinates	Grain size/Texture	Composition	Deformation/ Sedimentary Structures	Diagnostic Description	Rock name	Basin Evolution; depositional Environment and Age (Baiyegunhi, 2015; Branch et al., 2007; Geel et al., 2013; Johnson et al., 1997; Nyathi, 2014; Viljoen, 1994; Visser, 1992)
Collingham	26° 62′ 63″ E 33° 21′ 55″ S	Fine-grained deposit	Clay and silt	Well-laminated Thinly bedded Tuff beds	Tabular-bedded shales Fine-grained particles Clay and silt-sized particles Alternating beds of hard-grey siliceous shales and yellowish tuff beds Horizontal beds with an approximate thickness of 2– 9.5 cm	Shales	Turbidite influx Suspension setting in relatively deep water ~281–270 Ma

4.1.1 Prince Albert Formation lithologic description

The stratigraphic sequence is described from the oldest (Prince Albert) to the youngest (Collingham Formation). The lithostratigraphic units of the study area include the three Lower Ecca Group formations – the Prince Albert, Whitehill and Collingham Formations – underlain by the Dwyka Group and overlain by the sandstones of the Ripon Formation. These stratigraphic units comprise mudstones, carbonaceous shales and thin beds of siliceous mudrocks alternating with clayey material.

The Prince Albert Formation outcrop coordinates range between 26° 62′ 73″ E and 33° 21′ 62″ S and its thickness is about 100 m when exposed along the road cutting in the study area. The Prince Albert lithostratigraphic unit consists of fine-grained mudstones comprising clay and silt-sized particles. These mudstones are grey in colour, laminated, thinly bedded at the base and brownish at the top. The colours of the beds vary widely from light grey to red. The red colour is the result of iron staining (Figure 4.1). The thinly bedded mudstones are composed of beds with an average thickness of 2 mm.

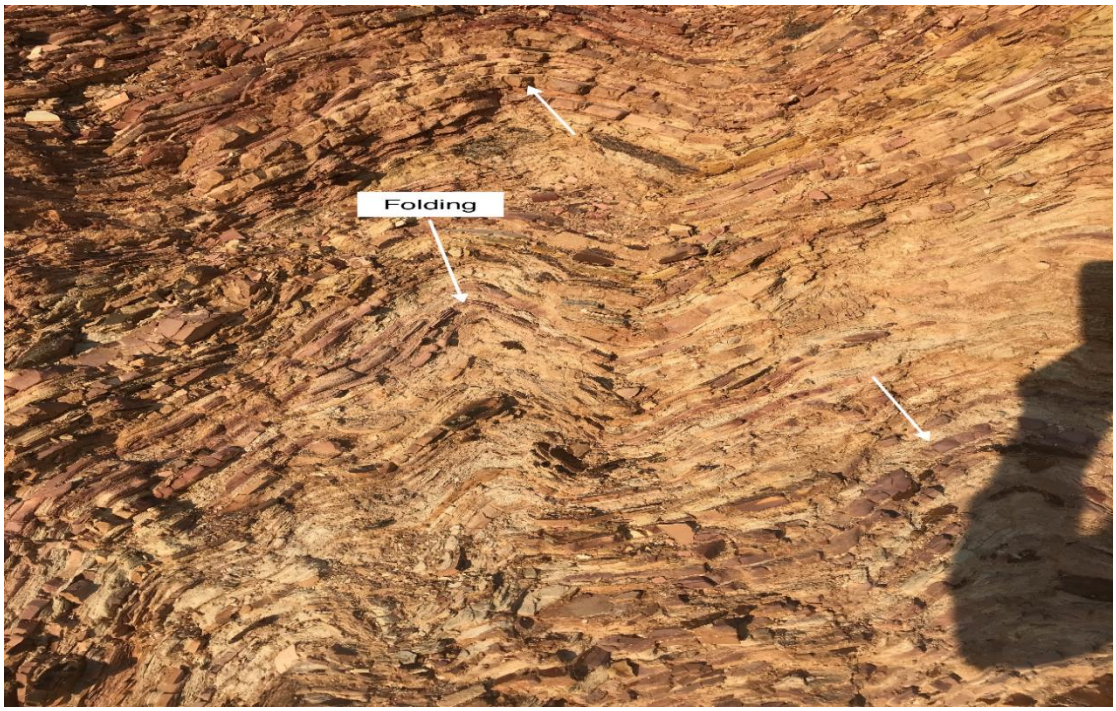


Figure 4.1: Shows mudstone foliation and red stain (due to high iron content) at the Prince Albert Formation (elevation 466 m; 26° 62′ 73″ E; 33° 21′ 62″ S)

The Prince Albert Formation in the study area is divided into two units: lower grey mudstones and upper brownish mudstones. These mudstones are organic carbon impoverished relative to the overlying Whitehill Formation. The Prince Albert Formation shows a gradational contact with the overlying dark grey carbonaceous shale facies. These mudstones are generally folded at the outcrop due to deformation and the folded bedding is moderately inclined. These mudstones are also fractured on a macro scale.

4.1.2 Whitehill Formation lithologic description

The Whitehill Formation of the Lower Ecca Group in the study area consists of fine-grained, dark grey to black shales comprising clay and silt-sized particles and breaks along the parallel bedding laminae. The formation is well-laminated and consists of carbonaceous-rich shales of the Early Permian age. At the base, the formation is thinly laminated and composed of firm dark grey rocks. Towards the top, the formation is characterised by a tuffaceous horizon with a distinctive white colour located in proximity to the overlying Collingham Formation (Figure 4.2). The actual colour is dark grey to black but turns white due to weathering. At the base, the formation is thinly laminated and composed of firm dark grey shales. The individual beds vary from 1 mm to 5 mm in thickness and the beds are horizontally laminated.



Figure 4.2: Shows tuffaceous zone within the Whitehill Formation (elevation 483 m; 26º 62′ 73″ E; 33º 21′ 62″ S)

The Whitehill Formation outcrop coordinates range between 26º 62′ 73″ E and 33º 21′ 62″ S and the formation has a thickness of approximately 22 m. The carbonaceous dark grey to black shales rest on the underlying non-carbonaceous mudstones of the Prince Albert Formation and are overlain by dark grey shales alternating with softer yellow beds. The carbonaceous shales comprise chert lenses and show the gradational lithological transition between the Prince Albert and Whitehill Formations.

4.1.3 Collingham Formation lithologic description

The Collingham Formation is tabular-bedded (flat-lying) and composed of fine-grained particles (mainly clay and silt-sized particles) which were deposited in the Late Permian age. The Collingham Formation in the study area is an interbedded lithostratigraphic unit with fine-grained beds, composed of alternating beds of hard dark grey siliceous shales and yellowish tuff beds (Figure 4.3) with an approximate thickness of 2 cm and 9.5 cm, respectively.

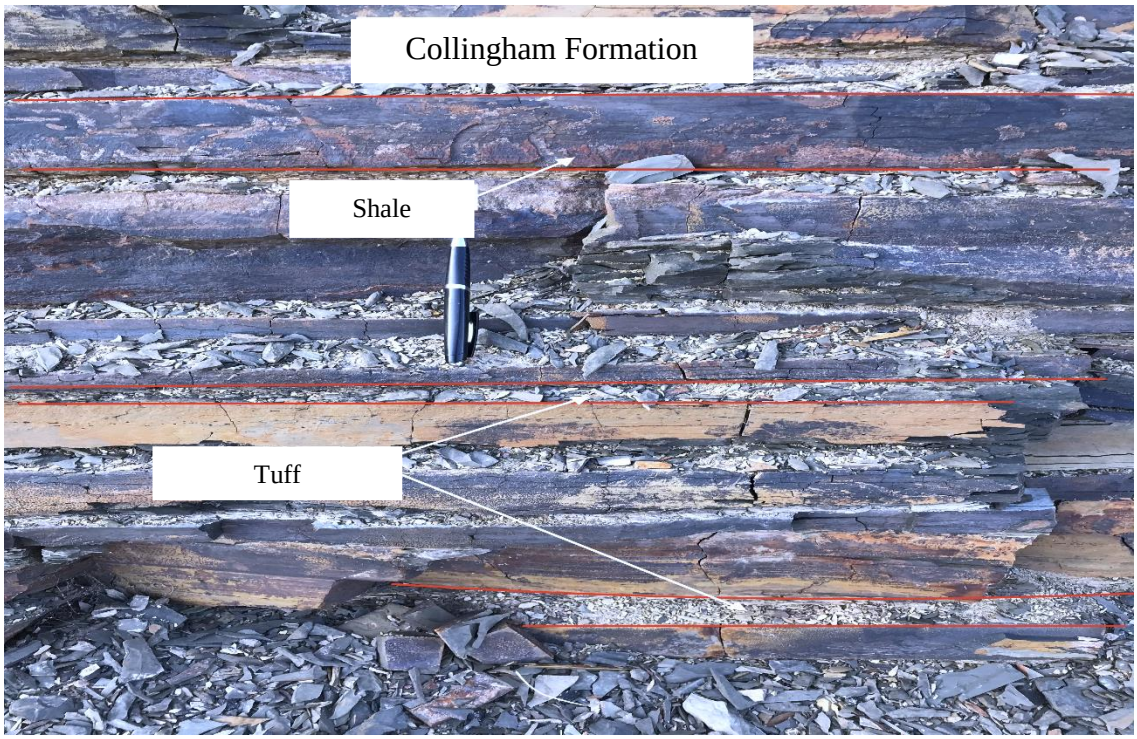


Figure 4.3: Shows shale and tuff interbeds of Collingham Formation (elevation 487 m; 26º 62′ 63″ E; 33º 21′ 55″ S)

The Collingham Formation overlies the carbonaceous shales of the Whitehill Formation and underlies the Ripon Formation at the outcrop. The Collingham Formation outcrop coordinates

range between 26° 62′ 63″ E and 33° 21′ 55″ S and the formation has a thickness of about 50 m.

4.2 Petrographic data

As clays and shales are extremely fine-grained for examination using microscopy, the petrographic analysis was supplemented by XRD analysis. Twelve unpolished thin sections (Figures 4.4, 4.5 and 4.6) were prepared using samples collected from the study area. Petrographic analysis was used to determine the mineral composition, textural variations (including grain size, shape and arrangement) and types of cementation. These observations were made to provide clues to the provenance of the sediments.

The grain size was measured under a petrographic microscope through thin section measurement (image analysis) on a millimetre (mm) scale. The petrographic data were obtained by petrographic microscopy analysis carried out in the laboratories of the School of Geosciences at the University of the Witwatersrand in Johannesburg. Petrographic studies were conducted under plane and reflected light on the prepared thin sections of rock samples varying from mudstones to shales. Four samples representative of the thin sections of each of the Prince Albert, Whitehill and Collingham Formations were studied. Tables 4.2 to 4.4 compare the field lithologic description data to the petrographic data.

4.2.1 Petrography of the Prince Albert Formation

The Prince Albert mudstones depict the following features as observed under microscopy (Figure 4.4):

(A) The thin section photomicrograph viewed under plane polarised light shows fine to medium grain size (0.1– 0.3 mm), moderately sorted and rounded to well-rounded grain shape. The mudstone contains small to large calcite grains. Apart from these features, calcite is the main cement replacing the original matrix and grains identified in the sample. The thin section also depicts smaller fractures filled with hematite cement (red stain). Air bubbles in the thin section may be a result of an error during preparation.

(B) The thin section photomicrograph viewed under plane polarised light shows moderately sorted grains, fine to medium in grain size and with a well-rounded grain shape. Calcite

grains are rounded to sub-rounded in shape. Calcite remains the dominant cementation in the sample together with hematite stained grains and hematite pellets.

(C) This thin section is stained reddish-brown due to iron and was viewed under plane polarised light. The mineral grains are moderately sorted and moderately packed. The overall shape of the grains is rounded to well-rounded. The sample is dominated by moderate to large calcite grains in a fine rock matrix. Hematite pellets also form part of the mudstone sample.

(D) The thin section comprises well-sorted grains with rounded calcite grains when viewed under plane polarised light. As observed in other Prince Albert mudstone samples, the thin section is composed of medium to large calcite grains in a fine to medium-grained matrix. Calcite precipitation together with reddish-brown stained grains (thick band) were also observed under the microscope.

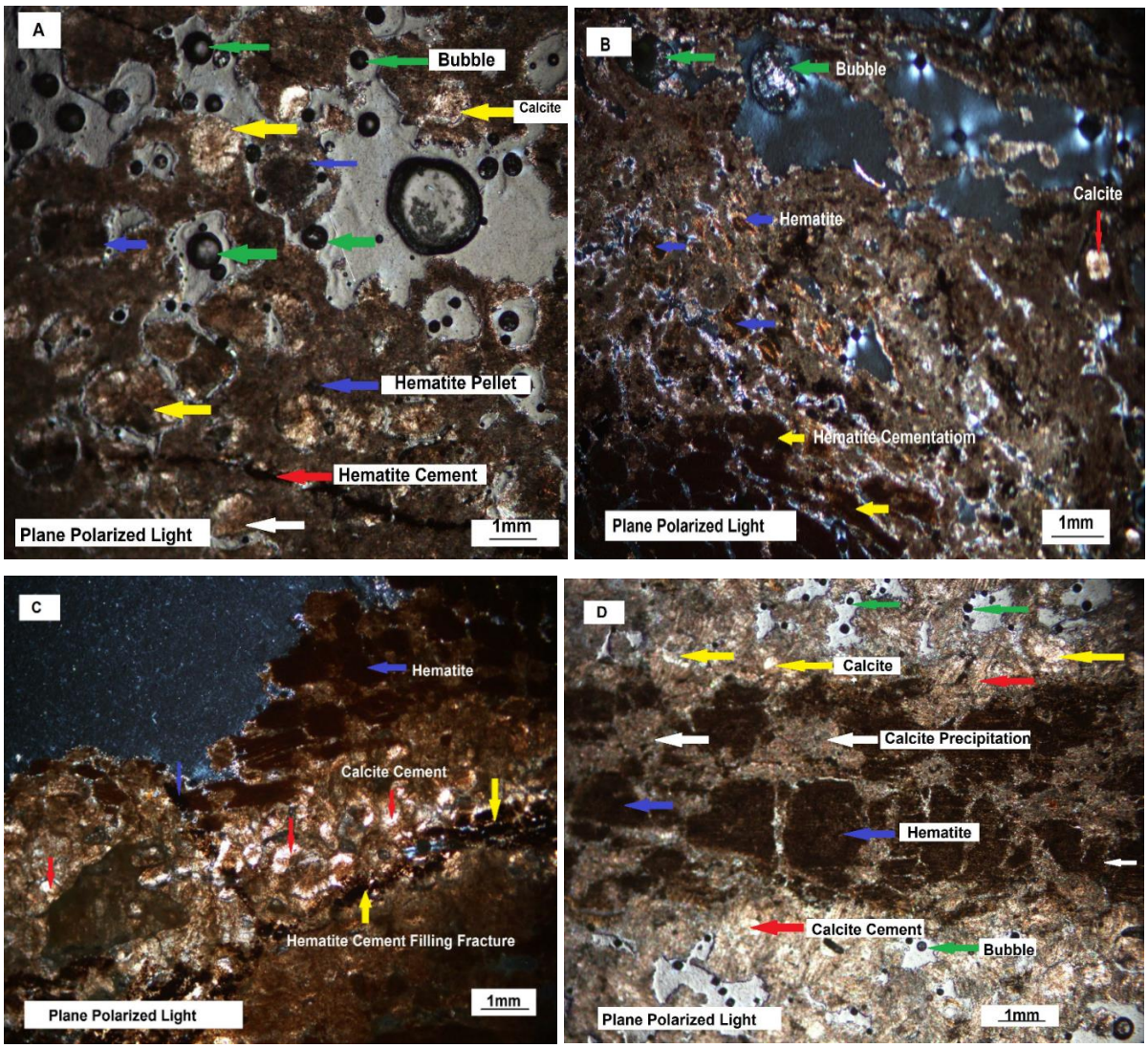


Figure 4.4: Thin section photomicrographs of the Prince Albert Formation viewed under plane polarised light

Table 4.2: Comparison of the lithologic description data to the petrographic data in the Prince Albert Formation

Formation	Lithologic Description	Petrographic Description
Prince Albert	The Prince Albert mudstones lithologic characteristics are as follows: • Fine-grained texture. • Clay and silt-sized particles. • Well-laminated. • Thinly bedded (red and light grey layers). • The red colour is the result of iron staining. • The mudstones are grey in colour. • Mudstones are folded due to deformation. • Mudstones are commonly developed in the form of thin laminae. • Grey at the base and brown at the top.	Prince Albert petrographic characteristics are as follows: • Clay and silt-sized particles (0.1–0.3 mm). • Moderately sorted and moderately packed. • Rounded to well-rounded grain shape. • Thin sections are stained reddish-brown due to iron. • Contain small to large calcite grains. • Calcite grains are rounded to sub-rounded in shape. • Calcite is the main cementing agent. • Fractures are filled with hematite cement (red stain). • Hematite stained grains and hematite pellets are present.

4.2.2 Petrography of the Whitehill Formation

The Whitehill Formation petrographic analysis indicates the following (Figure 4.5):

(A) The shales contain well-sorted, rounded detrital silt grains (0.03 mm) viewed under cross polarised light. The rock is resplendent with low angle laminations of organic-rich (dark) and hematite stained grains. The organic-rich laminae alternate with organic poor laminae and the shales also contain hematite pellets.

(B) The photomicrograph was viewed under a plane polarised light and shows sorted to well-sorted shale particles with scattered hematite pellets of less than 1 mm at this magnification. The rock sample is represented by medium to course silt grains (0.03–0.05 mm) and thick iron-stained laminae alternating with light coloured laminae. The mineral grains lie parallel to the laminations. The sample is thinly laminated between thick lamination.

(C) The degree of sorting under plane polarised light is moderate to well-sorted. The grains are rounded and represented by medium to coarse detrital silt. Hematite is the most occurring cementing agent in the shales together with hematite pellets. The hematite pellets change from well-rounded to subangular in shape. The shales show fine discontinuous parallel laminations.

(D) The shales under plane polarised light are moderately sorted and include grain sizes from silt to sand. The overall shape of the particles varies widely from well-rounded to sub-rounded. Hematite stained laminae alternate with lighter-coloured laminae of granular sample materials. The thin section also shows large, scattered quartz grains ranging from sub-rounded to angular. The sample is predominantly composed of hematite pellets. The fractures are filled with quartz cement.

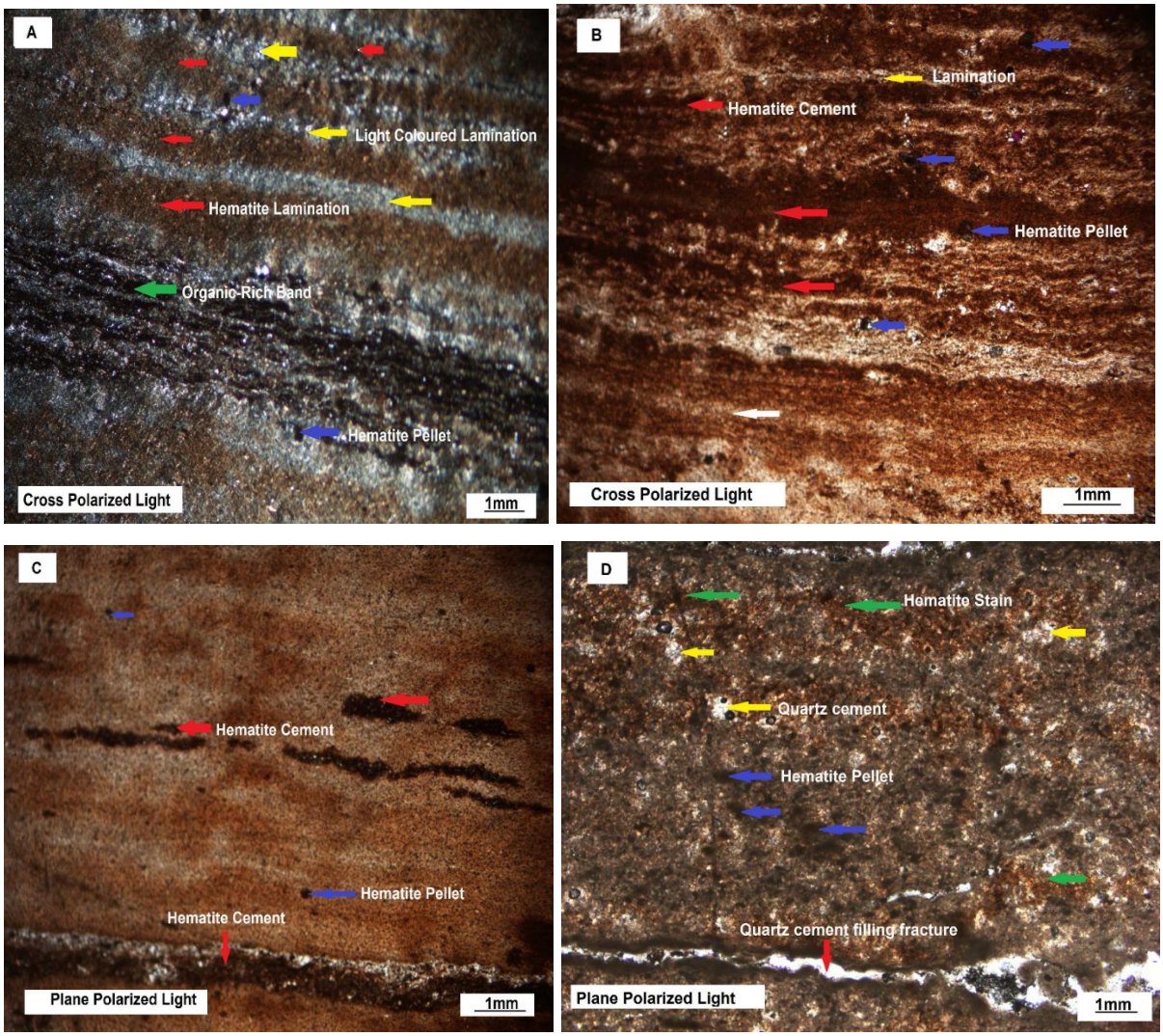


Figure 4.5: Thin section photomicrographs of the Whitehill Formation viewed under plane and cross polarised light

Table 4.3: Comparison of the lithologic description data to the petrographic data in the Whitehill Formation

Formation	Lithologic Description	Petrographic Description
Whitehill	Whitehill shales lithologic characteristics are as follows: • Carbonaceous dark grey to black shales with chert lenses. • Gradational lithological transition with underlying mudstones. • Organic-rich. • Tuffaceous zone with a distinctive white colour at the top of the formation. • At the base, the formation is thinly laminated and composed of firm dark grey shales.	Whitehill petrographic characteristics are as follows: • The organic-rich laminae alternate with organic poor laminae and the shale also contains hematite pellets. • Moderate to well-sorted, rounded detrital silt grains (0.03 mm) to course silt grains (0.05 mm). • The grains are rounded in shape. • Low angle laminations (organic-rich). • Hematite stained laminae alternate with lighter-coloured laminae of granular rock materials. • Sorted to well-sorted particles. • Thick iron-stained laminae alternating with light coloured laminae. • The mineral grains lie parallel to the laminations. • The shales are thinly laminated between thick lamination. • Hematite is the most occurring cementing agent. • The hematite pellets change from well-rounded to subangular in shape. • The shales show fine discontinuous parallel laminations.

4.2.3 Petrography of the Collingham Formation

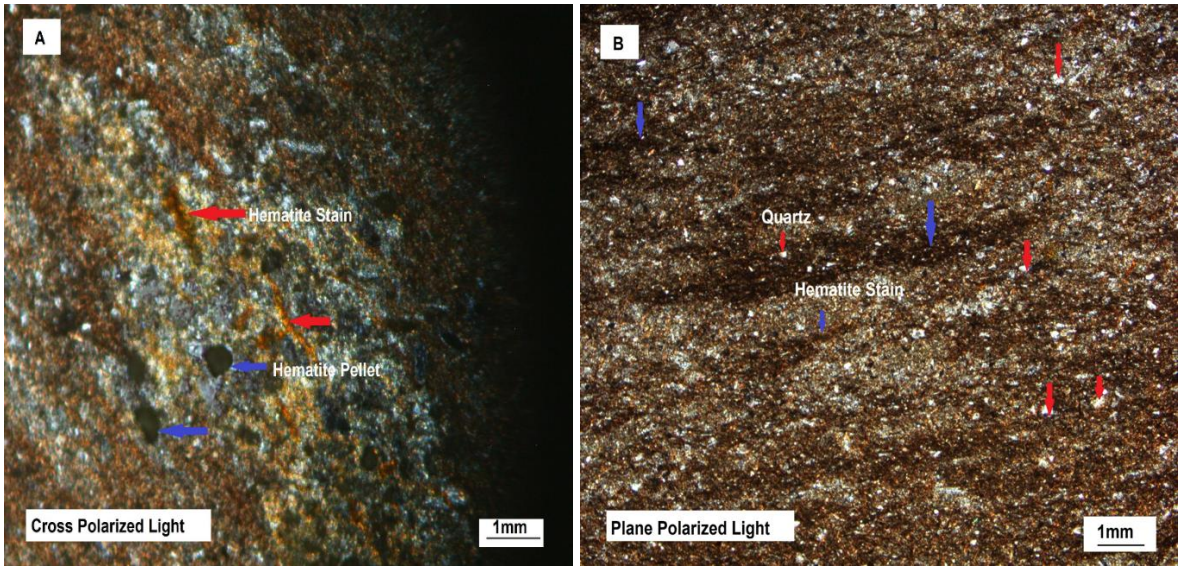
The Collingham Formation petrographic samples depict the following features under the microscope (Figure 4.6):

(A) The petrographic investigations were viewed under cross polarised light and show that the grains are moderately sorted, rounded to well-rounded in shape and with fine to medium-grained rock material (silt) in which hematite pellets are embedded.

(B) The sample is moderately sorted and composed of calcite particles and relict laminations; the grains are rounded under plane polarised light.

(C) The photomicrograph was viewed under polarised light and shows that the mudstone grains are moderate to well-sorted with a medium to coarse-grained texture. The sample is composed of small to medium calcite grains and hematite pellets. Calcite is the main cement viewed in the sample.

(D) The sample is composed of moderately sorted rock particles with fine to medium-grained texture under cross polarised light. The shales are thinly laminated (brown-reddish laminae); particles vary from sub-rounded to very angular. Quartz cement fills the horizontal fracture parallel to the grains.



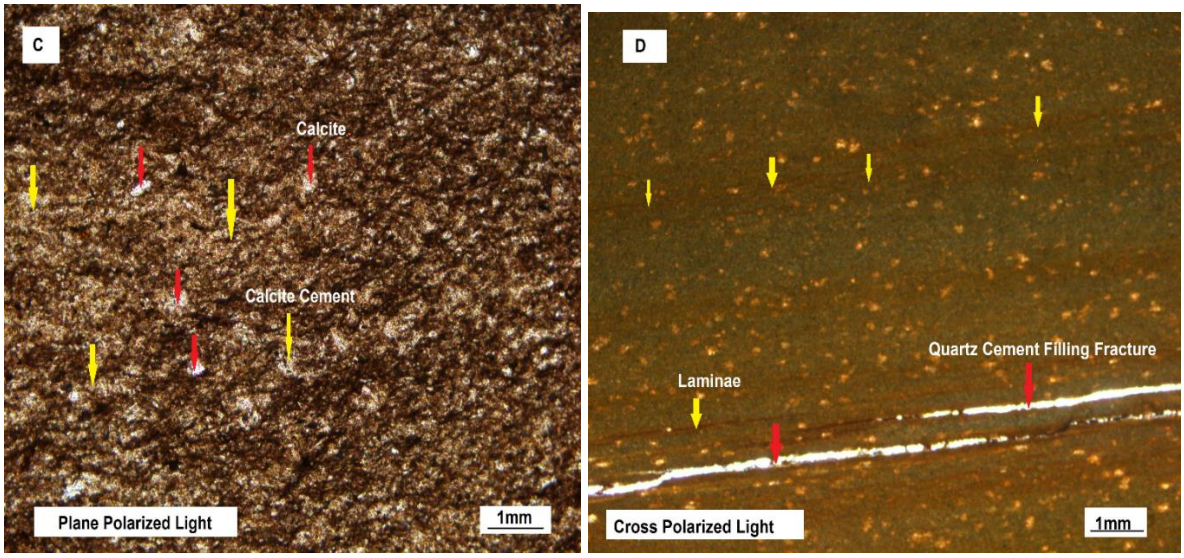


Figure 4.6: Thin section photomicrographs of the Collingham Formation in the Karoo Basin viewed under plane and cross polarised light

Table 4.4: Comparison of the lithologic description data to the petrographic data in the Collingham Formation

Formation	Lithologic Description	Petrographic Description
Collingham	Collingham shale lithologic characteristics are as follows: • Interlayered horizontal beds. • Rhythmically bedded grey coloured shales (hard) and yellow coloured tuff (soft). • Approximate thickness of 2 mm and 9.5 cm, respectively.	Collingham shale petrographic characteristics are as follows: • Moderately to well-sorted grains, rounded to well-rounded in shape. • Fine to coarse-grained texture. • Composed of calcite particles and relict laminations. • Small to medium calcite grains and hematite pellets. • Calcite is the main cementing agent. • Quartz precipitates. • Thinly laminated (brown-reddish laminae).

4.3 Mineralogical data

Twelve samples were examined by the XRD technique to determine the clay and non-clay mineral content present in the mudstones and shales from the study area. The results (Table 4.5) show that the Prince Albert, Whitehill and Collingham Formations have different

mineralogical compositions, consisting of quartz, illite, smectite, chlorite, calcite and dolomite as the main mineral content. Quartz is the most abundant mineral in all three formations, while clay and non-clay minerals are the second most abundant phases.

Table 4.5: Qualitative and quantitative XRD laboratory test results of the three formations reported in weight% (wt.%)

Formation	Sample	Quartz	Calcite	Dolomite	Illite	Chlorite	Plagioclase	Jarosite	Diopside	Halite	Smectite	Geothite
Prince	01	32	51.3	2.5	11.2	0	0	0	0	0.1	0	2.8
Albert	02	69.1	0.3	0	17.8	0	0.8	0.1	0.1	1.2	8.5	2.2
	03	51.8	23.3	1.1	8	4.9	0	0.1	0	1.8	3.4	5.5
	04	41.5	29.5	5.4	15.9	0.6	0,1	0	0	3.7	0	3.4
Whitehill	05	90	0	0	9.1	0.3	0.1	0	0	0.5	0	0
	06	89.2	0	0	8.9	0.3	0	1.4	0	0.1	0	0
	07	91.7	0	0	7.5	0.2	0.2	0	0	0.4	0	0
	08	48.4	41.6	5.3	3.2	0	0.7	0	0.7	0	0	0
Collingham	09	82.1	0	0	13.5	0.2	4.2	0	0	0	0	0
	10	78.2	0.1	0	15.1	0.3	6.3	0	0	0	0	0
	11	71.7	0.1	0	22.7	0.4	5	0	0	0	0	0
	12	77.6	0.1	0	13.5	7.1	1.6	0,1	0	0	0	0
Average		68.60	12.19	1.19	12,2	1.19	1.58	0.14	0.06	0.65	0.99	1.15

0 = not detected above the detection limit of 0.5–3 weight%

4.3.1 Prince Albert Formation

In the Prince Albert Formation of the Karoo Basin, shales have a quartz content of 32–69.1 wt.% with an average of 48.6 wt.%. This includes calcite (26.1 wt.%), illite (13.22 wt.%), smectite (2.97 wt.%), dolomite (2.25 wt.%) and chlorite (1.37 wt.%; Table 4.5). The quartz content is lowest in the Prince Albert Formation compared to the Whitehill and Collingham Formations. The mudstones from the Prince Albert Formation contain a large amount of quartz, secondarily carbonate and the least amount of clay minerals (Figure 4.7). Illite is the dominant clay mineral with comparatively small amounts of chlorite and smectite. Calcite is the dominant carbonate mineral with a comparatively small amount of dolomite.

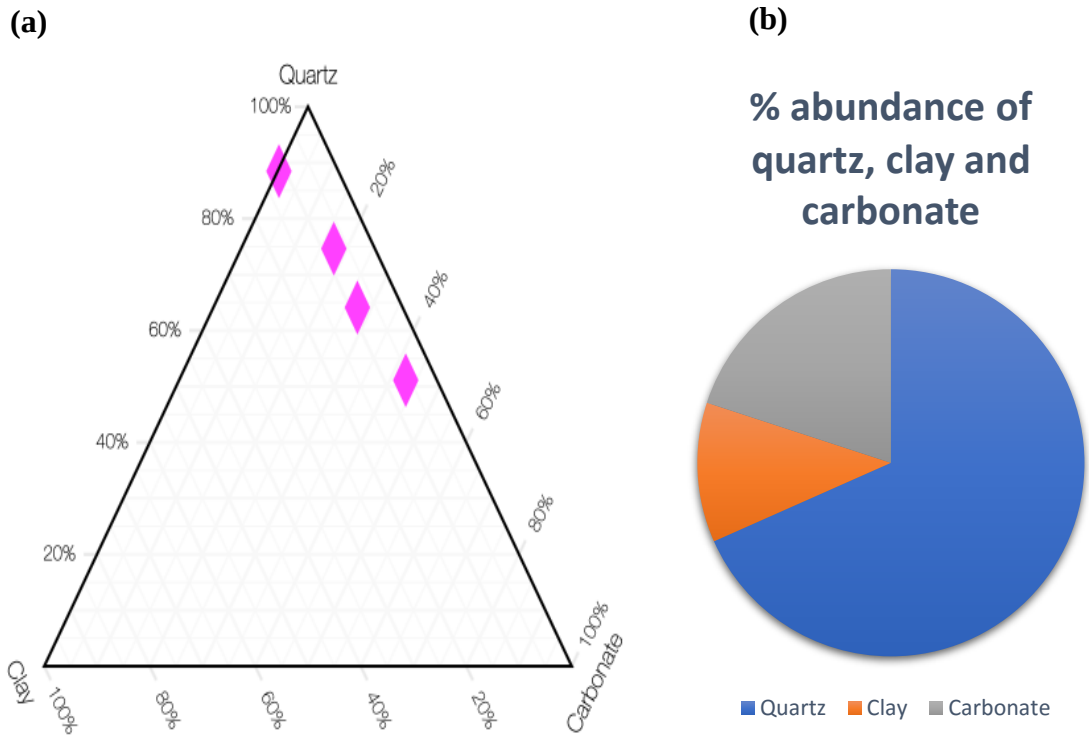


Figure 4.7: (a) A ternary plot showing the mineral composition as a percentage of three major components (i.e., quartz, clay and carbonate); (b) pie chart depicting the percentage distribution of quartz, clay and carbonate minerals in mudstones across the Prince Albert Formation

4.3.2 Whitehill Formation

In the Whitehill Formation, shales have the highest quartz content ranging from 48.4–92 wt.% with an average of 79.82 wt.%. The calcite, illite and dolomite content averages 10.4 wt.%, 7.17 wt.% and 1.32 wt.%, respectively, with no presence of smectite. The shale samples from the Whitehill Formation contain a large amount of quartz, secondarily carbonate and the least amount of clay minerals (Figure 4.8).

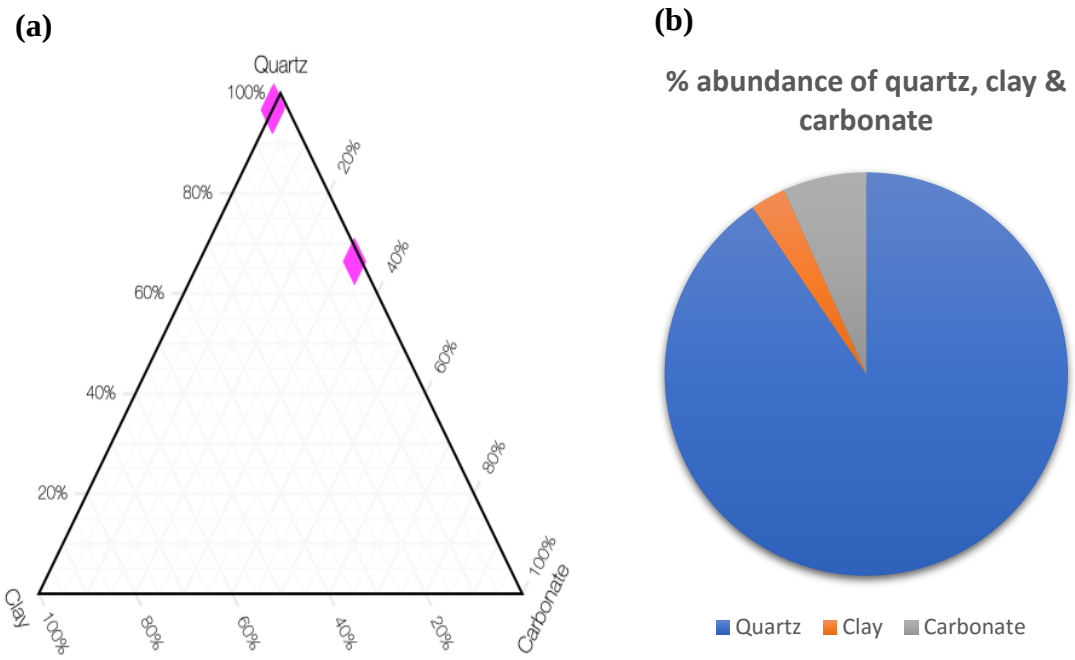


Figure 4.8: (a) A ternary plot showing mineral composition as a percentage of three major components (i.e., quartz, clay and carbonate); (b) pie chart depicting the percentage distribution of quartz, clay and carbonate minerals in shales across the Whitehill Formation

4.3.3 Collingham Formation

The Collingham Formation samples have the second-highest percentage of quartz ranging from 71.7 wt.% to 82.1 wt.% with an average of 77.4 wt.%. The illite, chlorite and calcite content averages 16.2 wt.%, 2.00 wt.%, 0.07 wt.%, respectively, with no presence of dolomite and smectite. The Collingham Formation contains a large amount of quartz, secondarily of clay and the least amount of carbonate minerals (Figure 4.9). Unlike in the Prince Albert and

Whitehill Formations, the Collingham Formation has a higher number of clay minerals than carbonate.

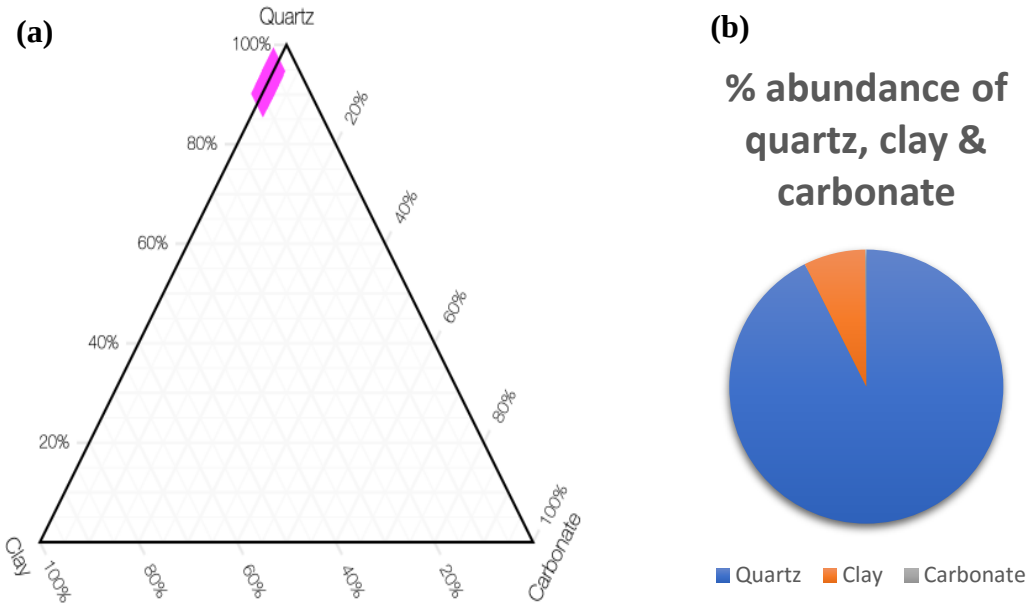


Figure 4.9: (a) A ternary plot showing the mineral composition as a percentage of three major components (i.e., quartz, clay and carbonate); (b) pie chart depicting the percentage distribution of quartz, clay and carbonate minerals in shales across the Collingham Formation

X-ray diffraction versus petrography

XRD and petrological analyses indicate that the mudstones and shales from the study area are chiefly composed of quartz and carbonate minerals, mainly calcite. Quartz generally constitutes more than 48 wt.% in the Prince Albert Formation and > 70 wt.% in the Whitehill and Collingham Formations. The average proportion of other minerals such as calcite, dolomite, illite, smectite and chlorite is usually less than 30 wt.%. The comparison of the mineralogical and petrographic characteristics of the shales and mudstones from the three formations is as follows: minerals that have been identified by the petrographic microscopy and XRD include calcite and quartz. The petrographic data indicate that calcite and quartz remain the dominant cementation, while the XRD data (mineralogical data) indicate that calcite is the highest constituent in the mudstones of the Prince Albert Formation.

4.4 Major element data

The geochemical analysis for this study involves the rock chemistry of major and trace elements carried out using traditional non-portable XRF and ICP-MS, respectively. The main objective of the XRF major element data is to better define chemical variations throughout the formations of the Lower Ecca Group. The XRF data for each element were reported in wt.%, while the ICP-MS data were reported in parts per million (ppm) because of the very small concentration of the element present. The following section presents the abundance and distribution of major elements in the study area. The summary statistics for whole-rock data from the 12 samples are given in Figures 4.10 to 4.12 and Table 4.6. The XRF provides for 12 major oxides including SiO_2, Al_2O_3, Fe_2O_3, MnO, MgO, CaO, Na_2O, K_2O, TiO_2, P_2O_5, Cr_2O_3 and NiO.

4.4.1 Prince Albert Formation

The ternary plots using major oxides determined by XRF and mineralogical data determined by XRD (Figure 4.10) show a similar distribution pattern of mineral composition and major oxides in the mudstones of the Prince Albert Formation. The ternary plots depict that the mudstones are rich in quartz and secondarily carbonate minerals. According to the XRD ternary plot, the mudstones in the Prince Albert Formation have higher concentrations of quartz than clay and carbonate, while the ternary plot of major elements (SiO_2, Al_2O_3, CaO) indicate that the mudstones are enriched in SiO_2 relative to Al_2O_3 and CaO.

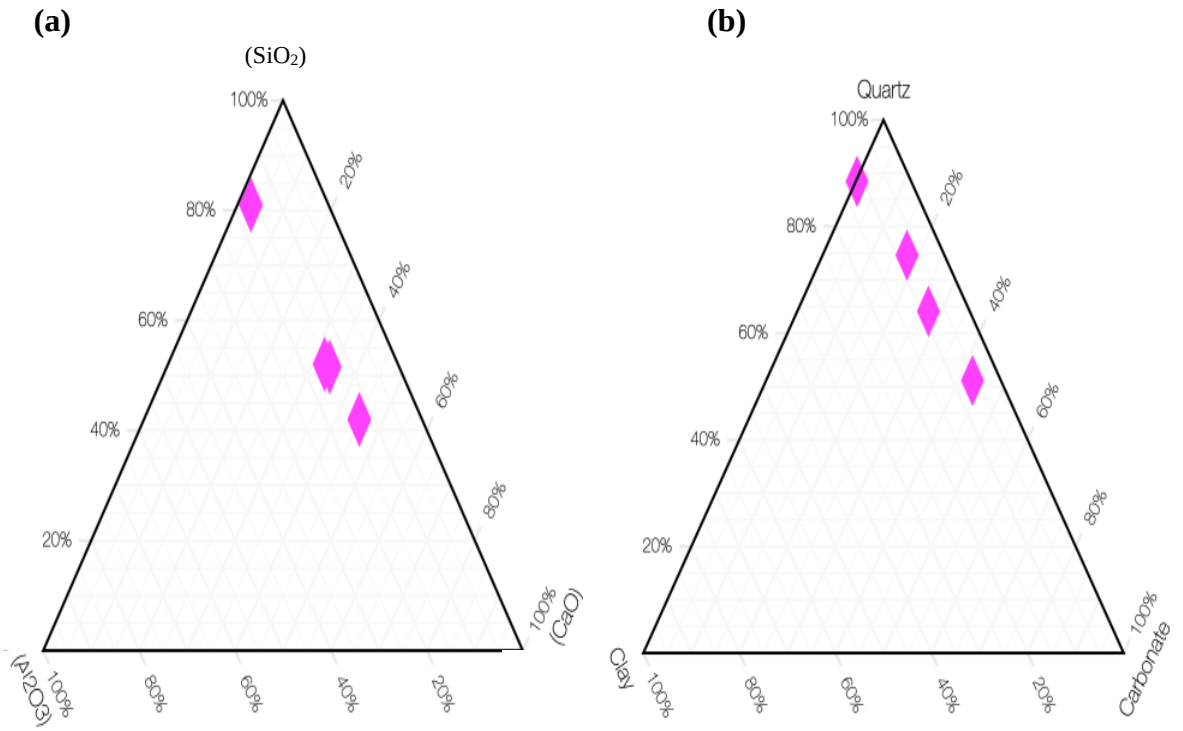


Figure 4.10: (a) A ternary plot of the major oxides (XRF) showing the Prince Albert mudstones rich in SiO_2 relative to Al_2O_3 and CaO; (b) a ternary plot showing mineral composition (XRD) as a percentage of three major components (i.e., quartz, clay = illite + chlorite + smectite and carbonate = calcite + dolomite) in mudstones across the Prince Albert Formation

4.4.2 Whitehill Formation

The ternary plots using major oxides determined by XRF and mineralogical data determined by XRD (Figure 4.11) show a similar distribution pattern of mineral composition and major oxides in the shales of the Whitehill Formation. The ternary plots of major elements (SiO_2, Al_2O_3, CaO) show that the Whitehill Formation is richer in SiO_2 than Al_2O_3 and CaO.

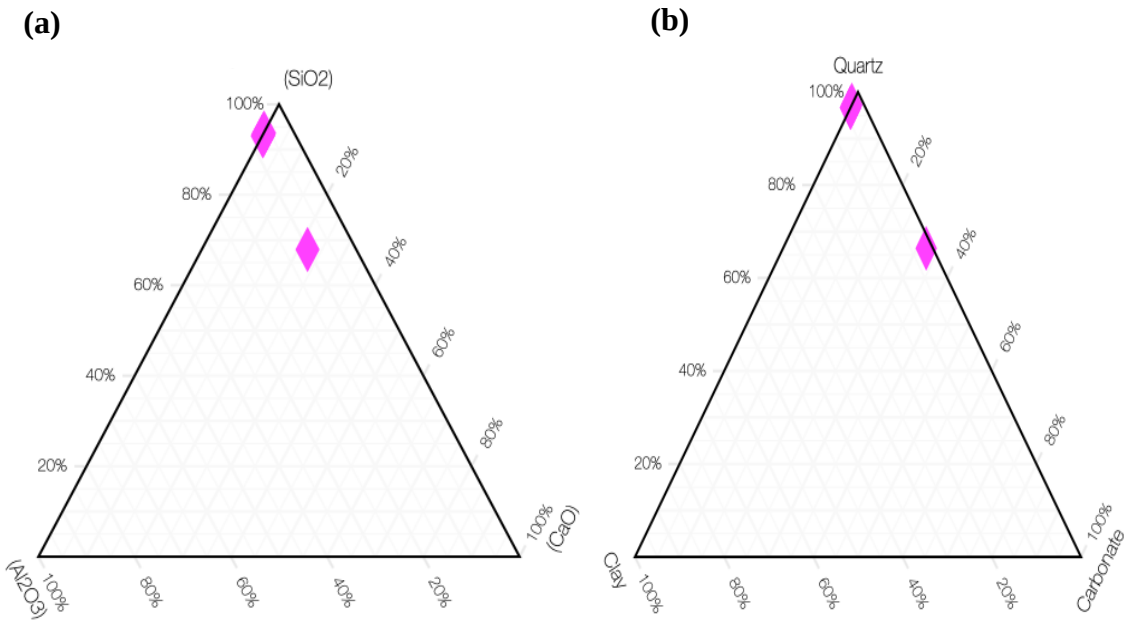


Figure 4.11: (a) A ternary plot of the major oxides (XRF) showing Whitehill shales rich in SiO_2, relative to Al_2O_3 and CaO. (b) a ternary plot showing the mineral composition (XRD) as a percentage of three major components (i.e., quartz, clay = illite + chlorite + smectite and carbonate = calcite + dolomite) across shales in the Whitehill Formation

4.4.3 Collingham Formation

The ternary plots using major oxides determined by XRF and mineralogical data determined by XRD (Figure 4.12) show a similar distribution pattern of mineral composition and major oxides in the shales of the Collingham Formation. Unlike in the Prince Albert and Whitehill Formations, the ternary plots indicate that the Collingham Formation is enriched in quartz and secondarily clay minerals. The shales in the Collingham Formation have higher concentrations of quartz than clay and carbonate minerals.

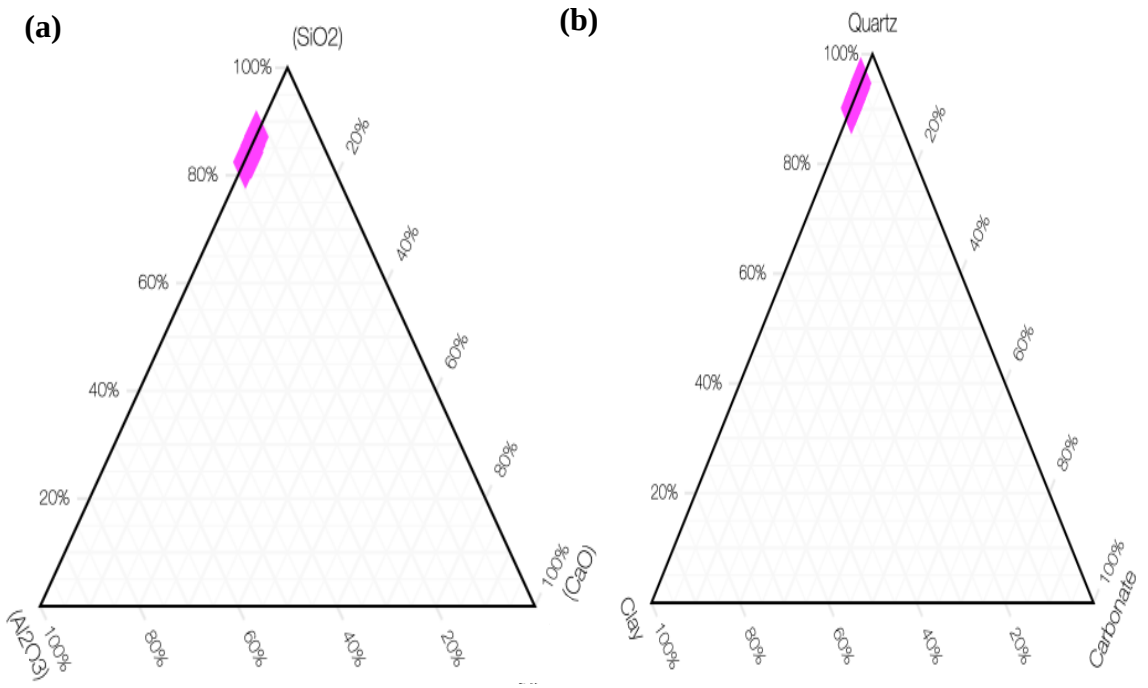


Figure 4.12: (a) A ternary plot of the major oxides (XRF) showing Collingham shales rich in SiO_2 relative to Al_2O_3 and CaO. (b) a ternary plot showing mineral composition (XRD) as a percentage of three major components (i.e., quartz, clay = illite + chlorite + smectite and carbonate = calcite + dolomite) across shales in the Collingham Formation

Table 4.6: Major element concentrations of the studied samples reported in weight%

Formation	wt.%	SiO_2	Al_2O_3	Fe_2O_3	MnO	MgO	CaO	Na_2O	K_2O	TiO_2	P_2O_5	Cr_2O_3	NiO
Prince	P01	26.6	8.29	4.06	0.01	2.75	28.45	0.18	0.94	0.31	0.19	0.01	0.00
Albert	P02	61.05	12.21	12.35	0.01	1.30	2.12	1.07	1.83	0.61	0.47	0.01	0.00
(Mudstones)	P03	31.57	9.28	10.22	0.02	3.49	19.81	0.79	0.82	0.29	0.33	0.02	0.00
	P04	32.04	9.01	4.84	0,.01	4.31	21.10	1.07	0.76	0.36	0.23	0.01	0.00
Whitehill	W05	87.62	6.25	0.37	0.00	0.43	0.12	0.37	1.54	0.44	0.12	0.01	0.00
(Shales)	W06	85.75	6.33	0.89	0.00	0.42	0.11	0.17	1.63	0.36	0.07	0.01	0.00
	W07	87.55	5.88	0.30	0.00	0.42	0.07	0.29	1.43	0.37	0.07	0.00	0.00
	W08	51.49	7.68	1.29	0.00	2.10	16.67	0.15	1.65	0.45	0.11	0.00	0.00
Collingham	C09	78.67	11.49	2.57	0.00	0.51	0.12	0.32	2.30	0.46	0.08	0.01	0.00
(Shales)	C10	75.39	12.45	3.40	0.07	0.90	0.21	0.60	2.71	0.39	0.10	0.01	0.00
	C11	70.71	14.80	3.90	0.07	1.05	0.22	0.54	3.27	0.42	0.09	0.01	0.00
	C12	70.33	12.69	7.80	0.07	1.72	0.40	0.30	2.15	0..28	0.08	0.01	0.00
Average		63.19	9.70	4.33	0.02	1.62	7.45	0.49	1.75	0.40	0.16	0.01	0.00

4.5 Trace element data

This section presents the abundance and distribution of trace elements in the samples. The distribution of trace element analysis in the mudstones and shales of the Lower Ecca Group normalised to UCC values are shown in Figure 4.13 and the results are reported in Table 4.7.

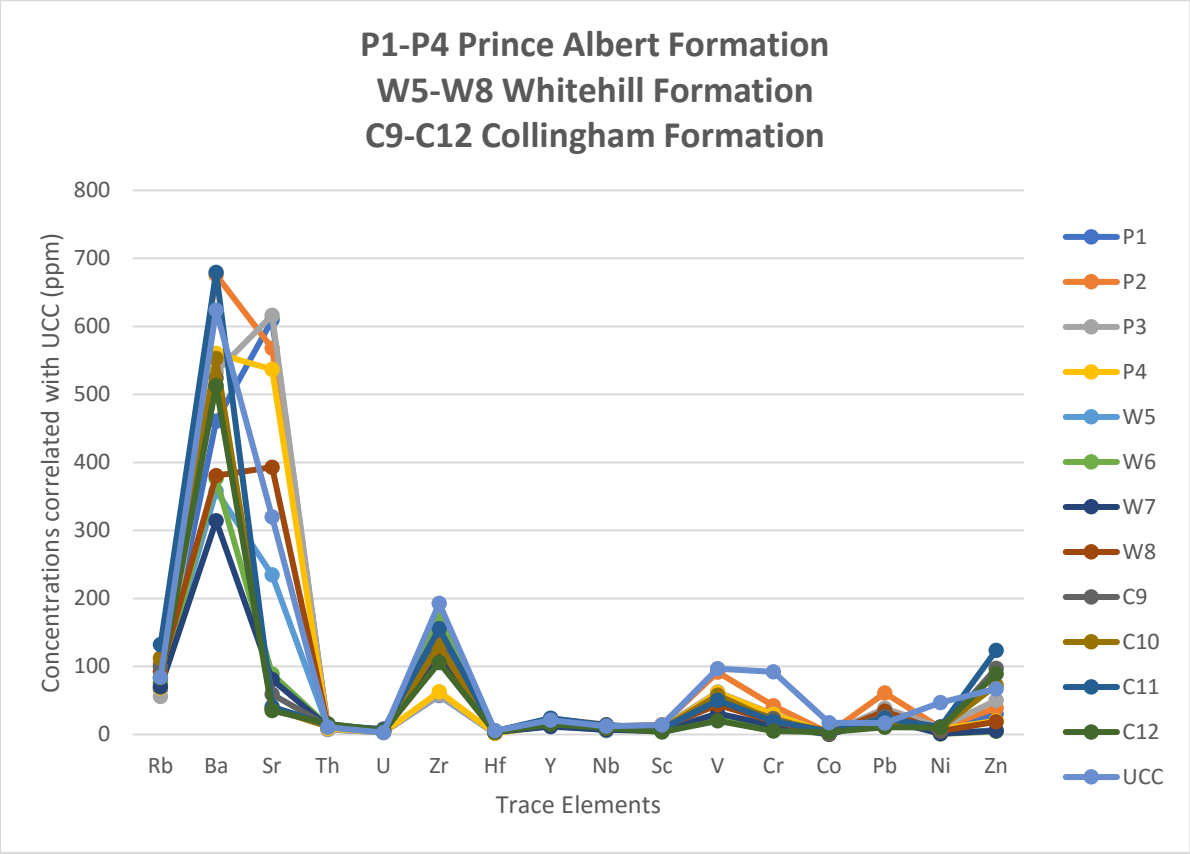


Figure 4.13: UCC normalised trace element concentrations of mudstones and shales of the Prince Albert, Whitehill and Collingham Formations (arranged in LILE, HFSE and TTE)

The trace element distribution varies significantly across the studied samples. On average, elemental content data show that the most abundant trace elements in the studied samples are Ti (2011.02 ppm), P (677.07 ppm), Ba (494.00 ppm), Sr (275.06 ppm), Rb (86.35 ppm) and Ce (79.29 ppm). Ti records the highest concentrations in all studied samples with an average ranging from 1873.54 ppm to 2246.44 ppm. The concentrations of elements such as Cu, Pb, Zn, Ga, V, La, Nd, Th and Y are relatively low, average < 50 ppm. Other elements show very low concentrations with averages below 10 ppm. The Prince Albert mudstones have the highest

concentrations of Ti, Pb, P, Sr, V, Cr, Co, Cu, Sb, Sm and Eu compared to shales from the Whitehill and Collingham Formations.

4.5.1 Prince Albert Formation

Large-ion lithophile elements (LILE; Rb, Ba, Sr, Th and U), compared to UCC, are mostly depleted in the Prince Albert mudstones except for Sr (Table 4.7). High field strength elements (HFSE; Zr, Hf, Y and Nb), compared to UCC, are depleted. UCC normalised concentrations of HSFE in the Prince Albert mudstones indicate that Zr is the most depleted trace element. Transition trace elements (TTE; Sc, V, Cr, Co, Pb, Ni and Zn), compared to UCC, are mostly depleted, while Pb is enriched in the mudstones of the Prince Albert Formation.

4.5.2 Whitehill Formation

LILE (Rb, Ba, Sr, Th and U), compared to UCC, are mostly depleted in the shales of the Whitehill Formation. The UCC normalised concentrations of LILE show that Th and U are enriched in the Whitehill shales. Ba is the most depleted trace element when compared to UCC normalised concentrations. HSFE (Zr, Hf, Y and Nb), compared to UCC, are mostly depleted. Zr is enriched in the shales of the Whitehill Formation. TTE (Sc, V, Cr, Co, Pb, Ni and Zn), compared to UCC, are highly depleted in the Whitehill Formation.

4.5.3 Collingham Formation

LILE (Rb, Ba, Sr, Th and U), compared to UCC, show that Ba and Sr are depleted, while Rb, Th and U are enriched in the shales of the Collingham Formation. HSFE (Zr, Hf, Y and Nb), compared to UCC, are mostly depleted in the shales of the Collingham Formation except for Y. TTE (Sc, V, Cr, Co, Pb, Ni and Zn), compared to UCC, are mostly depleted, while Zn is enriched in the Collingham Formation.

Table 4.7: Trace element composition in ppm (arranged in LILE, HFSE and TTE groups). (UCC values from Rudnick & Gao, 2003)

Element Group	Elements	Prince Albert Formation Mudstones (ppm)				Whitehill Formation Shales (ppm)				Collingham Formation Shales (ppm)				UCC (ppm)
		01	02	03	04	05	06	07	08	09	10	11	12	UCC
LILE	Rb	66.4	104.1	55.9	68.5	75.2	76	69.9	92.4	100	112.5	132.3	83	84
	Ba	460.8	675.7	533	560.3	358.1	376.3	314	380.8	523.9	552.9	679.3	513	624
	Sr	609.6	568	616.3	536.7	234.9	88.6	80.6	393	59.2	37.8	40.8	35.3	320
	Th	7.5	14.3	7.8	8.7	11.1	12.5	11.6	12.7	12.6	11.5	14.5	15.9	10.5
	U	3.0	4.1	3.3	2.9	3.9	4.8	4	6.1	7.8	6.1	7.2	5.7	2.7
HFSE	Zr	57.1	108.2	58.4	62.9	112.6	173.9	111.7	129	137.6	130.4	155.6	105.9	193
	Hf	1.6	3.3	1.7	1.8	4	5.5	3.5	3.1	3.8	3.8	4.8	3.7	5.3
	Y	15.4	21.2	19.8	13.5	13.1	15.4	11.5	22.5	23.2	23.1	24	14.8	21
	Nb	6.2	11.6	5.6	7.2	6.3	7	7	10.9	14.2	9.4	12.9	9.9	12
TTE	Sc	8.9	14,3	10.6	8	8.1	5.6	5.2	10	8	8.2	8.3	3.5	14
	V	53.8	91.6	62.6	61.4	47.1	27.1	31	43.4	50.5	57.9	50.4	20.1	97
	Cr	26.1	42.1	29.8	29.4	21.6	10.2	13	18.9	23.2	20.7	19.6	4.9	92
	Co	4.3	2	1.8	1.7	0.2	0.1	0.2	0.9	1.1	4.9	4.1	3.6	17.3
	Pb	18.9	61.1	38.6	22.4	33.2	25.6	22	34	26.6	17.8	23.2	10.7	17
	Ni	8.2	9.7	10.7	7.7	1.2	1	1.1	5	5.6	9.8	10.9	10.2	47
	Zn	29.9	38.7	50.3	20.2	6.4	4.5	5.6	18.8	97.3	72.1	123.6	89.3	67

*LILE = Large-ion Lithophile Elements *HFSE = High Field Strength Elements *TTE = Transition Trace Elements

CHAPTER 5: DATA ANALYSIS AND INTERPRETATION

Chapter 5 discusses the research data – fieldwork, petrographic, mineralogical (XRD), major element (XRF) and trace element (ICP-MS) data. This chapter also aims to compare the lithology, petrology, mineralogy and geochemistry of the formations in the United States (i.e., the Barnett and Marcellus Shales) and in South Africa (i.e., Ecca Group). Several previous works conducted in the Barnett and Marcellus Shales have been reported by many researchers (e.g., Abouelresh, 2014; Abouelresh & Slatt, 2012; Bowker, 2007; Bruner & Smosna, 2011; Chen, 2012; Colwell, 2014; Ding et al., 2012; Gale, et al., 2007; Han et al., 2015; Hupp & Donovan, 2018; Jarvie et al., 2001; Loucks & Ruppel, 2007; Milliken et al., 2012; Montgomery et al., 2005; Perez, 2010; Pollastro et al., 2007; Soeder, 2010; Tian, 2010; Tian & Ayers, 2010; Vermylen, 2011; Werne et al., 2002).

Barnett Shale is an organic and silica-rich black mudstone of the middle to late Mississippian age (Vermylen, 2011). It is the most productive, world-class unconventional gas play in the United States (Montgomery et al., 2005; Tian, 2010) due to its brittle mineral composition (Tian, 2010), among other characteristics. The Fort Worth Basin was formed during the Palaeozoic period mainly during the Mississippian and Pennsylvanian ages. However, Barnett is entirely Mississippian (Bowker, 2007). Marcellus Shale, on the other hand, is organic-rich and contains a significant amount of natural gas. It is located in the Appalachian Basin in the northeastern United States (Soeder, 2010).

This study was also compared to the previous mineralogical and geochemical investigations in the Ecca Group (e.g., Baiyegunhi, 2015; Ferreira, 2014; Geel et al., 2015; Nyathi, 2014).

5.1 Fieldwork data analysis

To fulfil the basic requirements for shale gas generation, the following must be considered: high organic carbon content, thickness and depth (Liu et al., 2017; Zhang et al., 2018). Black carbonaceous shales are chiefly located in the Whitehill Formation which can be regarded as a favourable area selection for shale gas development because of its enriched organic carbon content. The thickness of the Prince Albert, Whitehill and Collingham Formations at the study area is above 15 m and meets one of the prerequisites to determine whether the shale reservoir

has any value for commercial development. According to Zhang et al. (2018), the accumulated thickness of the shale reservoir must reach at least 15 m to contain enough resources and the depth of shale must be < 4000 m to achieve commercial development value. According to previous investigations in the Main Karoo Basin, the average thickness of the Prince Albert Formation is approximately 200 m (Mosavel & Cole, 2019) and the Whitehill Formation 50m to 70 m (Branch, Ritter, Weckmann, Sachsenhofer & Schilling, 2007) while the thickness of the Collingham Formation is approximately 70 m (Nxantsiya, 2017).

The foliations, laminations and hematite stained layers observed in the field are in agreement and correlate very well with the petrographic analysis. The thin-bedded laminations and fine-grained particles suggest deposition under weak hydrodynamic conditions and suspension setting as indicated by Zhao et al. (2017). Bedding and laminae observed in the outcrop at the study area may significantly improve the horizontal seepage capability of the shale reservoir and enhance shale gas output as suggested by Zou et al. (2017).

The laminae indicate vertical changes in texture and composition, while planes exhibit weaknesses that influence the efficiency of hydraulic fracturing. However, a high laminae density is not beneficial for the formation of vertical artificial cracks during hydraulic fracturing (Wang et al., 2019). The Barnett Shale is composed of a mixture of laminated siliceous and argillaceous mudstones, while shale is dominated by fine-grained sediment and flat-lying thin laminae that range up to 0.15 mm (Loucks & Ruppel, 2007).

5.2 Petrographic data analysis

The primary diagenetic cement observed in the studied samples includes carbonate (calcite), quartz and iron (hematite). These cements occur mainly as fracture filling and also as rock matrix and grain replacement. Apart from the cementation, the petrographic investigations indicate that the shales and mudstones are made up of organic-rich bands and low angle laminations. The laminations and lenticular bedding indicate the suspension deposition of the sediments (Zhao et al., 2017). Hematite stained grains and hematite pellets are prevalent in the studied shales and mudstones. According to Baiyegunhi et al. (2017a), a high concentration of iron-bearing minerals (such as hematite) in the rocks could be due to a source of iron in the Prince Albert, Whitehill and Collingham Formations.

The petrographic observations also show that the physical characteristics of the studied shales and mudstones have been altered mainly due to cementation. The original grains were partly replaced by calcite and quartz cemented material. Post-depositional diagenesis, such as the precipitation of calcite cements, has been observed mainly in the Prince Albert Formation. This suggests that the sediments have gone through a recrystallisation process, resulting in the formation of new mineral grains replacing the original grains. The carbonate mineral cements (calcite) mainly occur in the Prince Albert and Collingham Formations, while the Whitehill Formation is characterised by quartz cements mainly filling the natural fractures. The mudstones are fine to medium in grain size, moderately to well-sorted and mainly rounded in grain shape. Sediment distribution includes thin and thick laminations and interbedded layers which correspond with field observations.

In summary, the sediments were partially affected by diagenetic alteration due to cement filling the pore spaces during diagenesis. According to Geel et al. (2021), quartz and calcite veins are common throughout the Lower Ecca Group and the diagenetic precipitation of iron-rich carbonates such as calcite was a result of the high maturity of the source rock (Geel & Bordy, 2021). Quartz cement is the main factor influencing reservoir quality in siliciclastic sandstones (Molenaar et al., 2007).

Investigations indicate that diagenetic alteration due to cementation may reduce the porosity and permeability of the rock (Baiyegunhi et al., 2017a; Flewelling & Sharma, 2014; Lin et al., 2017; Wagen, 2000) and low permeability of the source rocks may degrade reservoir quality (Akinlua et al., 2016). The lower formations of the Ecca Group have low permeability. The low porosity and low permeability make these formations unfavourable for shale gas production in the absence of hydraulic fracturing operations (Baiyegunhi et al., 2017a) and may increase the requirement of an additional method to enhance recovery and flow capacity (Wang, 2017; Wang et al., 2014).

Fagereng (2012) documented that folding in the CFB was largely accomplished by brittle process assisted by dissolution. The folded rocks include, among others, the Ecca Group of the Karoo Supergroup and folds are common in the mudstone-dominated Prince Albert Formation. Fractures are common within folded and more competent (generally quartz-rich) layers in mudstone sequences.

The rocks of the Ecca Group in the study area were deformed either by brittle process or solution transfer (Fagereng, 2012). However, according to Baiyegunhi et al. (2017b), partial dissolution of silicate grains and recrystallisation of fine minerals were accommodated by the compaction of the Ecca Group sediments during burial diagenesis. This resulted in high temperatures and an increase in overburden pressure causing the dissolution of the silicate materials. The cracks and fractures in the mudrocks of the Ecca Group are evidence of their compaction during their progressive burial.

According to Geel et al. (2021), the Lower Ecca Group is highly fractured, particularly in the regions of thrust faulting and the fractures are filled with quartz or calcite precipitates. The fault planes are accommodated by the displacement of the Whitehill Formation during CFB formation. The high maturity of the Lower Ecca Group influences diagenetic mineral precipitation, causing an impact on the overall brittleness.

Field and petrographic observations within the Lower Ecca Group in this area recognise various structures (fractures and folds). This study recognises suggestions made by previous studies (Fagereng, 2012; Geel et al., 2021) linking the deformation of the Lower Ecca Group units largely with CFB deformation assisted by dissolution (Baiyegunhi et al., 2017b). However, other prime target areas for shale gas outside the CFB may likely experience diagenetic mineral precipitation accommodated by dissolution. This is as a result of the compaction of the sediments as suggested by Baiyegunhi et al. (2017b) and also as a result of the high maturity of the Lower Ecca Group (Geel et al., 2021).

Comparison of the Barnett Shale with the current study

Petrographic observations indicate that the Barnett Shale is composed of layers of thin beds with laminae of organic-rich skeletal siliceous mudstone in between (Loucks & Ruppel, 2007) and calcite-dominated skeletal fragments are common (Han, Mahlstedt & Horsfield, 2015). The Lower Ecca Group of the Main Karoo Basin, particularly the Whitehill Formation, is composed of organic-rich laminae with organic poor laminae in between. Quartz and clay minerals mostly chlorite, calcite, pyrite, dolomite and phosphatic grains (Abouelresh, 2014) have been observed under petrographic microscopy.

Most of the natural fractures observed in the Barnett Shale are filled with calcite (principal), quartz and chlorite cements (Gale et al., 2017; Milliken et al., 2012; Montgomery et al., 2005) and are highly clustered (Gale et al., 2007). Original sedimentary signatures in the Barnett Shale have been altered due to progressive burial and diagenesis (Han et., 2015). The Ecca Group mudstones and shales have also been altered due to deformation and progressive burial. Sediment alteration in the Barnett Shale includes mechanical and chemical modifications and calcite particles were locally dolomitised and replaced by silt-sized dolomite rhombs (Han et al., 2015). The Barnett and Lower Ecca Group Formations share features in that most of the fractures are filled with quartz and calcite cements and the sediments have been altered due to burial diagenesis.

Comparison of previous investigations with the current study

The petrographic observations of previous investigations (Baiyegunhi, 2015) in the study area are principally in agreement with the observations of the current study outlined above. The previous investigations in the Ecca Group indicate that the mudstones of the Prince Albert Formation are folded and characterised by minor detrital grains of quartz, feldspar and muscovite. The formation of hematite around the mineral grains could be due to the relatively low content of hornblende. The intragranular micropores are mostly filled with quartz cement.

The Whitehill Formation, on the other hand, consists of micro-quartz cement, hematite cement, quartz overgrowths, carbonaceous fragments and detrital quartz grains. Calcite is the most abundant and main cement mineral identified in the Collingham Formation. A recent study undertaken by Geel and Bordy (2021) documented that fractures in the Lower Ecca Group are filled with either quartz or calcite precipitates. The petrographic investigation also indicates that the Lower Ecca Group shales are distinctly laminated and demonstrate soft-sediment deformation structure, particularly in the Collingham Formation.

5.3 Mineralogical data analysis

In summary, the following findings regarding the mineralogical composition of the studied mudstones and shales were made: the mudstones and shales are mainly composed of quartz and carbonate minerals and secondarily of clay minerals. The XRD analysis indicates that clay minerals are mainly represented by illite with minor amounts of smectite and chlorite but no

presence of kaolinite. Quartz, dolomite and calcite are the dominant non-clay minerals together with small amounts of plagioclase and halite detected. The average content of quartz and carbonate is 68.60 wt.% and 6.69 wt.%, respectively. The average clay content is 4.79 wt.% with the illite content being the highest. The Lower Ecca Group formations are dominated by high strength and brittle mineral phases such as quartz and carbonates (calcite and dolomite). The mineralogical data analysis is divided into three parts: silica, carbonate and clay mineralogy.

5.3.1 Silica mineralogy

Quartz is the dominant mineral in the studied mudstones and shales. The average quartz content ranges from 48.6 wt.% at the Prince Albert Formation to 77.4 wt.% at the Collingham Formation and 79.82 wt.% at the Whitehill Formation (Figure 5.1). This study shows that the Whitehill and Collingham Formations are characterised by siliceous shales as the average content of silica is above 65 wt.%. According to Liang et al. (2016), siliceous shales are rich in silica (above 65%), while Zhao et al. (2017) documented that shale with a quartz content of greater than 45% is classified as siliceous shale. Organic-rich shale and siliceous shale of greater than 65% and deposited from suspension near upwelling zones are key exploration targets for shale gas. The lithofacies influenced by suspension and upwelling are rich in silica (up to 85%) and have high brittle mineral content (quartz) which is conducive to hydraulic fracturing.

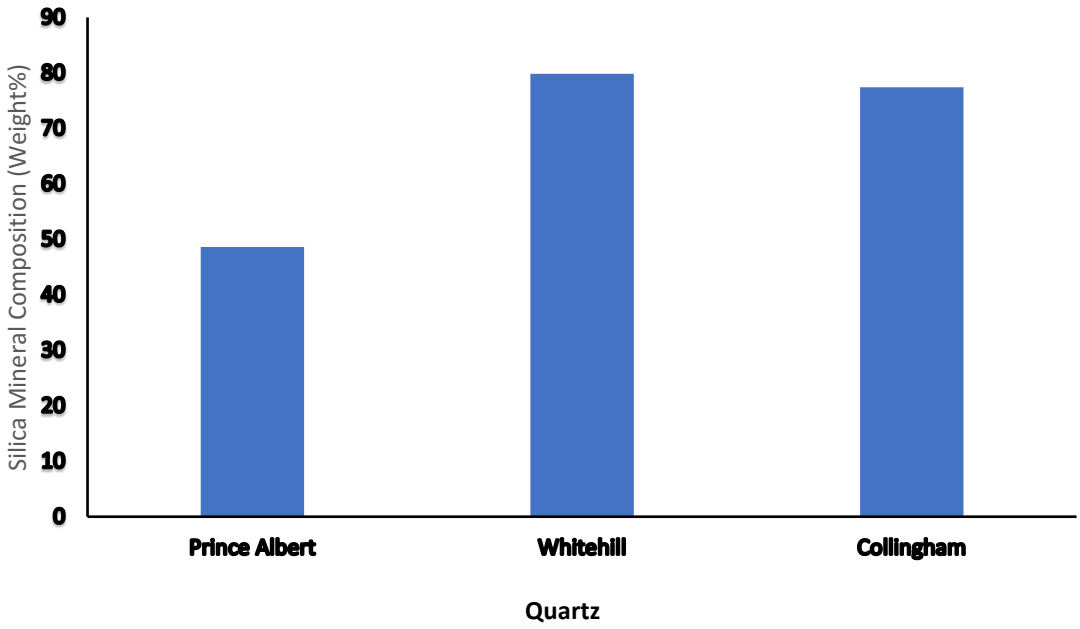


Figure 5.1: Silica mineral composition in the three formations

5.3.2 Carbonate mineralogy

Carbonate minerals are the second most abundant minerals in the studied mudstone and shale samples. The carbonates detected by XRD are calcite and dolomite (Figure 5.2). Calcite is the most dominant carbonate mineral in the studied mudstones and shales. The average calcite content ranges from 0.07 wt.% at the Collingham Formation to 10.4 wt.% at the Whitehill Formation and 26.1 wt.% at the Prince Albert Formation. This study suggests that the Prince Albert Formation is composed of calcareous mudstones as the average content of calcite is above 20 wt.%.

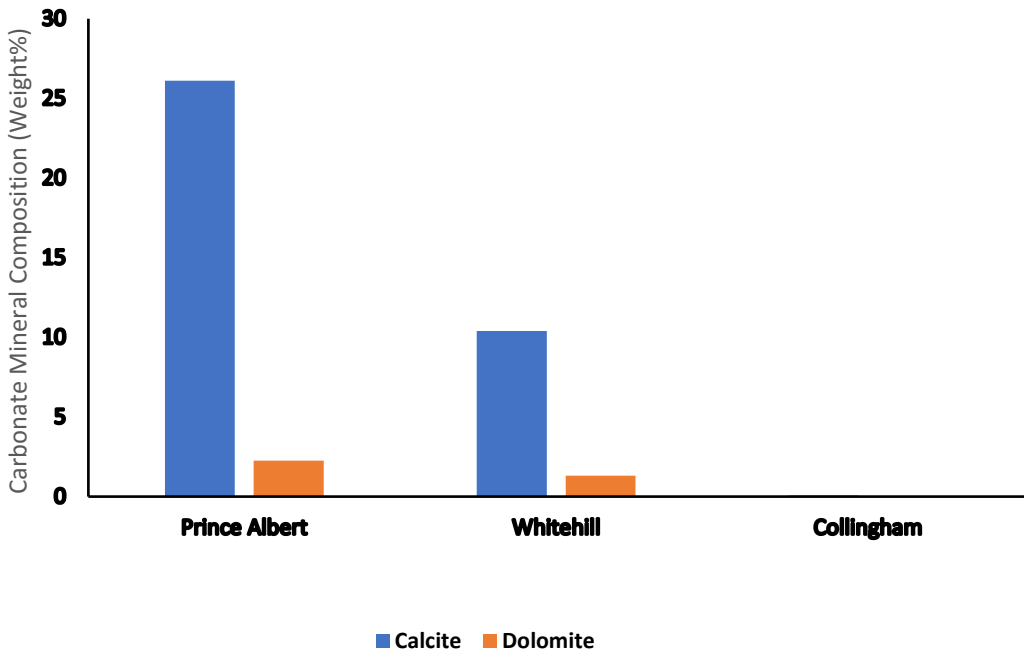


Figure 5.2: Carbonate mineral composition in the three formations

According to Liang et al. (2016), the calcite content in the calcareous shale ranges from 20% to 50%. Zhao et al. (2017) indicate that the carbonate content of calcareous shale, mainly calcite and seldom dolomite, is greater than 10%. The presence of calcite in the studied samples may indicate and support that the deposition of the sediments occurred in a marine environment (El-Anwar et al., 2018).

Dolomite is the least abundant carbonate mineral in the studied mudstones and shales. Its average content ranges from 0.00 wt.% at Collingham Formation to 1.32 wt.% at Whitehill Formation and 2.25 wt.% at the Prince Albert Formation (Figure 5.2). This study determined that the content of carbonates decreases gradually upwards in the formations – the Prince Albert Formation having the highest concentration and the Collingham Formation having the lowest concentration.

5.3.3 Clay mineralogy

Clay minerals are classified into four main groups: smectites (montmorillonite), illite, kaolinite and chlorite (Okeke & Okogbue, 2011). Clay minerals are the least dominant minerals in the studied samples. Illite is the most dominant constituent of the clay minerals in the mudstones and shales (Figure 5.3). The average content of illite in the mudstones and shales ranges from

7.17 wt.% at the Whitehill Formation to 13.22 wt.% at the Prince Albert Formation and 16.2 wt.% at the Collingham Formation (Figure 5.3). Chlorite is the second most abundant clay mineral and its average content ranges from 0.2 wt.% at the Whitehill Formation to 1.37 wt.% at the Prince Albert Formation and 2.00 wt.% at the Collingham Formation.

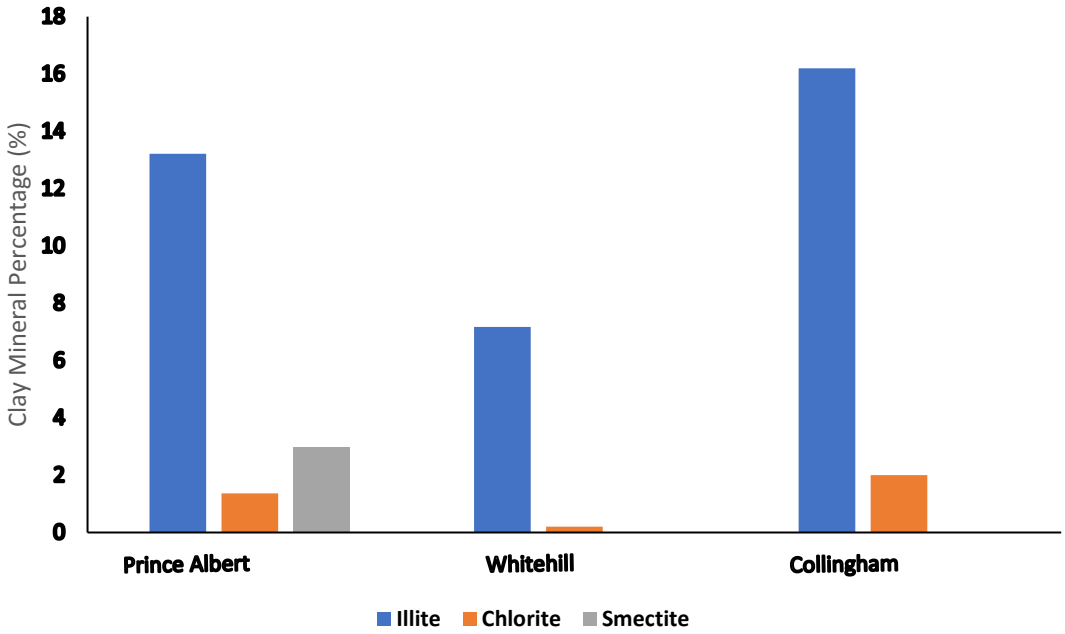


Figure 5.3: Clay mineral composition in the three formations

Illite is a common mineral in sedimentary rocks, particularly shales, and it may precipitate in the pores of the reservoirs, impeding fluid flow (Pevear, 1999). According to Weaver (1956), illite is dominant in organic-rich marine shales and old sediments. Kaolinite dominates continental and near-shore sediments but is rarely present in old sediments. Kaolinite-rich sediments are poorly represented in older geologic times.

Smectite is the least abundant clay mineral in the studied samples. It was detected only in the Prince Albert Formation (Figure 5.3). The average content of smectite in the studied mudstones and shales ranges from 0.00 wt.% at the Whitehill and Collingham Formations to 2.97 wt.% at the Prince Albert Formation. Smectite expands (Altaner, 1978; Okeke & Okogbue, 2011) and contracts upon wetting and drying (Altaner, 1978). Generally, smectites occur in a low-energy marine alkaline environment (Okeke & Okogbue, 2011). Other clay minerals such as illite, chlorite and kaolinite are non-expansive (Okeke & Okogbue, 2011; Shoieb et al., 2017). They

occur in a high-energy non-marine neutral/acidic environment where the rate of leaching is high (Okeke & Okogbue, 2011). A high smectite content indicates good gas storage capability (Deng et al., 2018).

This study suggests that the Prince Albert Formation mudstones are likely to be affected by swelling and shrinking due to the presence of smectite constituents compared to the other two formations. On the other hand, the Prince Albert Formation mudstones have better gas storage capacity due to the availability of smectite compared to the Whitehill and Collingham Formations.

Comparison of the Barnett Shale with the current study

The Upper Barnett Shale is calcite-rich, averages ~20%, and dark to light grey interlaminations predominate. Calcareous shale together with low TOC is associated with shallow water and oxic conditions (Abouelresh & Slatt, 2012). In the current study, the lowest of the Ecca Group unit – the Prince Albert Formation – has low TOC content with averages of 0.181 wt.% (Geel & Bordy, 2021; Geel et al., 2021) and is composed of calcareous mudstones; calcite averages at 26 wt.%. The low TOC content in the lowermost Ecca Group formation indicates a lack of organic matter preservation. High calcareous and low TOC content suggests that the Prince Albert sediments were deposited in relatively shallow water, oxic conditions.

The Lower Barnett Shale comprises both detrital and biogenic quartz and is composed of black, massive, organic-rich siliceous non-calcareous mudstones. The high TOC in the Lower Barnett Shale indicates a low-energy, anoxic depositional environment (Abouelresh & Slatt, 2012). The mineralogical and geochemical descriptions of the Lower Barnett Shale correspond with the Whitehill Formation of the Lower Ecca Group which consists of black carbonaceous siliceous shales and has a high TOC content. Recent investigation shows high TOC content (~5 wt.%) in the Whitehill Formation which suggests anoxic conditions (Geel & Bordy, 2021). The Prince Albert Formation indicates deposition in oxic conditions, while the Whitehill Formation shows deposition under an anoxic environment.

A research study by Chen (2012) indicates that samples representing the Barnett Shale are mainly composed of quartz, clay minerals, pyrite and carbonate. The XRD results indicate that quartz is the more dominant mineral than clay and carbonate. According to Bruner and Smosna

(2011), the quartz content in the Barnett Shale is around 35%–50%, calcite and dolomite 8%–19% and illite 27%. Essentially, XRD results have been obtained from Newark East and the results indicate that the Barnett Shale is composed of ~45% quartz, ~27% clay (mainly illite and a small amount of smectite) and ~8% calcite and dolomite (Bowker, 2007).

On the other hand, the Ecca Group of the Main Karoo Basin has an average quartz content of 68.6 wt.% with 4.8 wt.% clay (mainly illite and a small amount of smectite) and 6.7 wt.% calcite and dolomite. Shale develops natural and induced fractures during hydraulic fracturing treatments (external forces) when it has high quartz, feldspar and carbonate content because of a low Poisson's ratio, high Young's nodulus and high brittleness (Ding et al., 2012).

The Lower Ecca Group has low clay and high quartz content relative to the Barnett Shale. The clay content averages 4.79 wt.% in the Lower Ecca Group and 31 wt.% in the Barnett Shale (Milliken et al., 2012). The quartz content averages 68.60 wt.% at the study area and 43 wt.% in the Barnett Shale. The quartz content in the Prince Albert averages 48.6 wt.% with Whitehill, 79.8 wt.% and Collingham 77.4 wt.% – higher than in the Barnett Shale. The clay content in the Prince Albert averages 5.85 wt.% with Whitehill 8.1 wt.% and Collingham 6.1 wt.% – lower than in the Barnett Shale. Dolomite is the dominant carbonate mineral and averages 8 wt.%, while calcite averages 5 wt.% in the Barnett Shale (Milliken et al., 2012). In the current study, calcite is the dominant carbonate mineral and averages 12.19 wt.%, while dolomite averages 1.19 wt.%. The dominant minerals in the Barnett Shale are quartz, calcite, dolomite, clay minerals, feldspar and muscovite (Perez, 2010).

The Barnett Shale can be divided into three facies. Facies 1 has the highest quartz content; it is easier to initiate hydraulic fracturing in it and it represents the best reservoir rock. Facies 2 is constituted of moderate calcite content and facies 3 is rich in calcite (Perez, 2010). Based on the mineral types and their relative concentrations, determined using the XRD and petrographic data, the shales in the present study can be classified into two facies. Facies 1 (calcareous mudstone) has calcite-rich mudstone with greater than 20 wt.% calcite and the lowest quartz concentration; only lithofacies with a measured amount of smectite occur. Facies 2 (siliceous shale) has quartz-rich shale with the highest silica content – a range of 48.4 to 91.7 wt.% and an average of 78.6 wt.%. These lithofacies have a low concentration of clays and an absence of smectite.

The Barnett Shale in the United States has been successfully developed using hydraulic fracturing processing. Therefore, based on the comparative mineralogical data derived from the XRD analysis of the Barnett Shale in the United States and Ecca Group in South Africa, hydraulic fracturing treatments in the Ecca Group formations would be successful.

Comparison of previous investigations with the current study

According to previous investigations by Geel et al. (2015), the Whitehill Formation is largely composed of illite, quartz and muscovite and, in the current study, the formation mostly consists of quartz and illite. The Whitehill Formation is higher in clay minerals and relatively lower in silica content than the Collingham and Prince Albert Formations. In the present study, the Prince Albert Formation is higher in clay minerals and relatively lower in silica than the Whitehill and Collingham Formations. The Collingham Formation has the highest percentage of quartz (62%) relative to the lower two formations. In the present study, the Whitehill Formation has the highest percentage of quartz (averages 81.3 wt.%).

Mews et al. (2019) suggest that an effective hydraulic fracturing candidate requires high amounts of brittle minerals such as quartz and carbonate. Quartz is regarded as a mechanically strong mineral, while carbonate (calcite and dolomite) and clay (chlorite, illite and smectite) minerals are mechanically intermediate and mechanically weak, respectively (Geel & Bordy, 2021; Mews et al., 2019). In the present study, the Whitehill and Collingham Formations are mechanically strongest due to their high content of strong and brittle mineral phases, while the Prince Albert Formation is the weakest of the Lower Ecca Group due to its lowest content of strong and brittle mineral phases. However, recent work conducted by Geel and Bordy (2021) suggests that the Prince Albert Formation is mechanically strongest, followed by the Collingham Formation; the Whitehill Formation is the weakest due to the highest content of weak and ductile mineral phases.

The presence of clay minerals such as illite and smectite in the studied mudstones and shales is in agreement with results from previous studies (Nyathi, 2014; Ferreira, 2014). Nyathi (2014) documented that the Prince Albert Formation is dominated more by illite than kaolinite. The results obtained by Ferreira (2014) indicate that kaolinite, illite and smectite are the dominant clay minerals in the studied samples. Kaolinite is believed to have originated from the replacement of chlorite by smectite and also from further chemical alteration. Illite is believed

to have been formed from the weathering of feldspar and is present in the Prince Albert, Whitehill and Collingham Formations. Smectite was found to be present in the Whitehill Formation samples (Ferreira, 2014) and, in the current study, smectite was found to be present in the Prince Albert Formation mudstones.

The overall interpretation is that the mineralogy of shale and mudstone in the study area shows suitable brittleness as a result of high quartz and carbonate content rather than clay. This interpretation is in agreement with the interpretation of Geel et al. (2015) who indicated that the mineralogy of shale suggests suitable brittleness due to high quartz, calcite and dolomite content.

During hydraulic fracturing, high quartz content and natural cracks promote the generation of network fractures (Shen et., 2017). The Lower Ecca Group, particularly the Whitehill Formation, is suggested as a potential shale reservoir due to the following characteristics: high organic richness, high TOC content (~5 wt.%), porosity resulting from the decomposition of organic matter and mineral induced brittleness, among others. The Whitehill Formation was deposited under suitable anoxic bottom water conditions that allow the preservation of organic matter (Geel et al., 2015; Geel et al., 2021).

5.4 Major element data analysis

The major element geochemistry of the shales and mudstones in the three formations (Prince Albert, Whitehill and Collingham) is distinguishable. SiO_2 is the dominant constituent of all studied samples and has an overall average content of 63.19 wt.%. The SiO_2 composition varies from 26.60 to 87.62 wt.% (Figure 5.4). The Prince Albert Formation has the lowest average concentration of SiO_2 (37.67 wt.%), while the Whitehill Formation has the highest average concentration (78.10 wt.%). The Prince Albert Formation has the lowest SiO_2 content and highest CaO constituents when compared to the other two formations. SiO_2 content tends to decrease with an increase in CaO content. This correlates very well with the petrographic and XRD analysis discussed above. The XRD analysis indicates that the Prince Albert Formation has the lowest quartz and highest carbonate (calcite, chlorite and dolomite) content.

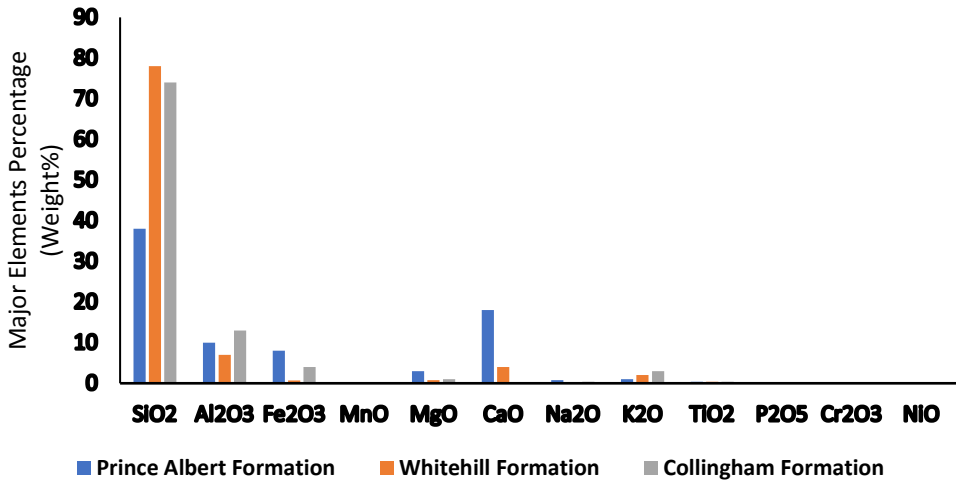


Figure 5.4: Major elements (reported in weight%) of shale samples from the three formations

The CaO content varies from 0.07 to 28.45 wt.%. The lowest concentration is in the Collingham Formation (0.24 wt.%), while the Prince Albert Formation has the highest CaO concentration (17.87 wt.%). The CaO concentrations in the studied mudstones and shales decrease gradually with the stratigraphy (from the oldest to the youngest), meaning that the CaO is highly concentrated at the lowest formation (i.e., Prince Albert). The high CaO content in the Prince Albert Formation could be due to calcite cementing material, as documented by Babu (2017). The significant enrichment of CaO in the Prince Albert Formation (silica poor formation) suggests a calcium dilution effect (Lone et al., 2018). This correlates very well with the observations made in the thin sections of the Prince Albert Formation that show calcite cements.

Comparison of the mineralogical (XRD) and major elements (XRF) data

A comparison of the XRD data with the major elements data suggests that the higher the carbonate mineral content (XRD), the higher the CaO content (XRF). The Prince Albert Formation is characterised by high CaO and Na_2O and low K_2O and TiO_2 (Figure 5.4) when compared with the Whitehill Formation. This study suggests that the high concentration of CaO in the Prince Albert Formation has been elevated by high carbonate content; a suggestion supported by Tobia and Shangola (2016). In summary, the Prince Albert Formation is high in CaO, Na_2O, MgO, P_2O_5 and low in SiO_2, K_2O, TiO_2.

Major elements plots

The bivariate diagrams (Figures 5.5a to 5.5d and 5.6a to 5.6d) of the major elements aim at characterising the geochemical composition of the source rocks and determining their possible provenance. Diagrams were plotted with the actual major elements results from the present study. The Al_2O_3 element was used as a normalisation factor because it is immobile during weathering and diagenesis (Ahari & Afarin, 2016).

The Hacker diagrams concerning SiO_2 correlate negatively with Na_2O, CaO, Fe_2O_3 and Al_2O_3. The negative correlations (Na_2O, CaO, Fe_2O_3 to SiO_2) suggest the non-association of major oxides with SiO_2 (Obasi et al., 2015; Ahari & Afarin, 2016) and indicate that much SiO_2 is present as quartz grains (Ahari & Afarin, 2016). The unstable minerals in the rock samples decrease with an increase in the maturity of the rocks (Hu et al., 2015). The SiO_2/Al_2O_3 ratio is mostly used to determine the maturity of sandstones (Roser et al., 1996).

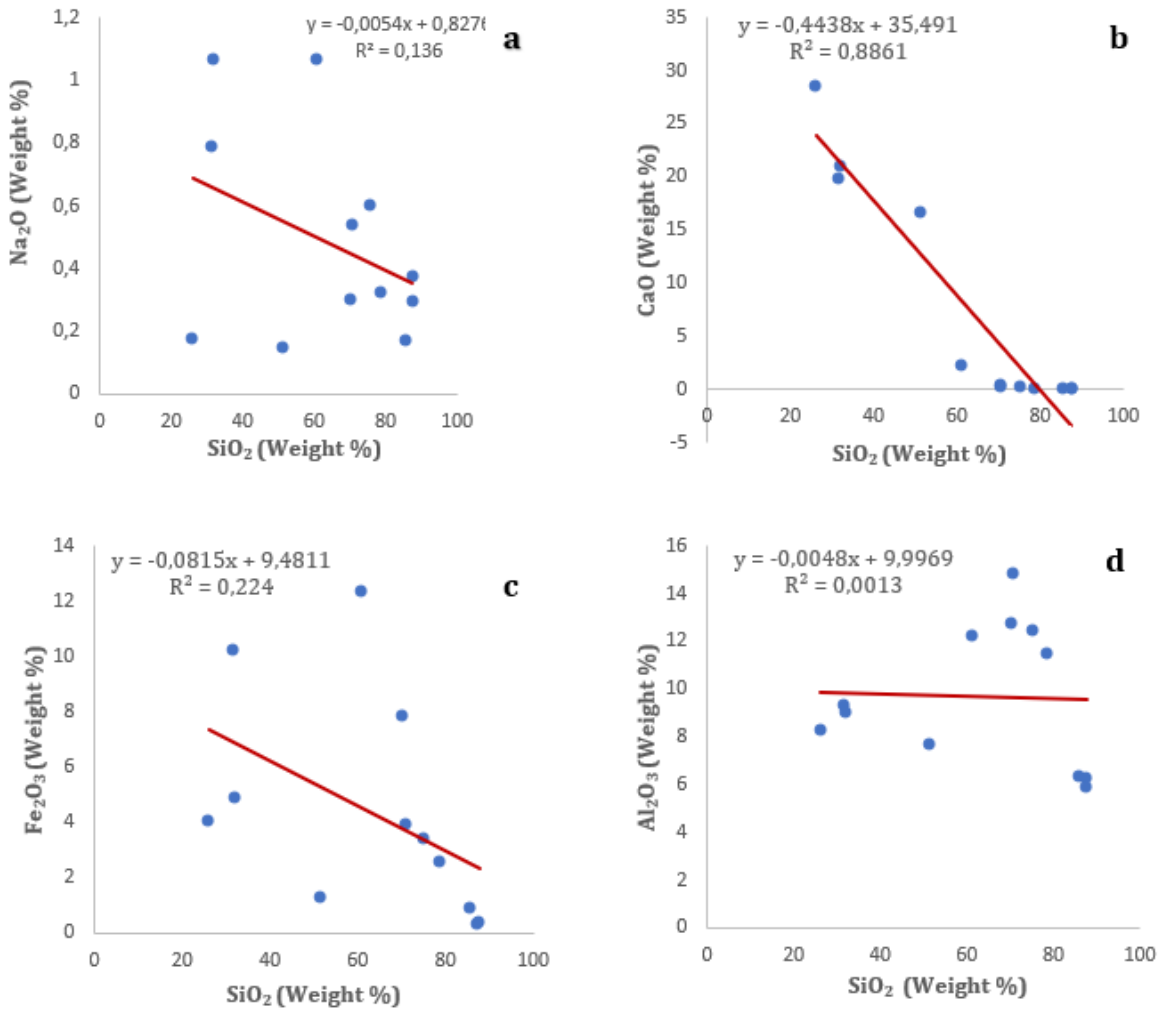


Figure 5.5: (a-d) Hacker diagrams of major oxides (Na_2O, CaO, Fe_2O_3 and Al_2O_3) versus SiO_2 (negative correlations)

The method used by Babu (2017) to obtain the distribution patterns of Al_2O_3 with other oxides, such as Fe_2O_3 and TiO_2, was also recommended for this study. Ratios of Fe_2O_3/Al_2O_3 and TiO_2/Al_2O_3 in the studied samples show that there is a good positive correlation (Figures 5.6a and 5.6b). Positive correlations between major oxides indicate that they are associated with clay and/or micaceous minerals (Obasi et al., 2015; Ahari & Afarin, 2016; Baiyegunhi et al., 2017b; Lone et al., 2018). Secondly, the K_2O/Al_2O_3 ratio of 0.499 and a good positive correlation (Figure 5.6c) may also suggest that the mudstone and shale samples contain a considerable amount of clay minerals, as indicated by Pandey and Parcha (2017). The enrichment of K_2O depends on clay minerals (Babu, 2017; Barbera et al., 2006).

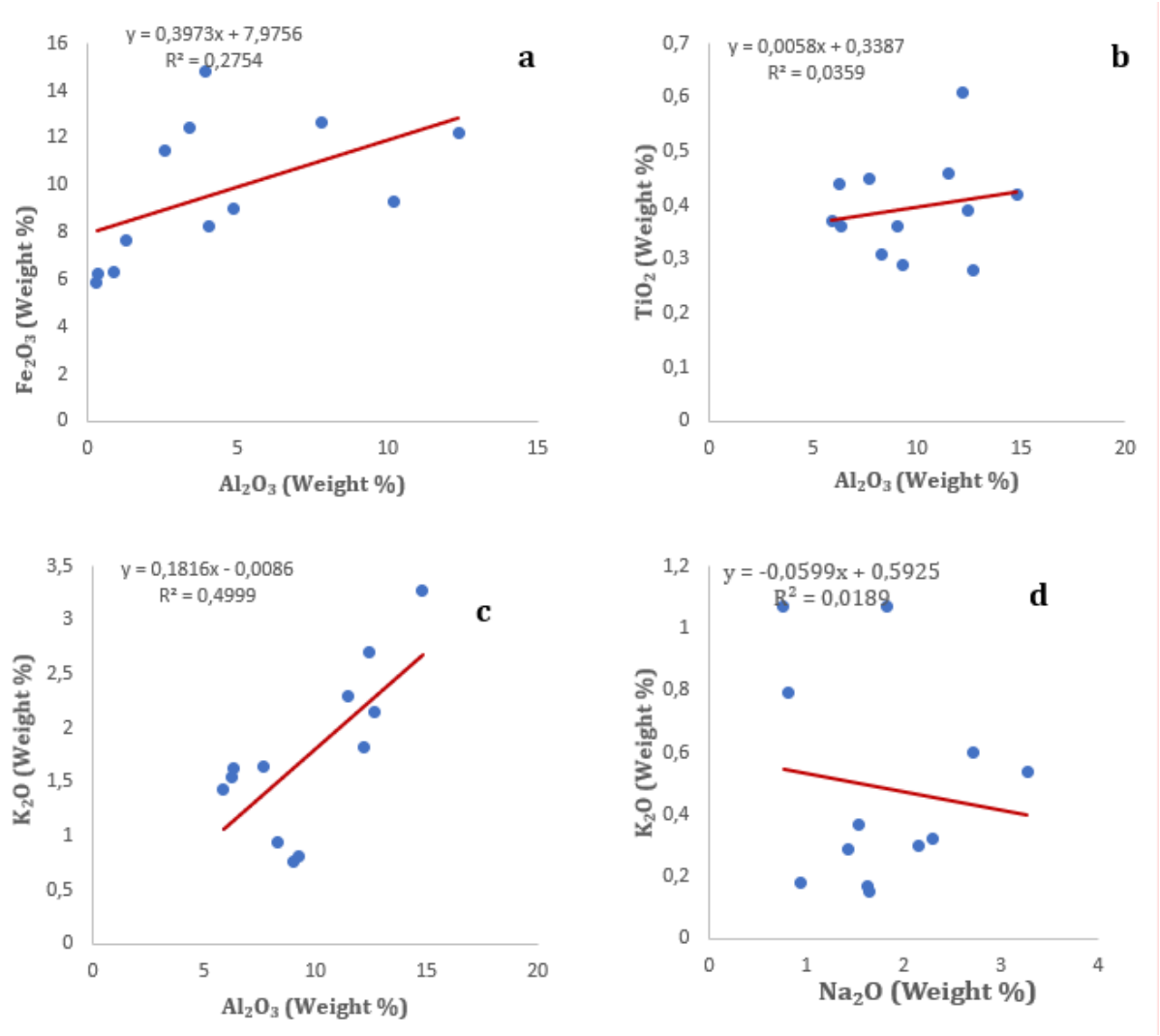


Figure 5.6: (a-c) Hacker diagrams of major oxides (Fe_2O_3, TiO_2 and K_2O versus Al_2O_3), positively correlated; (d) negatively correlated Na_2O/K_2O

Comparison of the Barnett Shale with the current study

The concentrations of the major elements in the present study are generally higher than in the Barnett Shale (Table 5.1), except for CaO, MgO and MnO. The SiO_2 content of the Barnett Shale averages 15.16 wt.% (Colwell, 2014). The SiO_2 content in the current study averages 63.19 wt.% – relatively higher than in the Barnett Shale (15.16 wt.%). The SiO_2 content in the Prince Albert Formation averages 37.82 wt.%, Whitehill 78.1 wt.% and Collingham 56.1 wt.%. The amount of silica content in the Barnett Shale makes it a better target for hydraulic fracturing (Tian & Ayers, 2010), suggesting that the hydraulic fracturing treatments in the study area would be a success because of the higher brittle content than clay. It is suggested that high SiO_2 and low clay content in the Prince Albert, Whitehill and Collingham Formations

will enhance the development of natural and induced fractures under external forces (fracking), as suggested by Ding et al. (2012).

Table 5.1: XRF data (major elements) of the Barnett Shale compared with the current study (Ecca Group)

	XRF Major elements in weight per cent (wt.%)							
Formations	Al_2O_3	K_2O	TiO_2	SiO_2	CaO	MgO	MnO	Fe_2O_3
Barnett Shale (Colwell, 2014)	2.7	0.95	0.2	15.16	13.9	2.99	0.03	1.63
Current Study	9.7	1.75	0.4	63.19	7.45	1.62	0.02	4.33

Comparison of previous investigations with the current study

The SiO_2 content varies from 26.60 to 87.62 wt.% in the present study and is slightly lower compared to those which range from 55.94 to 87.99 wt.% obtained by Baiyegunhi et al. (2017b). The CaO content varies from 0.07 to 28.45 wt.% – higher than the concentration documented by Baiyegunhi et al. (2017b). The low concentrations of TiO_2, MnO, MgO, Na_2O, K_2O and P_2O_5 in the Prince Albert, Whitehill and Collingham Formations conforms to the results obtained by Baiyegunhi et al. (2017b).

5.5 Trace element data analysis

Trace element data for this study were grouped into LILE (Rb, Ba, Sr, Th and U), HSFE (Zr, Hf, Y and Nb) and TTE (Sc, V, Cr, Co, Pb, Ni and Zn). The average Cu, Zn and Pb content in the studied mudstones and shales are 35.25, 46.40 and 27.84 ppm, respectively (Figure 5.7).

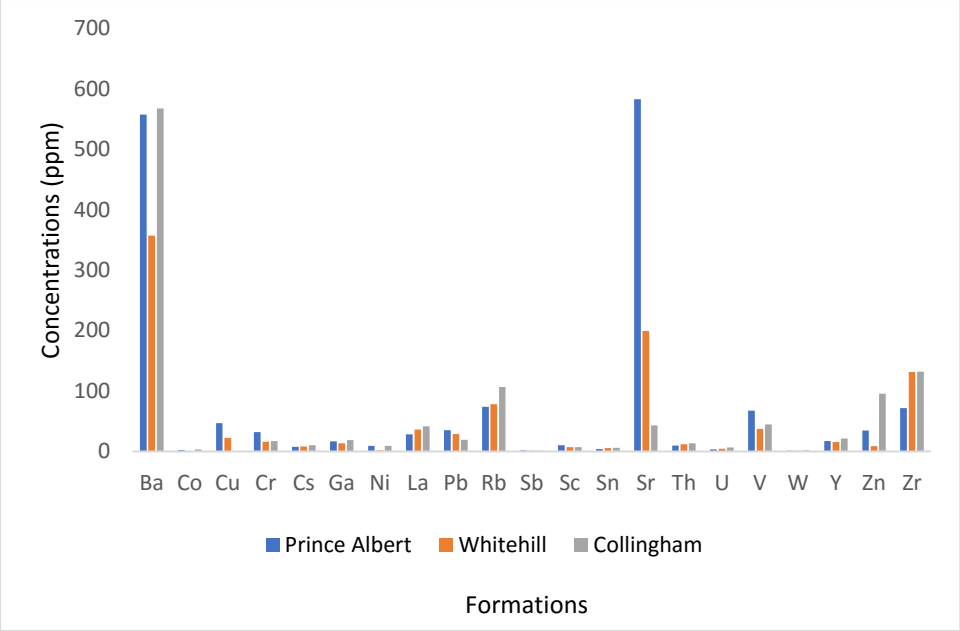


Figure 5.7: Average trace elements (ppm) in the studied samples

The Prince Albert Formation has the highest concentrations of Cu and Pb and also represents the second most abundant Zn concentration of the studied mudstones and shales. The high concentrations of Cu and Pb in the Prince Albert Formation suggest that it contains a significant amount of organic matter compared to the Whitehill and Collingham Formations, however, it has lower TOC content than the Whitehill Formation.

Elements such as Ni, Cu and Zn are deposited with the organic matter (Xu et al., 2018). However, Hofmeyr (1971) indicates that the Pb content is higher in South African shales compared to the average continental crust and shales from other parts of the world. Cr average concentrations in the Prince Albert, Whitehill and Collingham Formations are 31.85, 15.95 and 17.06 ppm, respectively. The Prince Albert Formation has the highest Cr concentration compared to the other two upper formations. The Cr is associated with clay minerals (Tao et al., 2017).

The studied mudstone and shale samples show average Co and Ni content of 2.09 and 6.75 ppm, respectively. Under coastal sediments, the Ni concentration is less than 39 ppm. The high concentration of Ni content indicates high productivity (El-Anwar, 2018). V average concentration varies from 20.12 ppm to 91.58 ppm in the studied mudstones and shales. The highest average value of V at 67.34 ppm in the current study was recorded in the Prince Albert Formation and the lowest average value at 37.15 ppm was recorded in the Whitehill Formation.

The high concentration of V in the Prince Albert Formation may be the result of oxidation and the weathering of organic matter, as suggested by El-Anwar (2018).

Trace element plots

The nature of the sedimentary rocks within the depositional basin is linked to their provenance. The geochemical composition of the mudrocks commonly reflects the provenance of their detrital source rocks (Dickinson & Suczek, 1979). The HFSE (Nb, Zr, Sc, Ti and Hf) were selected because they are immobile and thought to resemble provenance compositions (Bhatia & Crook, 1986). There are four tectonic settings recognised: oceanic island arc, continental island arc, active continental margin and passive margin. The geochemical signatures of the rock are important in characterising various plate tectonic regimes (Bhatia & Crook, 1986). The Main Karoo represents a retro-arc foreland system (Catuneanu et al., 2002; Johnson, 1991).

A good correlation observed in the ratio diagram (Figure 5.8) of K_2O/Rb indicates that the Rb content is mainly controlled by K-rich minerals such as illite (Hu et al., 2015). The positively correlated Cr/Ni ratio denotes that the mudstones and shales of the study area have suffered weak weathering (Hu et al., 2015). There is an excellent positive correlation between Zr and Hf, indicating similar geochemical behaviour (Figure 5.8). Ratio Al_2O_3/Rb shows a good positive correlation, which indicates that K_2O and Rb enrichments are a result of clay minerals (Barbera et al., 2006; Pandey & Parcha, 2017) correlating very well with the major element data.

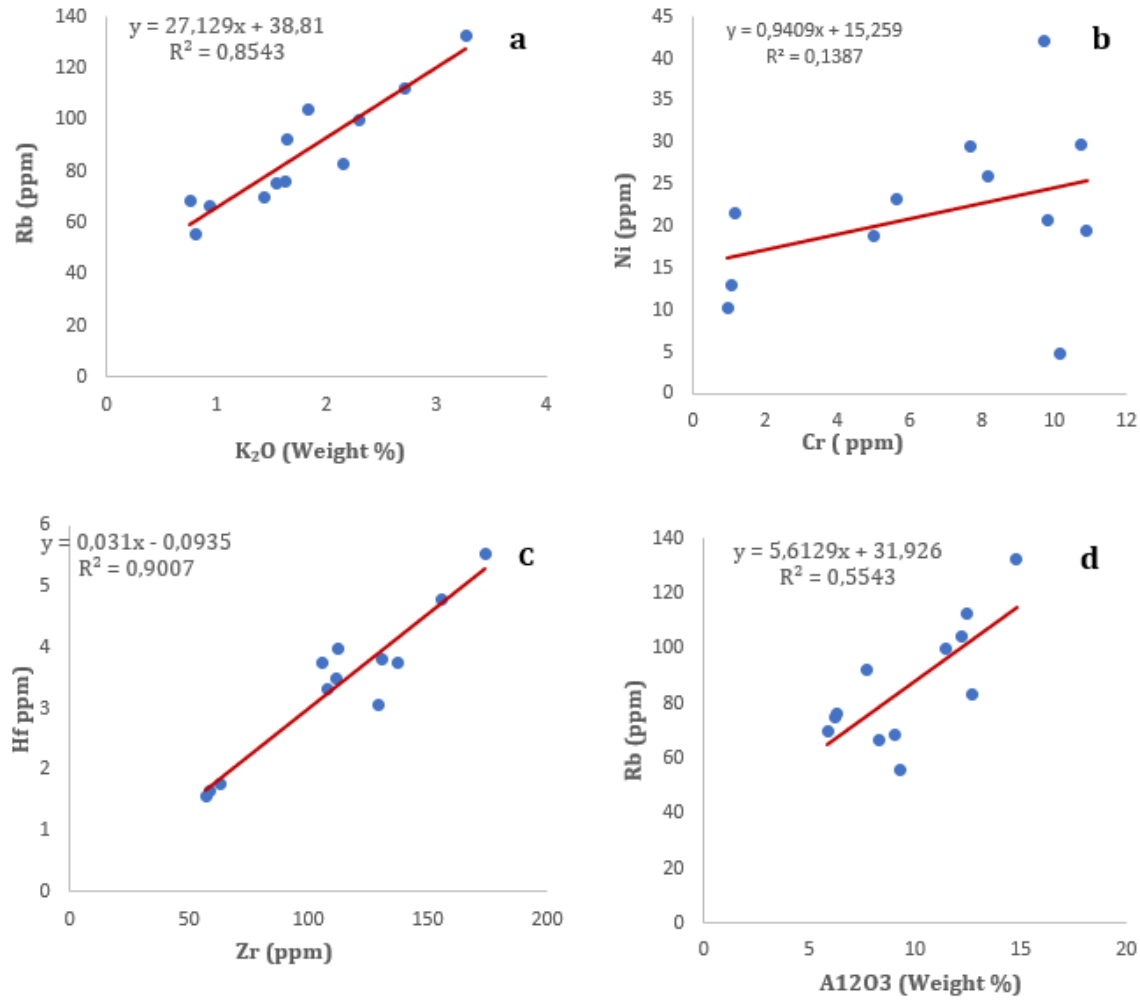


Figure 5.8: (a-d) Bivariate plot diagrams of K_2O and Rb, Cr and Ni, Zr and Hf and Al_2O_3 and Rb showing good strong correlations

According to the Ni versus TiO_2 plots diagram of Floyd, Winchester and Park (1989), the rocks of the Lower Ecca Group were derived primarily from acidic magmatic sources (Figure 5.9).

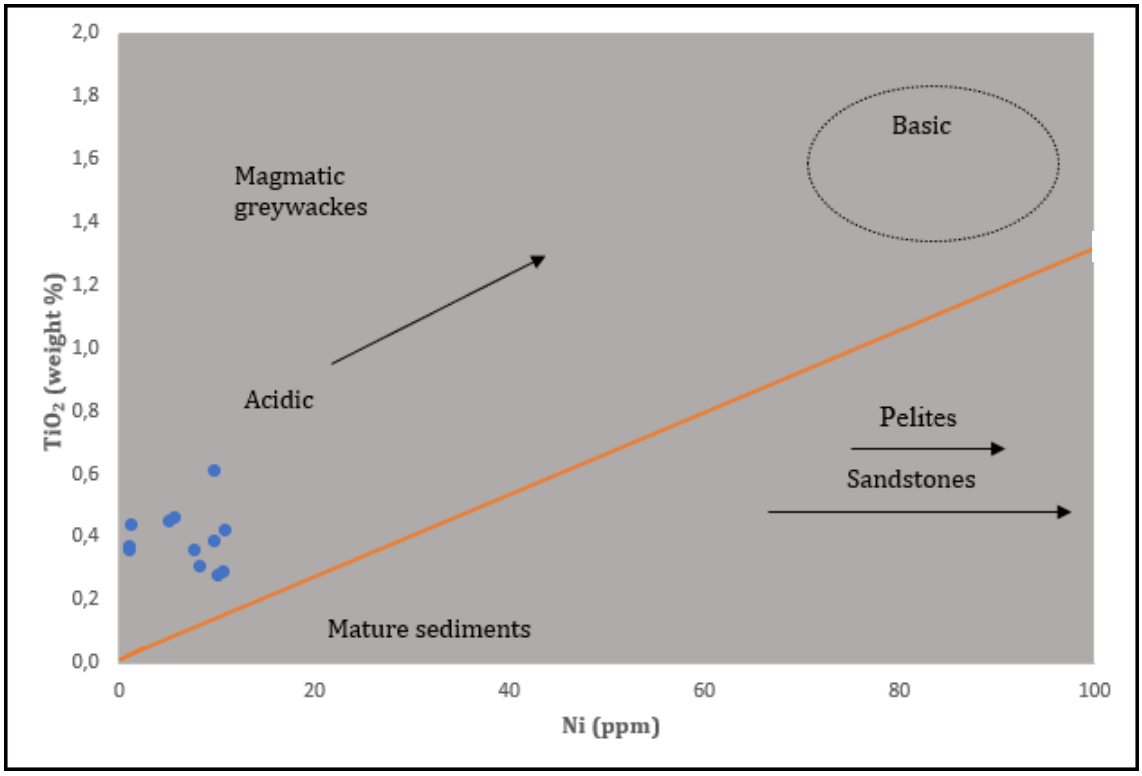


Figure 5.9: Ni versus TiO_2 plot diagram to characterise source rock composition in the study area (Floyd et al., 1989)

To determine the origin of the sediments in the study area, a Zr versus TiO_2 binary plot was considered. A Zr versus TiO_2 plot is useful to deduce the provenance of the sediments (Lone et al., 2018). According to the Zr versus TiO_2 plot diagram (Lone et al., 2018), the mudstones and shales were mainly derived from felsic igneous provenance (Figure 5.10). These findings are also supported by the Ni versus TiO_2 plot diagram (Figure 5.9), which indicates that the sediments of the Lower Ecca Group were derived from acidic magmatic rocks.

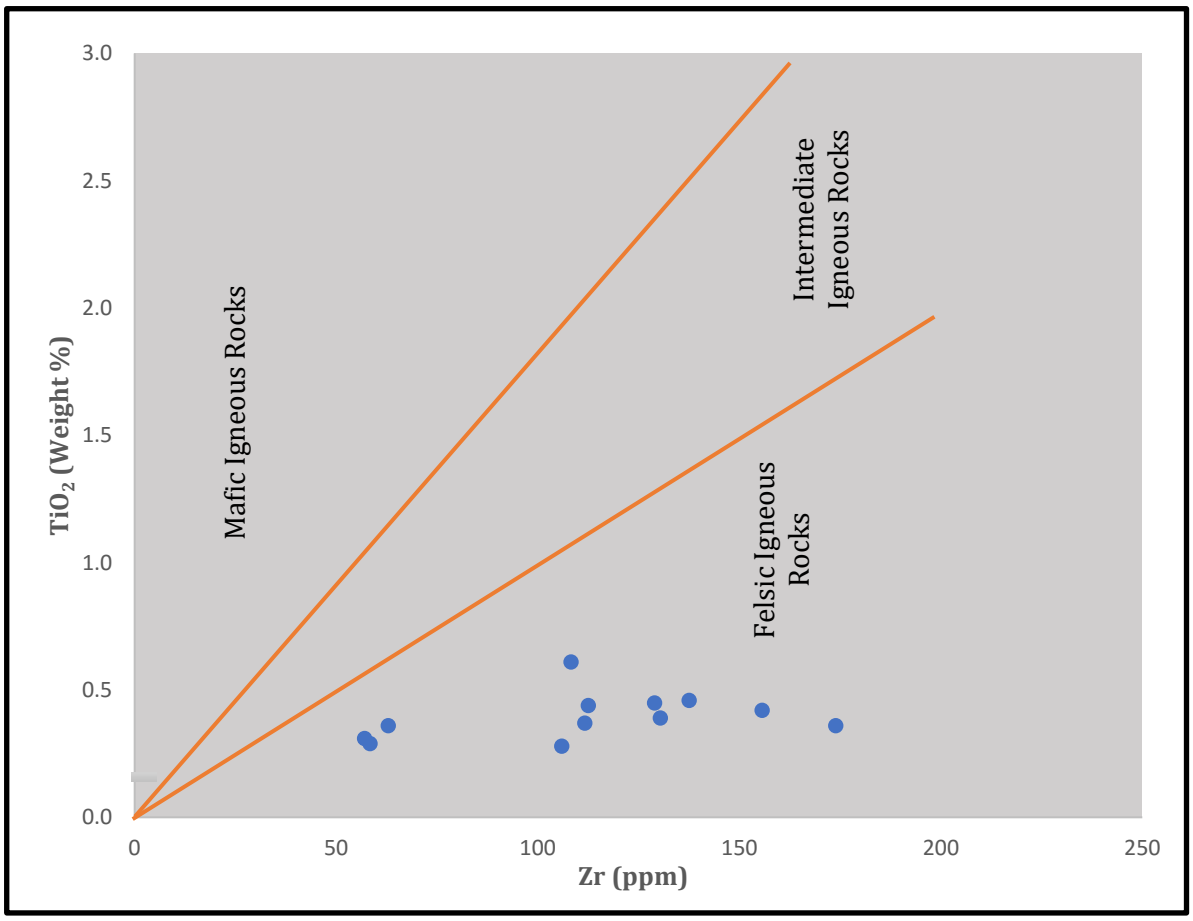


Figure 5.10: Zr versus TiO_2 plots diagram to discriminate provenance of the rocks in the study area (Lone et al., 2018)

These study findings correlate positively with the findings by Baiyegunhi et al. (2017b) in the Karoo Basin of South Africa and Berti (2014) in the Karasburg Basin of southern Namibia. According to Harkness et al. (2018), the Ecca Group rests on top of the acidic Archean granites and metamorphosed felsic volcanic rocks which form the basement. On the other hand, Findlay III (2016) suggests that the rocks of the Ecca Group were sourced from Permian granite and rhyolite of the Gondwanide Magmatic Arc and the Palaeozoic-Palaeoarchean sedimentary rocks of the CFB. However, a recent study in the Lower Ecca Group indicates that the Prince Albert, Whitehill and Collingham Formations plot in mafic, intermediate and felsic igneous fields (Geel & Bordy, 2021).

Comparison of the current study with the upper continental crust

Carbonaceous black shale such as that of the Whitehill Formation of the Ecca Group is expected to be enriched in trace elements such as Co, Cr, Cu, Ni, V and Zn (El-Anwar, 2017).

However, this study indicates that most of these elements are depleted in the mudstones and shales of the Prince Albert, Whitehill and Collingham Formations relative to UCC.

Comparison of the Barnett Shale with the current study

The Barnett Shale is enriched with Ni (75.83 ppm), Zn (190.52 ppm), U (11.32 ppm) and V (118.32 ppm) trace elements, while the Prince Albert, Whitehill and Collingham Formations are enriched with Th, Rb and Zr (Table 5.2). The concentration of Cu is relatively high in the Prince Albert Formation compared to that in the Barnett Shale, while the concentrations are lower in the Whitehill and Collingham Formations.

Table 5.2: Trace element data of the Barnett Shale compared with the current study (Colwell, 2014)

	Trace elements in parts per million (ppm)							
Formations	Ni	Cu	Zn	Th	Rb	U	Zr	V
Barnett Shale	75.83	36.92	190.52	4.92	57.68	11.32	58.63	118.32
Prince Albert	9.1	46.8	34.8	9.58	73.73	3.33	71.6	67.3
Whitehill	2	22.6	8.8	11.96	78.38	4.7	131.8	37.2
Collingham	9.1	32.8	95.6	13.63	106.95	6.7	132.4	44.7

According to Dean et al. (1984), trace elements such as Cd, Cu, Zn, V, Ni and Cr are enriched in organic carbon-rich shales. The enrichment of these trace elements in organic-rich sediments may be associated with chemical sorption and precipitation with organic detritus under anoxic conditions. The enrichment may reflect the deposition of sediment under anoxic conditions in the deep sea. The comparative trace element data suggest that the Barnett Shale is enriched in organic carbon due to high levels of Ni, Zn and V compared to the Lower Ecca Group formations.

Comparison of the Marcellus Shale with the current study

A comparison of the Marcellus Shale trace element data relative to the current study reveals that the mudstones and shales from the study area have low concentrations of Co, Cr, Cu, Ni, V, Zn and Y and a high concentration of Ba. The Whitehill and Collingham Formations have

high concentrations of La and Zr relative to the Marcellus Shale, while the Prince Albert Formation has a high concentration of Sr. The Prince Albert, Whitehill and Collingham trace element concentrations are generally lower relative to the concentrations of the reference shale (the Marcellus Shale). The comparative trace element data reveal that the Marcellus Shale is enriched in Cu, Zn, V, Ni and Cr trace elements relative to the Lower Ecca Group formations (Table 5.3). These trace elements are known to be high in sediments enriched with organic carbon. This suggests that the Prince Albert, Whitehill and Collingham Formations are organic carbon impoverished compared to the Marcellus and Barnett Shales of the United States.

Table 5.3: Comparison of the Marcellus Shale trace element data to this study (Werne et al., 2002)

Trace element (ppm)	Marcellus Shale: Oatka Creek Formation	Prince Albert Formation	Whitehill Formation	Collingham Formation
Ba	282.8	557.4	357.3	567.3
Co	21.3	2.5	0.4	3.5
Cr	66.9	31.9	15.9	17.1
Cu	113.3	46.8	22.6	32.8
La	30.8	28.4	36.1	41.7
Ni	119.2	9.1	2	9.1
Sr	255.1	582.7	199.2	43.3
V	134.9	67.3	37.2	44.7
Zn	398.3	34.8	8.8	95.6
Zr	101.5	71.6	131.8	132.4
Y	26.6	17.5	15.6	21.3

Comparison of the previous investigations with the current study

Trace element data of the current study are in agreement with those of previous investigation (Baiyegunhi et al., 2017b) which document that TTE (Sc, V, Cr, Ni and Zn) in the Lower Ecca Group formations are depleted relative to UCC and PAAS except for Cu and Zn. Other trace elements which are depleted include Rb, Ba, Sr and Nb relative to UCC and PAAS

concentrations. Zr, Hf and Y are comparable with that of UCC and PAAS (Baiyegunhi et al., 2017b).

The overall interpretation suggests that trace element depletion in the mudstones and shales from the study area could be due to weathering. Weathering can disperse the elements hosted in shales and, during this process, some elements may be depleted and others enriched (El-Anwar, 2017). The Prince Albert Formation is enriched with Sr and Pb, the Whitehill Formation with Zr, while the Collingham Formation is enriched with Rb, Th, U and Zn. Shales with high TOC are strongly enriched in U, V, Zn and Pb (Algeo & Maynard, 2004).

Trace elements such as Ni and Cu indicate the presence of organic matter and their abundance may be retained within sediments hosted by pyrite. Ni and Cu may be attributed to the original presence of organic matter even if it is partially lost after deposition. U and V can be used to convert paleoredox conditions and their enrichments may indicate euxinic conditions (Tribovillard et al., 2016). According to Chermak and Schreiber (2014), trace elements can have a broad concentration range in shales within the same formation.

CHAPTER 6: CONCLUSIONS

The groundwork for understanding the characteristics of the mudstones and shales of the Lower Ecca Group has been previously established. In this research, the objective to determine whether the rocks of the Lower Ecca Group are conducive to hydraulic fracturing operation has been achieved. The Ecca Group of the Karoo Basin has been the main target for shale gas exploration in South Africa. Its development requires an integrated approach aimed at assessing the practicality of any proposed development using the hydraulic fracturing method.

One of the criteria for a commercially viable shale gas formation is to determine the percentage of brittle and ductile minerals in the shale. It is generally recognised that shale formations with a higher percentage of brittle minerals (quartz and carbonate) than ductile minerals (clay) contribute largely to a successful hydraulic fracturing operation (Chopra et al., 2014; Tang et al., 2015; Zhao et al., 2017). The integration of petrographic and mineralogical analyses revealed that the lower formations of the Ecca Group possess higher brittle mineral content than ductile mineral content, suggesting that the formations are conducive to hydraulic fracturing.

Although it is universally accepted that quartz and carbonate minerals promote rock brittleness, recent studies indicate that excessive quartz content of above 70% reduces the brittleness of the shale formation (Ye et al., 2020), thereby reducing the success rate of the hydraulic fracturing process. The Whitehill and Collingham Formations have a quartz content of greater than 70 wt.%, meaning that the success rate of the hydraulic fracturing process may be reduced. The Prince Albert Formation has quartz content between 20 and 70 wt.% and may be conducive to the hydraulic fracturing process.

Even though the petrographic, mineralogical and geochemical tests indicate the presence of the desired characteristics of rock materials, the impact of diagenetic transformations (cementation) on formation fracability cannot be ignored. This study indicates that the lower formations of the Ecca Group have suffered multiple diagenetic changes, including cementation. The common diagenetic cements in the Prince Albert and Whitehill Formations include quartz and carbonate (mostly calcite).

Field and petrographic observations within the Lower Ecca Group in the study area recognise various structures such as fractures and folds. This study recognises suggestions made by previous studies (Fagereng, 2012; Geel et al., 2021) largely linking the deformation of the Lower Ecca Group units with the CFB and assisted by dissolution (Baiyegunhi et al., 2017b). This study suggests that, other prime shale gas target areas which are less deformed due to CFB may likely experience diagenetic mineral precipitation accomplished by the dissolution of silicate materials and the recrystallisation of fine minerals due to the compaction of sediments, as suggested by Baiyegunhi et al. (2017b). The high maturity of the Lower Ecca Group may also play a role (Geel et al., 2021).

According to Geel et al. (2021), the brittleness of the Lower Ecca Group suggests easy hydraulic fracturing treatments; however, the brittleness may be affected by diagenetic mineral precipitation. Baiyegunhi et al. (2017b) and Geel et al. (2021) suggested that diagenetic alteration due to cementation may reduce the porosity and permeability of the Lower Ecca Group leading to poor reservoir quality and increasing the requirement for hydraulic fracturing and additional stimulation methods to enhance gas recovery and flow capacity.

The current study compared the significant geological characteristics of the Barnett and Marcellus Shales in the United States with the Lower Ecca Group formations in South Africa. The data provided a good indication that the mineralogical composition of the Lower Ecca Group compares favourably with the gas-producing shales (Barnett Shale) of the United States. The Lower Ecca Group contains high brittle mineral content and low ductile mineral content relative to the Barnett Shale.

The Whitehill Formation of the Main Karoo Basin and the Barnett Shale of the Fort Worth Basin share the following similarities: they are both composed of black carbonaceous siliceous shales and have a high TOC content accommodated by an anoxic depositional environment. However, concentrations of the TTE (Cu, Ni, Zn and V) are depleted in the Lower Ecca Group relative to the Barnett and Marcellus Shales.

The current study findings contribute to the existing literature on the Ecca Group and enable an understanding of the behaviour of the formations during shale gas production. However, shale gas development decision-making should also be influenced by studies on thermal

maturity, mechanical properties and total organic content/organic carbonaceous material, among others.

This research study provides insights into how the mineralogy of shales can affect the hydraulic fracturing process in the study area. This study of the Lower Ecca Group has led to several important insights: the Collingham Formation may enable a good seal and traps shale gas from migrating out of the formation below due to high clay content (ductile) relative to the Prince Albert and Whitehill Formations. The high brittle mineral content in the study area may cause natural fractures and the generation of induced network fractures during the hydraulic fracturing process. The study findings indicate that although a higher percentage of brittle minerals (quartz and carbonate) than ductile minerals (clay) is beneficial for shale gas recovery using hydraulic fracturing, diagenetic alteration due to cementation may affect the stimulation process. The mineralogical composition of the Lower Ecca Group compares favourably with the gas-producing shales (Barnett Shale) of the United States.

REFERENCES

Abanda, P.A. and Hannigan, R.E. (2006). Effect of diagenesis on trace element partitioning in shales. *Chemical Geology*, 230(1-2): 42-59.

Abouelresh, M.O. (2014). Core and petrographic sequential analysis of organic-rich shale. Paper presented at second EAGE/SPE/AAPG shale gas workshop, 21-24 September, Dubai. *European Association of Geoscientists and Engineers*. doi: 10.3997/2214-4609.20142272

Abouelresh, M.O. et al. (2017). *Understanding reservoir properties of the organic-rich Qusaiba Shale, a potential shale gas reservoir, Northwest Saudi Arabia: An outcrop approach.* Paper presented at AAPG Annual Convention & Exhibition, 2-5 April, Houston.

Abouelresh, M.O. and Slatt, R.M. (2012). Lithofacies and sequence stratigraphy of the Barnett Shale in east-central Fort Worth Basin, Texas. *American Association of Petroleum Geologists*, 96(1): 1-22. doi: 10.1306/04261110116

Adeniyi, E.O. (2016). *Thermal impact of dolerite sills on the shale gas potential of Ecca Group mudstone in a drill core from the central Main Karoo Basin*. (Unpublished master's thesis). University of Johannesburg, Johannesburg.

Adeniyi, E.O., Ossa, F.O., Kramers, J.D., De Kock, M.O., Belyanin, G., and Beukes, N.J. (2018). Cause and timing of the thermal over-maturation of hydrocarbon source rocks of the Ecca Group (Main Karoo Basin, South Africa). *Marine and Petroleum Geology*, 91: 480-500. doi: 10.1016/j.marpetgeo.2018.01.033

Ahari, R.M. and Afarin, M. (2016). Interpretation of the origin and tectonic setting of coastal sediments in the northeastern of Oman Sea. *International Journal of Waste Resources*, 6(2): 1-9.

Akinlua, A., Ngola, A., Fadipe, O.A. and Adekola, S.A. (2016). Petrography and geochemistry of sandstone samples of Vischkuil formation, Karoo Supergroup, South Africa. *Journal of Petroleum Exploration and Production Technology*, 6(2): 159-167.

Algeo, T.J. and Maynard, J.B. (2004). Trace-element behaviour and redox facies in core shales of Upper Pennsylvanian Kansas-type cyclotherms. *Chemical Geology*, 206: 289-318.

Almond, J.E. (2016*). Proposed Brandvalley Wind Energy facility near Laingsburg, Western & Northern Cape Provinces*. (Palaeontological heritage assessment-combined desktop and field-based study). Natura Viva cc., Cape Town, South Africa.

Altaner, S.P. (1978). ‘Smectite group’ in G.V. Middleton, M.J. Church, M. Coniglio, L.A. Hardie and F.J. Longstaffe (eds), *Encyclopedia of sediments and sedimentary rocks. Encyclopedia of earth sciences series* (pp. 1120-1124). doi: 10.1007/978-1-4020-3609-5_216

Andersson, P.O.D., Worden, R.H., Hodgson, D.M. and Flint, S. (2004). Provenance evolution and chemostratigraphy of a Palaeozoic submarine fan-complex: Tanqua Karoo Basin, South Africa. *Marine and Petroleum Geology*, 21(5): 555-577.

Babu, K. (2017). Geochemical characteristics of sandstones from Cretaceous Garudamangalam area of Ariyalur, Tamilnadu, India: Implications of provenance and tectonic setting. *Journal of Earth System Science*, 126(45): 1-13.

Baiyegunhi, C. (2015). *Geological and geophysical investigation of the Southeastern Karoo Basin, South Africa*. (Unpublished master’s dissertation). University of Fort Hare, South Africa.

Baiyegunhi, C., Liu, K. and Gwavava, O. (2017a). Diagenesis and reservoir properties of the Permian Ecca Group sandstones and mudrocks in the Eastern Cape Province, South Africa. *Minerals*, 7(6): 88.

Baiyegunhi, C., Liu, K. and Gwavava, O. (2017b). Geochemistry of sandstones and shales from the Ecca Group, Karoo Supergroup, in the Eastern Cape Province of South Africa: Implications for provenance, weathering and tectonic setting. *Open Geosciences*, 9(1): 340-360. doi: 10.1515/geo-2017-0028

Baiyegunhi, C., Nxantsiya, Z., Pharoe, K., Baiyegunhi, T.L. and Mepaiyeda, S. (2019). Petrographical and geophysical investigation of the Ecca Group between Fort Beaufort and Grahamstown, in the Eastern Cape Province, South Africa. *Open Geoscience*, 11(1): 313-326.

Barbera, G., Mazzoleni, P., Critelli, S., Pappalardo, A., Giudice, A.L., Cirrincione, R. (2006). Provenance of shales and sedimentary history of the Monte Soro unit, Sicily. *Journal of Mineralogy*, 75(2): 313-330.

Belica, M.E., Tohver, E., Poyatos-More, M., Flint, S., Parra-Avila, L.A., Lanci, L., Denyszyn, S., and Pisarevsky, S.A. (2017). Refining the chronostratigraphy of the Karoo Basin, South Africa: Magnetostratigraphic constraints support an early Permian age for the Ecca Group. *Geophysical Journal International*, 211: 1354-1374. doi: 10.1093/gji/ggx344

Bennett, R.H., O’Brien, N.R. and Hulbert, M.H. (1991). ‘Determinants of clay and shale microfabric signatures: Processes and mechanisms’, in W. Chiou et al. (eds), *Microstructure of fine-grained sediments*. Springer: New York.

Berti, M. (2014). *The evolution of marginal-marine systems of the Amibberg formation, Karasburg Basin, Southern Namibia: Implications for early-middle Permian palaeogeography in South Western Gondwana*. (Unpublished master's thesis). University of the Witwatersrand, Johannesburg.

Bhatia, M.R. and Crook, K.A.W. (1986). Trace element characteristics of graywackes and tectonic setting discrimination of sedimentary basins. *Contributions to Mineralogy and Petrology*, 92: 181-193.

Black, D.E., Booth, P.W.K. and De Wit, M.J. (2016). Petrographic, geochemical and petro-physical analysis of the Collingham Formation near Jansenville, Eastern Cape, South Africa – potential cap rocks to shale gas in the Karoo. *South African Journal of Geology*, 119(1): 171-186.

Bordy, E.M. and Eriksson, P. (2015). Lithostratigraphy of the Elliot Formation (Karoo Supergroup), South Africa. *South African Journal of Geology*, 118(3): 311-316.

Bordy, E.M. and Head, H.V. (2018). Lithostratigraphy of the Clarens Formation (Stormberg Group, Karoo Supergroup), South Africa. *South African Journal of Geology*, 121(1): 119-130.

Bowker, K.A. (2007). Development of the Barnett Shale play, Fort Worth Basin. *American Association of Petroleum Geologists*, 91(4): 4-11.

Brady, J.B., Newton, R.M. and Boardman, S.J. (1995). New uses for powder X-ray diffraction experiments in the undergraduate curriculum. *Journal of Geological Education*, 43: 466-470.

Branch, T., Ritter, O., Weckmann, U., Sachsenhofer, R.F. and Schilling, F.R. (2007). The Whitehill Formation – a high conductivity marker horizon in the Karoo Basin. *South African Journal of Geology*, 110(2-3): 465-476.

Brennan, R., Dulude, J. and Thomas, R. (2015). Approaches to maximize performance and reduce the frequency of routine maintenance in ICP-MS. *Spectroscopy*, 30(10): 12-25.

Broderick, J., Wood, R., Gilbert, P., Sharmina, M. and Anderson, K. (2011). *Shale gas: An updated assessment of environmental and climate change impacts*. (A report commissioned by The Co-operative and undertaken by researchers at the Tyndall Centre). University of Manchester, United Kingdom.

Bruner, K.R. and Smosna, R.A. (2011). *A comparative study of the Mississippian Barnett shale, Fort Worth Basin and Devonian Marcellus shale, Appalachian Basin*. Washington, D.C.: U.S. Department of Energy.

Burton, J., Skovgaard, J. and Rennkamp, B. (2018). *Sustaining carbon lock-in: Fossil fuel subsidies in South Africa*. Available online at: https://www.cambridge.org/core/terms

Butt, A.S. (2012). *Shale characterization using X-ray diffraction*. (Unpublished master's thesis). Dalhousie University, Nova Scotia.

Cadle, A.B., Cairncross, B., Christie, A.D.M. and Roberts, D.L. (1993). The Karoo Basin of South Africa: Type basin for the coal-bearing deposits of southern Africa. *International Journal of Coal Geology*, 23(1-4): 117-157.

Campbell, S.A., Mielke, P. and Götz, A.E. (2016). Geothermal energy from the Main Karoo Basin? New insights from borehole KWV-1 (Eastern Cape, South Africa). *Geothermal Energy*, 4(9): 1-19.

Catuneanu, O., Hancox, P.J., Cairncross, B., and Rubidge, B.S. (2005). The Karoo Basin of south-central Africa. *Journal of African Earth Science*, 43: 211-253.

Catuneanu, O., Hancox, P.J., Cairncross, B. and Rubidge, B.S. (2002). Foredeep submarine fans and forebulge deltas: Orogenic off-loading in the underfilled Karoo Basin. *Journal of African Earth Sciences*, 35:489-502.

Chen, D. (2012). *Microstructure study on Barnett Shale*. (Unpublished master's thesis). University of Houston, Texas.

Chermak, J.A. and Schreiber, M.E. (2014). Mineralogy and trace element geochemistry of gas shales in the United States: Environmental implications. *International Journal of Coal Geology*, 126: 32-44.

Chopra, S., Sharma, R. and Marfurt, K. (2014). *Shale gas reservoir characterization workflows*. Paper presented at the Unconventional Resources Technology Conference, 12-14 August, Denver (pp. 1905-1910).

Cole, D. and Mosavel, H. (2016). Shale gas developments in the Karoo Basin. *Geoclips*, 47: 1-8.

Colwell, C.L. (2014). *Correlation of chemostratigraphy, mechanical stratigraphy and total organic carbon using one core from the Barnett Shale, Fort Worth Basin, Hood County, Texas*. (Unpublished master's thesis). Texas Christian University, Texas.

Costin, G., Götz, A.E. and Ruckwied, K. (2019). Sedimentary organic matter characterization of the Whitehill shales (Karoo Basin, South Africa): An integrated quantitative approach using FE-EPMA and LA-ICP-MS. *Review of Palaeobotany and Palynology*, 268: 29-42.

Damiani, R.J. and Rubidge, B.S. (2003). A review of the South African temnospondyl amphibian record. *Palaeontologia Africana*, 39: 21-36.

Danchin, R.V. (1970). *The aspects of the geochemistry of some selected South Africa fine grained sediment*. (Unpublished doctoral thesis). University of Cape Town, Cape Town.

Dargahi, H.J., Rezaee, R. and Pejcic, B. (2013). *Clay mineralogy of shale gas reservoirs through integrating infrared spectroscopy and x-ray diffraction*. A paper presented at the Unconventional Resources Technology Conference, 12-14 August, Denver (pp. 2027-2035).

Day, M.O. and Rubidge, B.S. (2014). A brief lithostratigraphic review of the Abrahamskraal and Koonap formations of the Beaufort Group, South Africa: Towards a basin-wide stratigraphic scheme for the Middle Permian Karoo. *Journal of African Earth Sciences*, 100: 227-242.

Dean, W.E., Arthur, M.A. and Stow, D.A.V. (1984). Origin and geochemistry of Cretaceous deep-sea black shales and multi-colored claystones, with emphasis on Deep Sea Drilling Project Site 530, Southern Angola Basin. *Initial Reports of the D.S.D.P*, 75(2): 819-844.

Degens, E.T., Williams, E.G. and Keith, M.L (1957). Environmental studies of carboniferous sediments Part I: Geochemical criteria for differentiating marine from fresh-water shales. *American Association of Petroleum Geologists Bulletin*, 41(11): 2427-2455.

De Kock, M.O. et al. (2017). Deflating the shale gas potential of South Africa's Main Karoo Basin. *South African Journal of Science*, 113(9-10): 1-12.

Deng, H., Xie, X., Chen, K., Vij, C., Pang, Y., and Li, H.A. (2018). Mineralogical characteristics of continental shale: A case study in Yan-Chang Formation, Ordos Basin. *Australian Journal of Earth Sciences*, 65(11): 1-12.

Deshpande, V.P. (2008). *General screening criteria for shale gas reservoirs and production data analysis of Barnett Shale*. (Unpublished master's thesis). Texas A&M University, Texas.

Dickinson, W.R. and Suczek, C.A. (1979). Plate tectonics and sandstone compositions. *American Association of Petroleum Geologists Bulletin*, 63(12): 2164-2182.

Ding, W., Li, C., Li, C., Xu, C., Jiu, K., Zeng, W., and Wu, L. (2012). Fracture development in shale and its relationship to gas accumulation. *Geoscience Frontiers*, 3(1): 97-105.

Dondo, C. and Nhleko, L. (2008). Boreholes: 3D geological modelling and representation, *PositionIT*, Nov/Dec 2008: 49-51.

El-Anwar, E.A.A. (2017). Mineralogical, petrographical, geochemical, diageneses and provenance of cretaceous black shales, Duwi Formation at Quseir-Safaga, Red Sea, Egypt. *Egyptian Journal of Petroleum*, 26(4): 915-926.

El-Anwar, E.A.A., Mekky, H.S. and Wahab, W.A. (2018). Geochemistry, mineralogy and depositional environment of black shales of the Duwi Formation, Qusseir area, Red Sea coast, Egypt. *Carbonates and Evaporites*, 34(3): 883-892.

Eriksson, P.G. (1984). A palaeoenvironmental analysis of the Molteno Formation in the Natal Drakensberg. *South African Journal of Geology*, 87(3): 237-244.

Fagereng, A. (2012). A note on folding mechanisms in the Cape Fold Belt, South Africa. *South African Journal of Geology*, 115(2): 137-144. doi: 10.2113/gssajg.115.2.137

Ferreira, J.C. (2014). *Characterization of potential source rocks of the Prince Albert, Whitehill and Collingham formations in the Laingsburg sub-basin, South Africa*. (Unpublished master's thesis). University of the Western Cape, Cape Town.

Fildani, A., Weislogel, A., Drinkwater, N.J., McHargue, T., Tankard, A., Wooden, J., Hodgson, D., and Flint, S. (2009). U-Pb-zircon ages from the southwestern Karoo Basin, South Africa – implications for the Permian-Triassic boundary. *Geology*, 37(8): 719-722.

Findlay III, C.P. (2016). *Influence of the Gondwanide Magmatic Arc and Cape Fold Belt on the Karoo Basin, South Africa*. (Unpublished master's thesis). West Virginia University, West Virginia.

Finlay, A.J. and Martin, J. (2013). Understanding shale gas plays through the application of inorganic geochemistry. *Goldschmidt 2013 conference abstracts*, p. 1085.

Flewelling, S.A. and Sharma, M. (2014). Constraints on upward migration of hydraulic fracturing fluid and brine. *Groundwater*, 52(1): 9-19.

Flint, S.S., Hodgson, D.M., Sprague, A.R., Brunt, R.L., Van der Merwe, W.C., Figueiredo, J., Prelat, A., Box, D., Di Celma, C., and Kavanagh, J.P. (2011). Depositional architecture and sequence stratigraphy of the Karoo basin floor to shelf edge succession, Laingsburg depocenter, South Africa. *Marine and Petroleum Geology*, 28(3): 658-674.

Floyd, P.A., Winchester, J.A. and Park, R.G. (1989). Geochemistry and tectonic setting of Lewisian clastic metasediments from the Early Proterozoic Loch Maree Group of Gairloch, NW Scotland. *Precambrian Research*, 45(1-3): 203-214.

Gale, J.F.W., Reed, R.M. and Holder, J. (2007). Natural fractures in the Barnett Shale and their importance for hydraulic fracture treatments. *American Association of Petroleum Geologists Bulletin*, 91(4): 603-622.

Gąsiński, A. (2017). Mineral composition and preferred orientation of minerals in shales from Palaezoic Baltic Basin. *EGU General Assembly Conference Abstracts*, 19: 9334.

Geel, C. and Bordy, E.M. (2021). Palaeo-environmental and provenance reconstruction of the Lower Permian mudstones (lower Ecca Group) in the main Karoo Basin, South Africa. *Journal of African Earth Sciences*, 182: 1-18. doi: 10.1016/afrearsci.2021.104303

Geel, C., De Wit, Booth, P., M., Schulz, H.M. and Horsfield, B. (2015). Palaeo-environment, diagenesis and characteristics of Permian black shales in the lower Karoo Supergroup flanking the Cape Fold Belt near Jansenville, Eastern Cape, South Africa: Implication for the shale gas potential of the Karoo Basin. *South African Journal of Geology*, 118(3): 249-279.

Geel, C., Nolte, S. and Bordy, E.M. (2021). Geomechanical properties of the Permian black shales in the southern main Karoo Basin: Lessons from compositional and petrophysical studies. *South African Journal of Geology*, 124(3): 1-16. doi: 10.25131/sajg.124.0026

Geel, C., Schulz, H.M., Booth, P., De Wit, M.J. and Horsfield, B. (2013). Shale gas characteristics of Permian black shales in South Africa: Results from recent drilling in the Ecca Group (Eastern Cape). *Energy Procedia*, 40: 256-265.

Genhe, S., and Benson, P.M. (2019). Permeability enhancement through hydraulic fracturing: laboratory measurements combining a 3D printed jacket and pore fluid over-pressure. *Scientific Reports*,12573: 1-11. doi: 10.1038/s41598-019-49093-1

Haddad, M., Sanei, A. and Sepehrnoori, K. (2017). *Hydraulic fracturing fluid effect on clay swelling in stimulated naturally fractured reservoirs*. A paper presented at the Unconventional Resources Technology Conference, 24-26 July, Texas (pp. 1-15).

Han, Y., Mahlstedt, N. and Horsfield, B. (2015). The Barnett Shale: Compositional fractionation associated with intraformational petroleum migration, retention and expulsion. *American Association of Petroleum Geologists Bulletin*, 99(12): 2173-2202.

Harkness, J.S., Swana, K., Eymold, W.K., Miller, J., Murray, R., Talma, S., Whyte, C.J., Moore, M.T., Maletic, E.L., Vengosh, A., and Dorrah, T.H. (2018). Pre-drill groundwater geochemistry in the Karoo Basin, South Africa. *Groundwater*, 56(2): 187-203.

Herbert, C.T. and Compton, J.S. (2007). Depositional environments of the lower Permian Dwyka diamictite and Prince Albert shale inferred from the geochemistry of early diagenetic concretions, southwest Karoo Basin, South Africa. *Sedimentary Geology*, 194(3): 263-277.

Hodgson, D.M., Flint, S.S., Hodgetts, D., Drinkwater, N.J., Johannessen, E.P., and Luthi, S.M. (2006). Stratigraphic evolution of fine-grained submarine fan systems, Tanqua Depocenter, Karoo Basin, South Africa. *Journal of Sedimentary Research*, 76: 20-40. doi: 10.2110/jsr.2006.03

Hofmeyr, P.K. (1971). *The abundances and distribution of some trace elements in some selected South African shales*. (Unpublished doctoral thesis). University of Cape Town, Cape Town.

Hu, J., Li, Q., Fang, N., Yang, J. and Ge, D. (2015). Geochemistry characteristics of the Low Permian sedimentary rocks from central uplift zone, Qiangtang Basin, Tibet: Insights into source-area weathering, provenance, recycling and tectonic. *Arabian Journal of Geosciences*, 8(8): 5373-5388.

Hupp, B.N. and Donovan, J.J. (2018). Quantitative mineralogy for facies definition in the Marcellus Shale (Appalachian Basin, USA) using XRD-XRF integration. *Sedimentary Geology*, 371(C): 16-31.

Isbell, J.L., Cole, D.I. and Catuneanu, O. (2008). Carboniferous-Permian glaciation in the main Karoo Basin, South Africa: Stratigraphy, depositional controls and glacial dynamics. *The Geological Society of America*, Special Paper 441, pp. 71-82. doi: 10.1130/ 2008.2441(05)

Jarvie, D.M., Claxton, B., Henk, B. and Breyer, J. (2001). *Oil and shale gas from Barnett Shale, Ft. Worth Basin, Texas*. A paper presented at the American Association of Petroleum Geologists National Convention, 3-6 June, Denver (pp. 1-28).

Jarvie, D.M., Hill, R.J., Ruble, T.E. and Pollastro, R.M. (2007). Unconventional shale-gas systems: The Mississippian Barnett Shale of north-central Texas as one model for thermogenic shale-gas assessment. *American Association of Petroleum Geologists Bulletin*, 91(4): 475-499.

Jiang, Z. et al. (2016). Basic characteristics and evaluation of shale oil reservoirs. *Petroleum Research*, 1(2): 149-163.

Johansson, M. (2019). *Efficient modeling and control of crushing processes in mineral processing*. (Unpublished thesis). Chalmers University of Technology, Goteborg.

Johnson, M.R. (1976). *Stratigraphy and sedimentology of the Cape and Karoo sequences in the Eastern Cape Province*. (Unpublished doctoral thesis). Rhodes University, Grahamstown.

Johnson, M.R. (1991). Sandstone petrography, provenance and plate tectonic setting in Gondwana context of the southeastern Cape-Karoo Basin. *South African Journal of Geology*, 94(2-4): 137-154.

Johnson, M.R., Van Vuuren, C.J., Hegenberger, W.F., Key, R. and Show, U. (1996). Stratigraphy of the Karoo Supergroup in southern Africa: An overview. *Journal of African Earth Sciences*, 23(1): 3-15.

Johnson, M.R., Van Vuuren, C.J., Visser, J.N.J., Cole, D.I., Wickens, H.V., Christie, A.D.M., and Roberts, D.L. (1997). The Foreland Karoo Basin, South Africa. *Sedimentary Basins of the World*, 3: 269-317.

Johnson, M.R., Van Vuuren, C.J., Visser, J.N.J., Cole, D.I., De V. Wickens, H., Christie, A.D.M., Roberts, D.L., and Brandl, G. (2006). 'Sedimentary rocks of the Karoo Supergroup', in M.R. Johnson, C.R. Anhaeusser and R.J. Thomas (eds), *The geology of South Africa*. Johannesburg: Geological Society of South Africa.

Karpiński, B. and Szkodo, M. (2015). Clay minerals – mineralogy and phenomenon of clay swelling in oil and gas industry. *Advances in Materials Science*, 15(1): 37-55.

Kingsley, C.S. (1981). A composite submarine fan-delta-fluvial model for the Ecca and Lower Beaufort Groups of Permian Age in the Eastern Cape Province, South Africa. *South African Journal of Geology*, 84(1): 27-40.

Kogel, J.E. and Lewis, S.A. (2001). Baseline studies of the clay minerals society source clays: Chemical analysis by inductively coupled plasma-mass spectroscopy (ICP-MS). *Clays and Clay Minerals*, 49(5): 387-392.

Lanci, L., Tohver, E., Wilson, A. and Flint, S. (2013). Upper Permian magnetic stratigraphy of the lower Beaufort Group, Karoo Basin. *Earth and Planetary Science Letters*, 375: 123-134. doi: 10.1016/j.eps1.2013.05.017

Lavelle, G. (2014). Different coloration of Devonian shales. *The Juniata Journal of Geology*, 1: 1-6.

Liang, C., Jiang, Z., Cao, Y., Wu, M., Guo, L., and Zhang, C. (2016). Deep-water depositional mechanisms and significance for unconventional hydrocarbon exploration: A case study from the lower Silurian Longmaxi shale in the southeastern Sichuan Basin. *American Association of Petroleum Geologists Bulletin*, 100(5): 773-794.

Lin, W., Chen, L., Lu, Y., Hu, H., Liu, L., Liu, X., and Wei, W. (2017). Diagenesis and its impact on reservoir quality for the Chang 8 oil group tight sandstone of the Yanchang Formation (upper Triassic) in southwestern Ordos basin, China. *Journal of Petroleum Exploration and Production Technology*, 7: 947-959.

Liu, L., Qiao, J., Shen, B., Lu, X. and Yang, Y. (2017). Geological characteristics and shale gas distribution of carboniferous mudstones in the Tarim Basin, China. *Acta Geochimica*, 36(2): 260-275. doi 10.1007/s11631-017-0144-8

Lone, A.M., Shah, R.A., Achyuthan, H. and Fousiya, A.A. (2018). Geochemistry, spatial distribution and environmental risk assessment of the surface sediments: Anchar Lake, Kashmir Valley, India. *Environmental Earth Sciences*, 77(65): 1-20.

Loock, J.C., Brynard, H.J., Heard, R.G., Kitching, J.W. and Rubidge, B.S. (1994). The stratigraphy of the Lower Beaufort Group in an area north of Laingsburg, South Africa. *Journal of African Earth Sciences,* 18(3): 185-195.

Loucks, R.G. and Ruppel, S.C. (2007). Mississippian Barnett shale: Lithofacies and depositional setting of a deep-water shale-gas succession in the Fort Worth Basin, Texas. *American Association of Petroleum Geologists Bulletin*, 91(4): 579-601.

Maake, L.T. (2018). *Mineralogy and geochemistry of Karoo black shales and associated carbonates in the Lower Ecca Formations of Jansenville area, Southern Karoo Basin*. Nelson Mandela University, Port Elizabeth (pp.1). doi:10.13140/RG.2.2.34349.13289

Mepaiyeda, S., Madi, K., Gwavava, O. and Baiyegunhi, C. (2020). Geological and geophysical assessment of groundwater contamination at the Roundhill landfill site, Berlin, Eastern Cape, South Africa. *Heliyon*, 6(7): 1-9. doi: 10.1016/j.heliyon.2020.e04249

Merriman, R.J., Highley, D.E. and Cameron, D.G. (2003). Definition and characteristics of very-fine grained sedimentary rocks: Clay, mudstone, shale and slate. *British Geological Survey Commissioned Report, CR/03/281N*.

Mews, K.S., Alhubail, M.M. and Barati, R.G. (2019). A review of brittleness index correlations for unconventional tight and ultra-tight reservoirs. *Geosciences*, 9(7): 319. doi: 10.3390/geosciences9070319

Michaud, D. (2015). X-ray fluorescence spectroscopy report. Available online at: https://www.911metallurgist.com/blog/x-ray-fluorescence-spectroscopy

Milliken, K.L., Esch, W.L., Reed, R.M. and Zhang, T. (2012). Grain assemblages and strong diagenetic overprinting in siliceous mudrocks, Barnett Shale (Mississippian), Fort Worth Basin, Texas. *American Association of Petroleum Geologists Bulletin*, 96(8): 1553-1578.

Mohamed, I.M., Mohamed, S., Yakup, C., and Mazher, I. (2019). *Integrated approach to evaluate rock brittleness and fracability for hydraulic fracturing optimization in shale gas*. Paper presented at the SPE Oklahoma City Oil and Gas Symposium, 9-10 April, Oklahoma (pp. 1-21). doi: 10.2118/195196-MS

Molenaar, N., Čyžienė, J. and Sliaupa, S. (2007). Quartz cementation mechanisms and porosity variation in Baltic Cambrian sandstones. *Sedimentary Geology*, 195(3): 135-159.

Montgomery, S.L., Jarvie, D.M., Bowker, K.A. and Pollastro, R.M. (2005). Mississippian Barnett Shale, Fort Worth Basin, north-central Texas: Gas-shale play with multi-trillion cubic foot potential. *American Association of Petroleum Geologists Bulletin*, 89(2): 155-175.

Mosavel, H. and Cole, D.I. (2019) Lithostratigraphy of the Prince Albert Formation (Ecca Group, Karoo Supergroup). *South African Journal of Geology*, 122(4): 571-582.

Mowzer, Z. (2012). *Geochemical evaluation of source rocks within the upper Ecca, main Karoo*. (Unpublished master's thesis). University of the Western Cape, Cape Town.

Nicolas, M.P.B. and Bamburak, J.D. (2009). *Geochemistry and mineralogy of cretaceous shale, Manitoba (parts of NTS 62C, F, G, H, J, K, N): Preliminary results, in Report of activities*. Manitoba, Canada: Manitoba Geological Survey (pp. 165-174).

Niemack, A. (2009). The challenges of carbon mitigation and implications for South Africa in the post-2012 context. *South African Yearbook of International Affairs*, 2008/9: 67-84.

Nolte, S., Geel, C., Amann-Hildenbrand, A., Krooss, B.M. and Littke, R. (2019). Pretrophysical and geochemical characterization of potential unconventional gas shale reservoirs in the southern Karoo Basin, South Africa. *International Journal of Coal Geology*, 212: 1-16.

Nxantsiya, Z. (2017). *A study of the southwestern Karoo Basin in South Africa using magnetic and gravity data*. (Unpublished master's thesis). University of Fort Hare, Alice.

Nyakairu, G.W.A. and Koeberl, C. (2001). Mineralogical and chemical composition and distribution of rare earth elements in clay-rich sediments from central Uganda. *Geochemical Journal*, 35(1): 12-28.

Nyathi., N. (2014). *Stratigraphy, sedimentary facies and diagenesis of the Ecca Group, Karoo Supergroup in the Eastern Cape, South Africa*. (Unpublished master's thesis). University of Fort Hare, Alice.

Obasi, R.A., Madukwe, H.V. and Akinola, O.O. (2015). Geochemical, provenance tectonic setting, source-area weathering and maturity status of tar sands from Ode Aye area of Ondo State, Southwestern, Nigeria. *British Journal of Earth Sciences Research*, 3(1): 63-77.

Okeke, O.C. and Okogbue, C.O. (2011). Shales: A review of their classifications, properties and importance to the petroleum industry. *Global Journal of Geological Sciences*, 9(1): 55-73.

Olatunde, P.S. (2016). Geochemical techniques for the analysis of geochemical data and its application in the Nigerian oil and gas industries. *Chemical Sciences Journal*, 7(3).

Pandey, S. and Parcha, S.J. (2017). Provenance, tectonic and source-area weathering of the lower Cambrian sediments of the Parahio valley in the Spiti basin, India. *Journal of Earth System Science*, 126(27): 1-15.

Paulsen, G., Zacny, K., Dreyer, C.B., Szucs, A., Szczesiak, M., Santoro, C., Craft, J., Hedlund, M., and Skok, J. (2013). Robotic instrument for grinding rocks into thin sections (GRITS). *Advances in Space Research*, 51(11): 2181-2193.

Perez, R. (2010). *Application of LMR inversion and clustering analysis in the Barnett Shale*. Paper presented at SEG Denver 2010 Annual Meeting, 17-22 October, Oklahoma. doi: 10.1190/1.3513294

Pettijohn, F.J. (1975). Sedimentary rocks (3rd ed.). New York: Harper and Row.

Pevear, D.R. (1999). Illite and hydrocarbon exploration. *Proceedings of the National Academy of Sciences of the United States of America*, 96(7):3440-3446.

Pollastro, R.M., Jarvie, D.M., Hill, R.J. and Craig C.W. (2007). Geologic framework of the Mississippian Barnett Shale, Barnett-Paleozoic total petroleum system, Bend arch-Fort Worth Basin, Texas. *American Association of Petroleum Geologists Bulletin*, 91(4): 405-436.

Ratcliffe, H.G.K. and Schmidt, K. (2011). Application of inorganic whole-rock geochemistry to shale resource plays: An example from the Eagle Ford Shale, Texas. *Houston Geological Society Bulletin*, 2011 April: 31-38.

Ren, L., Zhao, J. and Hu, Y. (2014). Hydraulic fracture extending into network in shale: Reviewing influence factors and their mechanism. *The Scientific World Journal*, 2014: 1-9.

Rickman, R., Mullen, M.J., Petre, J.E. (2008). A practical use of shale petrophysics for stimulation design optimization: All shale plays are not clones of the Barnett shale. A paper presented at SPE Annual Technical Conference and Exhibition, Denver. Society of Petroleum Engineers, 1-11

Rodriguez, R., Crandall, D., Song, X., Verba, C. and Soeder, D. (2014). *Imaging techniques for analyzing shale pores and minerals*. NETL laboratory, Morgantown, p. 40.

Rogen, B. and Fabricius, I.L. (2002). Influence of clay and silica on permeability and capillary entry pressure of chalk reservoirs in the North Sea. *Petroleum Geoscience*, 8(3): 287-293.

Roser, B.P., Cooper, R.A., Nathan, S. and Tulloch, A.J. (1996). Reconnaissance sandstone geochemistry provenance and tectonic setting of the lower Paleozoic terranes of the West Coast and Nelson, New Zealand. *New Zealand Journal of Geology and Geophysics*, 39(1): 1-16.

Ross, D.J. and Bustin, R.M. (2009). The importance of shale composition and pore structure upon gas storage potential of shale gas reservoirs. *Marine and Petroleum Geology*, 26(6): 916-927.

Rubidge, B. and Hancox, J.P. (2002). The Karoo Supergroup. *Rocks and Minerals*, 77(1): 54-59. doi: 10.1080/00357529.2002.9926658

Rubidge, B.S., Hancox, J.P. and Catuneanu, O. (2000). Sequence analysis of the Ecca-Beaufort contact in the southern Karoo of South Africa. *South African Journal of Geology*, 103(1): 81-96.

Rudnick, R.L. and Gao, S. (2003). Composition of the continental crust. *Treatise on Geochemistry*, 3: 1-64. doi: 10.1016/b0-08-043751-6/03016-4

Rutherford, A.B., Rubidge, B.S. and Hancox, J.P. (2015). Sedimentology and palaeontology of the Beaufort Group in the Free State Province supports a reciprocal Foreland Basin model for the Karoo Supergroup, South Africa. *South African Journal of Geology*, 118(4): 355-372.

Scholle, P.A. and Ulmer-Scholle, D.S. (2003). A color guide to the petrography of carbonate rocks: grains, textures, porosity, diagenesis. *American Association of Petroleum Geologists Memoir*, 77.

Shen, Y., Meng, M., Liu, T., Ge, H. and Zhang, Y. (2017). Impact of petrophysical properties on hydraulic fracturing and development in tight volcanic gas reservoirs. *Geofluids*, 8: 1-13. doi: 10.1155/2017/5235140

Shoieb, M.A., Abidin, N.S.Z., Sum, C.W. and Ibrahim, Y. (2017). *Mineralogical and petrographic characterization: An indication of fracability of shale gas reservoir in the Blue Nile Basin, Sudan*. Singapore: Springer. doi: 10.1007/978-981-10-3650-7_21

Smithard, T., Bordy, E.M. and Reid, D. (2015). The effect of dolerite intrusions on the hydrocarbon potential of the lower Permian Whitehill Formation (Karoo Supergroup) in South Africa and southern Namibia: A preliminary study. *South African Journal of Geology*, 118(4): 489-510. doi: 10.2113/gssajg.118.4.489

Soeder, D.J. (2010). The Marcellus Shale: Resources and reservations. *EOS Transactions American Geophysical Union*, 91(32): 277-278. doi: 10.1029/2010E0320001

Spencer, R. and Weedmark, T. (2015). *Application of x-ray fluorescence (XRF) analyses to the characterization of tight reservoirs*. A paper presented at the Gas Mexico Congress, Mexico.

Środoń, J., Drits, V.A., McCarty, D.K., Hsieh, J.C. and Eberl, D.D. (2001). Quantitative x-ray diffraction analysis of clay-bearing rocks from random preparations. *Clays and Clay Minerals*, 49(6): 514-528.

Tamponi, M., Bertoli, M., Innocenti, F. and Leoni, L.D.S. (2003). X-ray fluorescene analysis of major elements in silicate rocks using fused glass discs. *Proceedings of the Tuscan Society of Natural Sciences – Memories Series A*, 108: 73-79.

Tang, X., Jiang, Z., Li, Zhuo., Gao, Z., Bai, Y., Zhao, S., and Feng, J. (2015). The effect of the variation in material composition on the heterogeneous pore structure of high-maturity shale of the Silurian Longmaxi Formation in the southeastern Sichuan Basin, China. *Journal of Natural Gas Science and Engineering*, 23: 464-473.

Tao, S., Xu, Y., Tang, D., Xu, H., Li, S., Chen, S., Liu, W., Cui, Y., and Gou, M. (2017). Geochemistry of the Shitoumei oil shale in the Santanghu Basin, Northwest China: Implications for paleoclimate conditions, weathering, provenance and tectonic setting. *International Journal of Coal Geology*, 184(2017): 42-56.

Tian, Y. (2010). *An investigation of regional variations of Barnett shale reservoir properties and resulting variability of hydrocarbon composition and well performance*. (Unpublished master's thesis). Texas A&M University, Texas.

Tian, Y. and Ayers, W.B. (2010). *Barnett Shale (Mississippian), Fort Worth Basin, Texas: Regional variations in gas and oil production and reservoir properties*. A paper presented at the Canadian Unconventional Resources and International Petroleum Conference, 19-21 October, Calgary (pp. 1-20). doi: 10.2118/137766-MS

Tobia, F.H. and Shangola, S.S. (2016). Mineralogy, geochemistry and depositional environment of the Beduh shale (Lower Triassic), Northern Thrust Zone, Iraq. *Turkish Journal of Earth Sciences*, 25(4): 367-391.

Tourtelot, H.A (1964). Minor-element composition and organic carbon content of marine and nonmarine shales of Late Cretaceous age in the western interior of the United States. *Geochinica et Cosmochimica Acta*, 28(10-11): 1579-1604.

Tribovillard, N.P., Algeo, T.J., Lyons, T.W. and Riboulleau, A. (2006). Trace metals as paleoredox and paleoproductivity proxies: An update. *Chemical Geology*, 232(1-2): 12-32.

Van der Walt, M., Day, M., Rubidge, B., Cooper, A.K. and Netterberg, I. (2010). A new GIS-based biozone map of the Beaufort Group (Karoo Supergroup), South Africa. *Palaeontology of Africa*, 45: 1-5.

Veevers, J.J., Cole, D.I. and Cowan, E.J. (1994). Southern Africa: Karoo Basin and Cape Fold Belt. *Geological Society of America Memoir*, 184: 223-279.

Vermylen, J.P. (2011). *Geomechanical studies of the Barnett Shale, Texas, USA*. (Unpublished doctoral thesis). Stanford University, USA.

Von Brunn, V. (1996). The Dwyka Group in the northern part of Kwazulu/Natal, South Africa: sedimentation during late Palaeozoic deglaciation. *Palaeogeography, Palaeoclimatology, Palaeoecology*, 125(1-4): 141-163.

Von Ketelhodt, A. and Wöcke, A. (2008). The impact of electricity crises on the consumption behavior of small and medium enterprises. *Journal of Energy in Southern Africa*, 19(1): 1-12.

Viljoen, J.H.A. (1994). Sedimentology of the Collingham Formation, Karoo Supergroup. *South African Journal of Geology*, 97(2): 167-183.

Visser, J.N.J. (1992). Deposition of the early to late Permian Whitehill Formation during a sea-level highstand in a juvenile foreland basin. *South African Journal of Geology*, 95(5-6): 181-193.

Wagen, M. (2000). Generation of overpressure by cementation of pore space in sedimentary rocks. *Geophysical Journal International*, 143(3): 608-620.

Walters, S.W. and Tucker, R.T. (2020). Resolving cryptic stratigraphy in the Ecca Group, Karoo Basin, South Africa: Elucidating the Ripon and Laingsburg depocenters. *Journal of African Earth Sciences*, 172: 1-21.

Wang, C. et al. (2019). Laminae characteristics and influence on shale gas reservoir quality of lower Silurian Longmaxi Formation in the Jiaoshiba area of the Sichuan Basin, China. *Marine and Petroleum Geology*, 109: 839-851.

Wang, H. (2017). A numerical study of thermal-hydraulic-mechanical simulation with application of thermal recovery in fractured shale-gas reservoirs. *SPE Reservoir Evaluation and Engineering*, 20(3): 513-531.

Wang, H., Ajao, O.O. and Economides, M.J. (2014). Conceptual study of thermal stimulation in shale gas formations. *Journal of Natural Science and Engineering*, 21: 874-885.

Wang, Q. and Li, R. (2017). Research status of shale gas: A review. *Renewable and Sustainable Energy Reviews*, 74(C): 715-720.

Wang, X., Ge, H., Wang, D., Wang, J. and Chen, H. (2017). A comprehensive method for the fracability evaluation of shale combined with brittleness and stress sensitivity. *Journal of Geophysics and Engineering*, 14(6): 1420-1429.

Wanniarachchi, W.A.M., Ranjith, P., Perera, M., Lashin, A., Al Arifi, N., and Li, J. (2015). Current opinions on foam-based hydro-fracturing in deep geological reservoirs. *Journal* of *Geomechanics and Geophysics for Geo-Energy and Geo-Resources,* 1(3): 121-134.

Weaver, C.E. (1956). A discussion on the origin of clay minerals in sedimentary rocks. *Clays and Clay Minerals*, 5: 159-173.

Werne, J.P., Sageman, B.B., Lyons, T.W. and Hollander, D.J. (2002). An integrated assessment of a "type euxinic" deposit: evidence for multiple controls on black shale deposition in the middle Devonian Oatka Creek Formation. *American Journal of Science,* 302(2): 110-143.

Wheeler, A.T. (2015). *Palaeoenvironmental and palaeoclimatic reconstruction of the Witbank coal deposits (Karoo Basin, South Africa)*. (Unpublished master's thesis). University of Pretoria, Pretoria.

Woodford, A.C., Chevallier, L. and Botha J.F. (2003). *Hydrogeology of the main Karoo Basin: Current knowledge and future research needs*. Gezina, South Africa: Water Research Commission.

Xia, Y., Zhou, H., Zhang, C., He, S., Gao, Y., and Wang, P. (2019). The evaluation of rock brittleness and its application: A review study. *European Journal of Environmental and Civil Engineering*. doi: 10-1080/19648189.2019.1655485

Xu, J., Cheng, B., Deng, Q., Liang, Y., Faboya, O.L., and Liao, Z. (2018). Distribution and geochemical significance of trace elements in shale rocks and their residual kerogens. *Acta Geochimica*, 37(6): 866-900. doi: 10.1007/s11631-018-02970

Xue, S., Lu, S., Xue, H., Yang, J., Tang, M., and Liu, S. (2015). Similarities and differences between marine and continental shale gas. *Acta Geologica Sinica*, 89(s1): 288-289.

Ye, Y., Tang, S. and Xi, Z. (2020). Brittleness evaluation in shale gas reservoirs and its influence on fracability. *Energies*, 13(2): 388.

Zhang, C., Gamage, R.P., Perera, M.S.A. and Zhao, J. (2013). Characteristics of clay-abundant shale formations: Use of CO_2 for production enhancement. *Energies*, 10: 2-27.

Zhang, D., Pathegama Gamage, R., Perera, M.S.A., Zhang, C. and Wanniarachchi, W.A.M. (2017). Influence of water saturation on the mechanical behaviour of low-permeability reservoirs rocks. *Energies*, 10(11): 1887.

Zhang, H., Shi, T. and Li, X. (2018). Optimization of shale gas reservoir evaluation and assessment of shale gas resources in the Oriente Basin in Ecuador. *Petroleum Science*, 15: 756-771.

Zhang, L., Chen, Z. and Zhao, Y. (2019). *Well production performance analysis for shale gas reservoirs*. doi: 10.1016/b978-0-444-64315-5.00001-2

Zhang, X., Shi, W., Zhai, G., Xu, G., Wang, R., Xu, Z., Wang, J., Wang, C., and Yuan, Q. (2017). Characteristics and controlling factors of shale gas reservoir in the Fuling area, Sichuan Basin. *Petroleum Research*, 2(1): 25-40.

Zhao, J., Jin, Z., Jin, Z., Wen, X., Geng, Y., Yan, C., and Nie, H. (2017). Depositional environment of shale in Wufeng and Longmaxi Formations, Sichuan Basin. *Petroleum Research*, 2(3): 209-221.

Zou, C., Zhao, Q., Dong, D., Yang, Z., Qiu, Z., Liang, F., Wang, N., Huang, Y., Duan, A., Zhang, Q., and Hu, Z. (2017). Geological characteristics, main challenges and future prospect of shale gas. *Journal of Natural Gas Geoscience*, 2(5-6): 273-288.